Journal of Medicinal Chemistry

pubs.acs.org/jmc

Article

Synthesis and Evaluation of Structurally Diverse C-2-Substituted Thienopyrimidine-Based Inhibitors of the Human Geranylgeranyl Pyrophosphate Synthase

Hiu-Fung Lee, Cyrus M. Lacbay, Rebecca Boutin, Alexios N. Matralis, Jaeok Park, Daniel D. Waller, Tian Lai Guan, Michael Sebag, and Youla S. Tsantrizos*

Cite This: https://doi.org/10.1021/acs.jmedchem.1c01913

Read Online

ACCESS | Metrics & More | Article Recommendations | Supporting Information

ABSTRACT: Novel analogues of C-2-substituted thienopyrimidine-based bisphosphonates (C2-ThP-BPs) are described that are potent inhibitors of the human geranylgeranyl pyrophosphate synthase (hGGPPS). Members of this class of compounds induce target-selective apoptosis of multiple myeloma (MM) cells and exhibit antimyeloma activity *in vivo*. A key structural element of these inhibitors is a linker moiety that connects their (((2-phenylthieno[2,3-*d*]pyrimidin-4-yl)amino)methylene)-bisphosphonic acid core to various side chains. The structural diversity of this linker moiety, as well as the side chains attached to it, was investigated and found to significantly impact the toxicity of these compounds in MM cells. The most potent inhibitor identified was evaluated in mouse and rat for liver toxicity and systemic exposure, respectively, providing further optimism for the potential value of such compounds as human therapeutics.

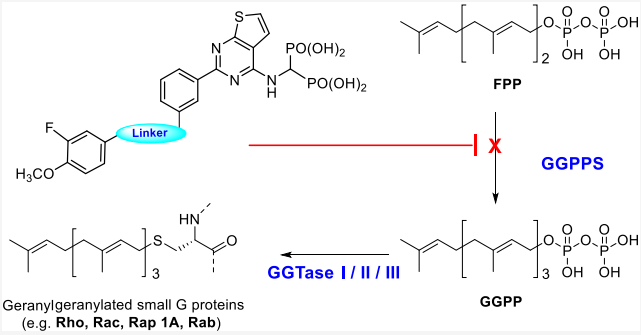

Downloaded via MCGILL UNIV on February 5, 2022 at 09:30:41 (UTC).
See https://pubs.acs.org/sharingguidelines for options on how to legitimately share published articles.

■ INTRODUCTION

Posttranslational modifications of small GTP-binding proteins (GTPases) with the lipidic side chain of either farnesyl pyrophosphate (FPP) or geranylgeranyl pyrophosphate (GGPP) provide these proteins with the ability to specifically associate with cellular membranes and act as molecular switches, which regulate numerous biochemical processes, including cell proliferation (Figure 1).[1,2] Previous biochemical studies have shown that dysregulation of protein prenylation plays a crucial role in tumor cell survival.[3] Mutated GTPases, such as the farnesylated H/K/N-Ras,[4] as well as geranylgeranylated GTPases, such as the Rho family (*e.g.*, RhoA/B/C) and the Ras-related proteins (*e.g.*, Rap 1A and Rab),[5] are presumed to mediate cell proliferation and metastasis in cancer and have been of interest in drug discovery for several decades.

Initially, efforts in oncology programs focused primarily on blocking protein farnesylation (directly or indirectly).[6] Numerous biochemical studies reported that zoledronic acid (**1**; ZOL; Figure 2), the most potent and selective inhibitor of the human farnesyl pyrophosphate synthase (hFPPS; Figure 1), inhibits the proliferation of various cancer cells, including breast,[7] multiple myeloma (MM),[8] prostate,[9] and osteosarcoma,[10] *albeit* at high concentrations. Although clinically relevant data in support of the *in vitro* observations are limited, some investigations have revealed evidence of longer disease-free survival for patients with MM when treated with standard chemotherapy plus ZOL (**1**).[11,12] Improved therapeutic outcomes were also reported for breast cancer patients treated with the standard of care chemotherapy plus ZOL (**1**),[13−16] although these results were less consistent and appeared to be dependent on age (*e.g.*, pre- *vs* postmenopausal women). However, the very modest therapeutic benefits observed with MM and breast cancer patients were attributed mainly to the poor physicochemical properties of bisphosphonate drugs and not the importance of hFPPS as a relevant biological target in oncology.

ZOL (**1**, ZOL) and risedronic acid (**2**, RIS) are among the most potent members of the nitrogen-containing bisphosphonate drugs (N-BPs) that are clinically used primarily for the treatment of bone-resorbing diseases, such as osteoporosis and lytic bone diseases associated with the progression of non-skeletal cancers, including MM. The bisphosphonate moiety of N-BPs is a chemically stable bioisostere of the pyrophosphate (diphosphate) moiety found in natural isoprenoid metabolites, and these drugs act as competitive inhibitors of the enzyme's substrates that bind in the allylic subpocket of the active site (*i.e.*, DMAPP and GPP; Figure 1).[17] At physiological pH, N-BPs are

Received: November 8, 2021

© XXXX American Chemical Society

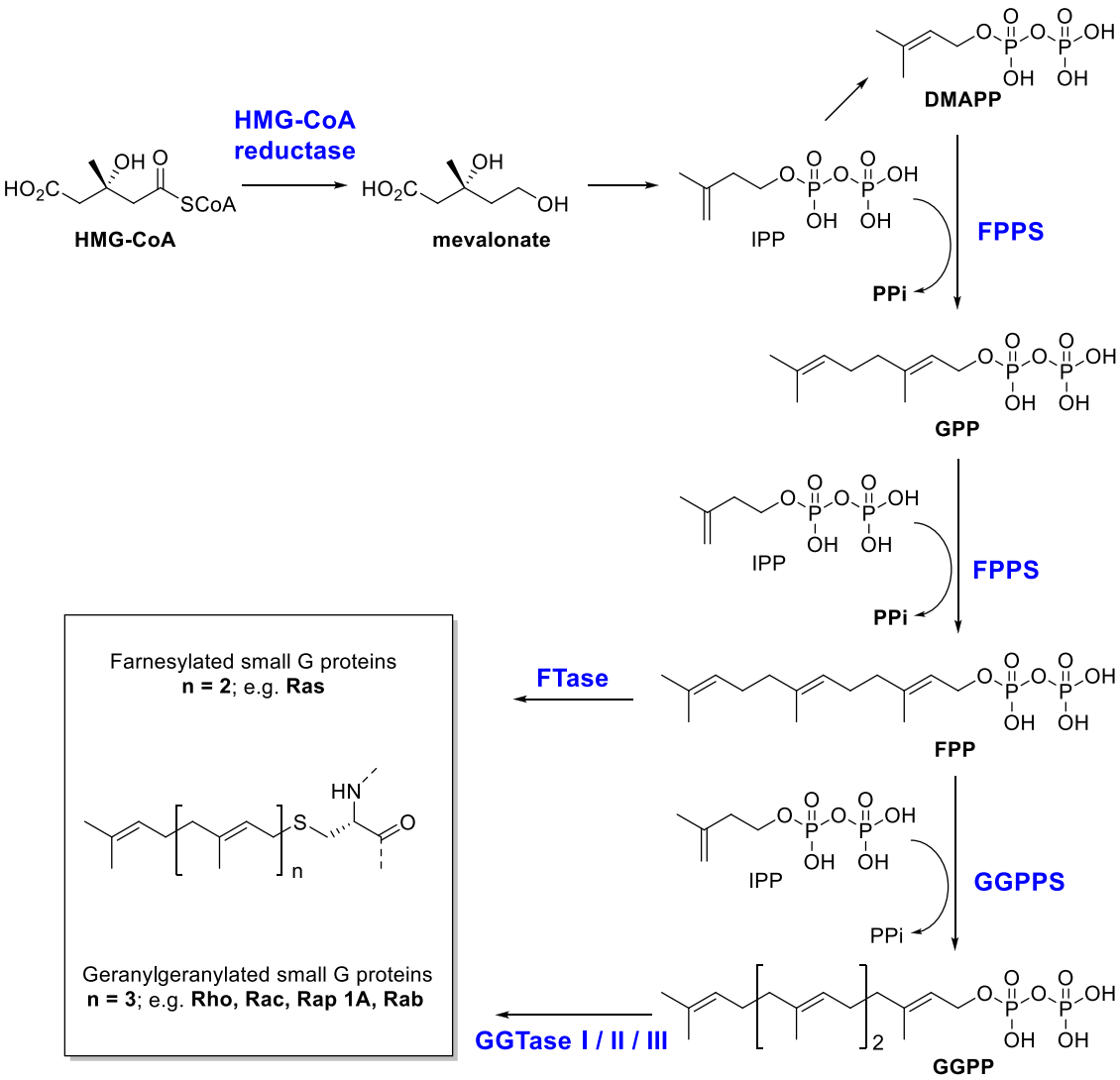

Figure 1. Biosynthetic pathway of isoprenoid metabolites and protein prenylation.

highly ionized (as the trianions) and consequently exhibit very poor cell-membrane permeability, suffer from rapid clearance from the systemic circulation through the kidneys, and have almost negligible distribution to nonskeletal tissues.[18,19]

In the hope of identifying therapeutics that block protein farnesylation of small GTPases and exhibit better biopharmaceutical properties than the previously approved N-BP drugs (*e.g.*, **1**, **2**), a number of different nonbisphosphonate chemotypes were also explored. Examples include allosteric inhibitors of hFPPS (*e.g.*, compounds **3**−**5**; Figure 2) that bind into a well-defined lipophilic pocket near the active site and interfere with the binding of the IPP substrate.[20] Additionally, compounds that block the farnesylation of GTPases by directly inhibiting the farnesyl transferase enzyme (FTase), such as tipifarnib (**6**) and lonafarnib (**7**), have also been explored as potential antitumor agents (Figure 2). Unfortunately, none of these approaches have been highly successful; the hFPPS allosteric inhibitors identified so far exhibit poor cell-based activity, whereas the FTase inhibitors have limited clinical efficacy, likely due to a redundancy mechanism, which allows geranylgeranylation and activation of oncogenic GTPases (*e.g.*, mutated K-RAS) when FTase is inhibited (Figure 1).[21] To overcome this redundancy mechanism, past efforts also attempted to design dual FTase/GGTase I inhibitors, such as the compound L-778,123 (**8**), which was advanced to phase I clinical trials for the treatment of pancreatic cancer, but was withdrawn from development due to toxicity.[22] Collectively, all of these examples highlight the significant drug discovery efforts devoted to exploring the direct, or indirect, inhibition of protein farnesylation, as a means of treating various cancers; unfortunately, these efforts have yet to identify a highly successful human therapeutic for the treatment of cancer.

More recently, our own group and those of others provided evidence that the inhibition of geranylgeranylation of relevant GTPases may provide a more efficient mechanism for treating MM, as compared to that of blocking farnesylation (Figure 1). MM is characterized by the accumulation of malignant plasma cells in the bone marrow, secretion of monoclonal immunoglobulins (known as M protein or paraprotein), and a constellation of target organ damage (known as CRAB: hyperCalcemia, Renal failure, Anemia, Bone disease).[23,24] This disease is the second-most common hematological malignancy in adults, currently leading to an estimated 38 000 new cases and 14 000 deaths per year in the United States and Canada. Recent advances in our knowledge of the pathophysiology and treatment of MM have led to patients living longer with MM, in spite of the

https://doi.org/10.1021/acs.jmedchem.1c01913
J. Med. Chem. XXXX, XXX, XXX−XXX

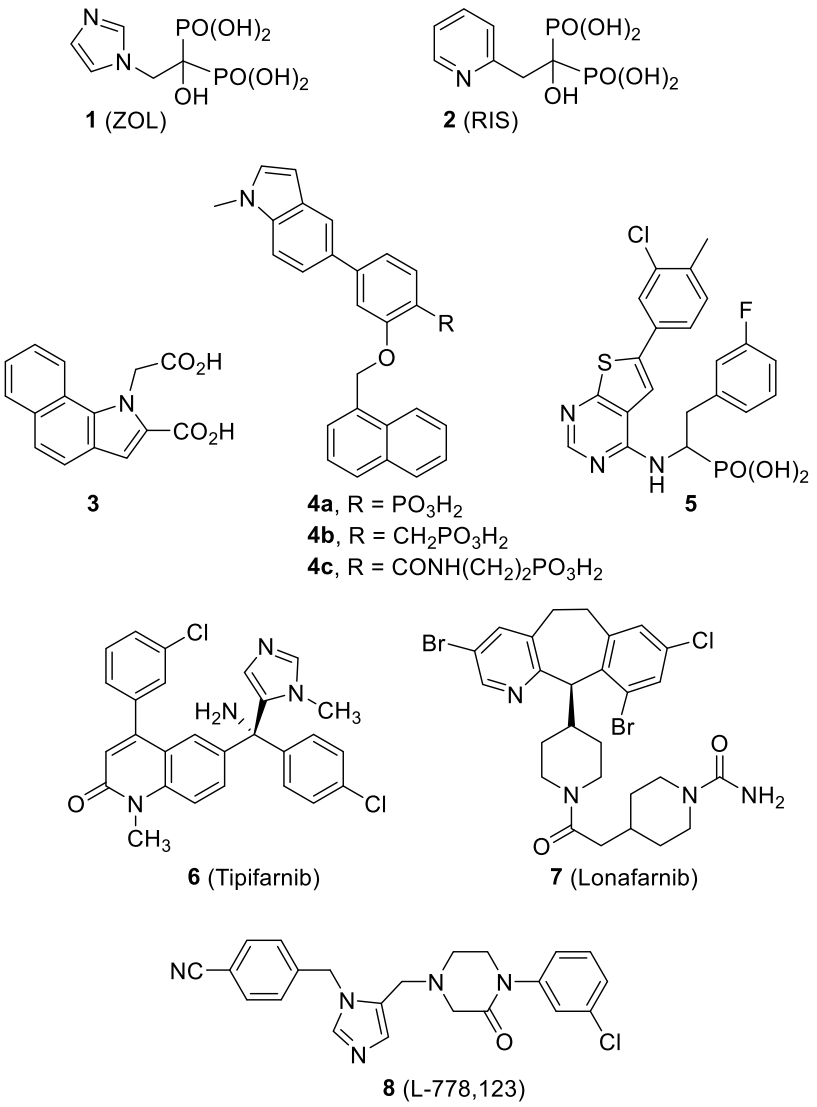

Figure 2. Compounds that block protein farnesylation. N-BP drugs **1** and **2** are clinically validated, active site inhibitors of hFPPS, exploratory compounds **3**−**5** are allosteric inhibitors of hFPPS, the drugs **6** and **7** are inhibitors of FTase (under further clinical investigation), and compound **8** is a dual inhibitor of FTase and GGTase I.

complications and side effects of the currently available treatments.[25] However, there is still no cure for this malignancy and drugs with novel mechanisms of action to treat/cure MM are of significant interest.

In contrast to hFPPS and FTase, drug discovery efforts focusing on the selective inhibition of the human geranylgeranyl pyrophosphate synthase (hGGPPS) enzyme have been very limited. To date, only a small number of potent inhibitors of this enzyme have been reported, including inhibitors **9**,[26] **10**,[27] **11**,[28] and **13c**[29] (Figure 3). This may be, in part, due to the long-held assumption that the selective inhibition of the upstream enzyme (*i.e.*, hFPPS) is more important for clinical efficacy in the treatment of cancer.[26a] In principle, this is a reasonable biochemical assumption since the inhibition of hFPPS will lead to intracellular depletion of the FPP substrate of hGGPPS (required for the biosynthesis of GGPP) and consequently expected to result in effective antitumor efficacy for cancers depending on either the upregulation of mutated farnesylated (*e.g.*, K-Ras) or geranylgeranylated GTPases (*e.g.*, Rho, Rab, Rap 1A). Consistent with this presumption, studies have shown that ZOL (**1**) can block geranylgeranylation of Rap 1A.[30] However, numerous other factors play an important role in the clinical efficacy of a therapeutic agent, including the intracellular concentration of the biological target and the extent (%) of target engagement that is required to achieve clinical efficacy. In the absence of any direct measurements of target engagement *in vivo* that can link the preclinical to the clinical readouts, it becomes very difficult to discern the value of a biological target, or its inhibitors, for the intended disease treatment.[31] Recently, we provided data from a large panel of human MM cell lines, as well as from bone marrow specimens obtained from MM patients, indicating that the mRNA levels of hFPPS are significantly higher than those of hGGPPS in these samples, suggesting that hGGPPS may be a more amenable therapeutic target (than hFPPS) for the treatment of multiple myeloma.[29] At that time, we disclosed only seven examples of a new chemotype, typified by the C-2 phenyl thienopyrimidine bisphosphonate (C2-ThP-BP) core **18b** (Figure 3), which were prepared during the method development of our synthetic methodologies. One of these compounds, CML-07-119 (analogue **13c**; Figure 3), was found to exhibit nanomolar potency in blocking the proliferation of various MM cells. Consistent with the expected

https://doi.org/10.1021/acs.jmedchem.1c01913
J. Med. Chem. XXXX, XXX, XXX−XXX

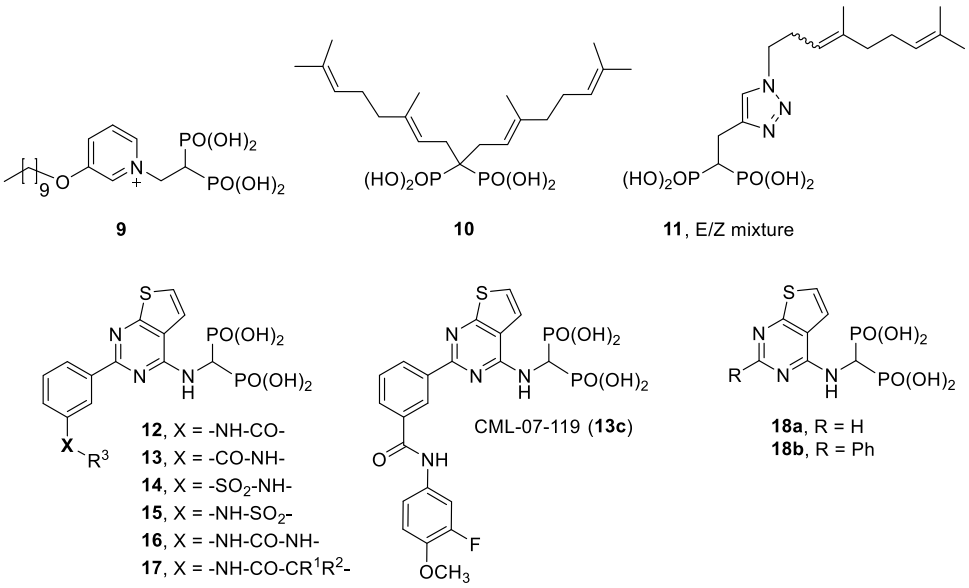

Figure 3. Exploratory compounds that block protein geranylgeranylation by targeting hGGPPS and inhibiting GGPP biosynthesis.

Scheme 1. Parallel Synthesis of Compound Library, Inhibitors 12−17[a]

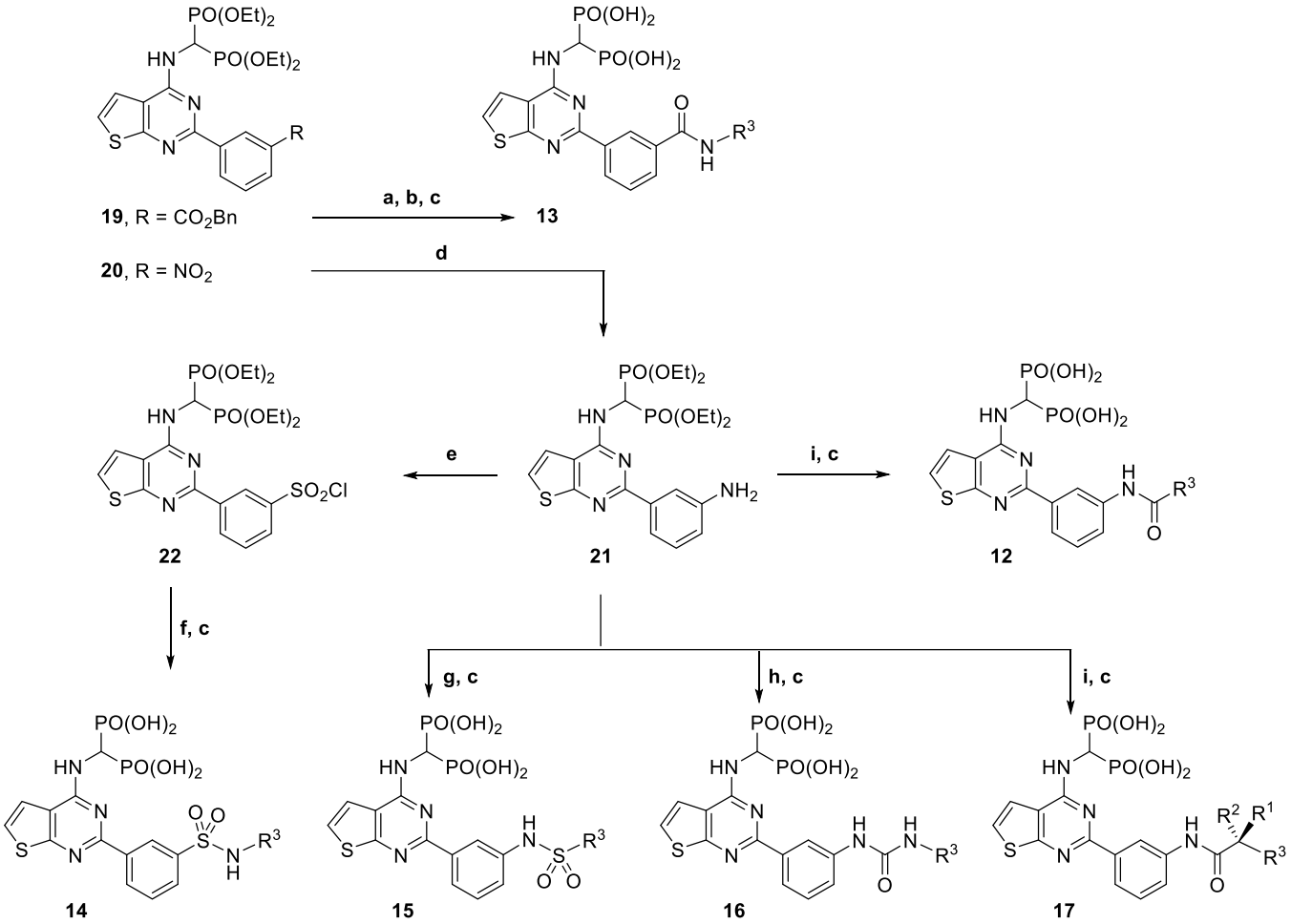

[a]Conditions: (a) TFA, 80 °C, 92−95%; (b) H_2N-alkyl/aryl/heteroaryl, HATU, DIPEA, DMF/DCM, RT, 50−80%; (c) (i) TMSBr, DCM/DMF, 0 °C to RT, (ii) MeOH, 15−95%; (d) $SnCl_2$, EtOH, 80 °C, 83%; (e) (i) $NaNO_2$, HCl aq., (ii) $SOCl_2/H_2O$, cat. CuCl, −5 °C to RT, 86%; (f) H_2N-alkyl/aryl/heteroaryl, pyridine, DCM, RT, 15−60%; (g) alkyl- or arylsulfonyl chloride, pyridine, DCM, RT, 30−55%; and (h) triphosgene, H_2NAr, Et_3N, DCM, RT, 40−70%; (i) RCO_2H, HATU, DIPEA, DCM/DMF, RT, 10−70%.

https://doi.org/10.1021/acs.jmedchem.1c01913
J. Med. Chem. XXXX, XXX, XXX−XXX

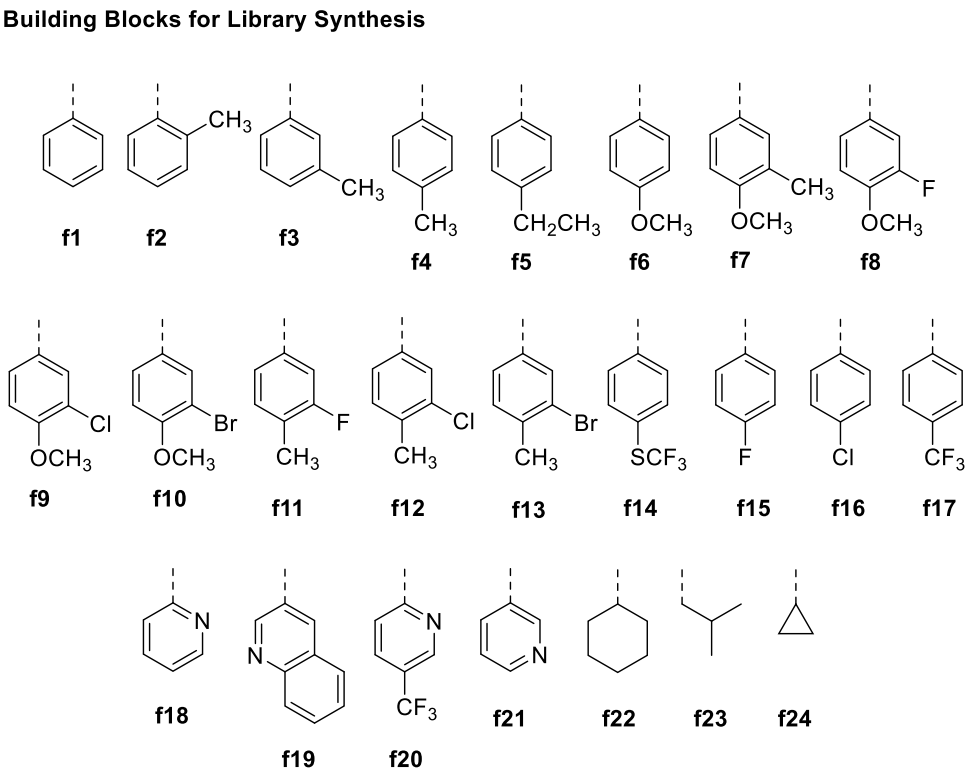

Figure 4. Examples of building blocks used as the R^3 substituent in the library synthesis of inhibitors **12**−**17**.

mechanism of action of this compound, we also demonstrated a direct correlation between the selective intracellular target engagement of hGGPPS and cell apoptosis.[29] Additionally, we used CML-07-119 to demonstrate *in vivo* antimyeloma efficacy in a genetically engineered mouse model that faithfully recapitulates the characteristics of the human MM disease and mimics the therapeutic responses of MM patients to known clinically validated drugs.[32] Inhibitor CML-07-119 is metabolically stable in mouse, rat, and human liver microsomes (half-life of 128 min in MLM, 187 min in RLM, and 154 min in HLM), with an intrinsic clearance of 27, 13, and 7 μL/(min mg) of proteins in mouse, rat, and human liver microsomes, respectively. In this report, we present additional preclinical studies on CML-07-119 (**13c**) and highlight some structural features of the linker moiety (*i.e.*, **X** moiety of analogues **12**−**17**; Figure 3) and the R^3 side chain of these compounds that modulate their potency and bone affinity.

■ RESULTS AND DISCUSSION

Synthesis of hGGPPS Inhibitors with Structurally Diverse Linkers and Side Chains. During the initial optimization of our synthetic methodologies, to render them amenable to modular parallel synthesis of large compound libraries, we reported the synthesis of the thieno[2,3-*d*]-pyrimidin-4-amine intermediates **19** and **20** and their conversion to a handful of final inhibitors with general structures **12** and **13** (Scheme 1).[29] Surprisingly, among that very small number of compounds (a total of only 7), we discovered analogue CML-07-119 (Figure 3, analogue **13c**), which is a potent hGGPPS inhibitor with antimyeloma activity *in vivo*.[29] Encouraged by this finding, we directed our efforts toward the preparation of a focused library of approximately 150 new analogues having an amide (**12**, **13**), sulfonamide (**14**, **15**), urea (**16**), or an extended and branched chiral linker (**17**) connecting the C-2 phenyl moiety of the basic scaffold **18b** to various side chains (*i.e.*, R^3). The general structures of these analogues are shown in Figure 3 and Scheme 1. Over 50 building blocks were used as the R^3 substituents, including those shown in Figure 4; some examples of the most potent hGGPPS inhibitors identified are shown in Figure 5.

The synthesis of the final inhibitors **12** and **13** was achieved as we previously reported with minor modifications (Scheme 1).[29] A two-step conversion of the aniline moiety of intermediate **21** to the corresponding sulfonyl chloride **22** was achieved by first preparing the aryl diazonium chloride, via a modified Sandmeyer/Meerwein protocol,[33] using $NaNO_2$ in concentrated HCl, followed by Cu-catalyzed addition of SO_2, which was generated *in situ* from the reaction of water with thionyl chloride, as previously described.[34] This optimized protocol provided the desired intermediate **22** in an excellent isolated yield (>85%) and purity (>90% without chromatography), minimizing any potential decomposition of either the diazonium intermediate or product **22** (due to the presence of excess water) and eliminated the inconvenience of using both acetic acid as the solvent and SO_2 gas. The final inhibitors **14** were obtained after coupling with various amines (alkyl/cycloalkyl/aryl/heteroaryl) under basic conditions, followed by deprotection of the bisphosphonate tetraesters using TMSBr and then MeOH.[35] The reversed sulfonamide analogues **15** were prepared by coupling intermediate **21** with the corresponding alkyl/aryl/heteroarylsulfonyl chloride under basic conditions. Urea analogues **16** were synthesized from various isocyanate precursors, which were first prepared from the reaction of anilines with triphosgene under basic conditions.[36] These isocyanate intermediates reacted with **21** to produce the bisphosphonate tetraesters of the urea analogues **16** in modest to good yields; a few representative examples are shown in Figure 5.

https://doi.org/10.1021/acs.jmedchem.1c01913
J. Med. Chem. XXXX, XXX, XXX−XXX

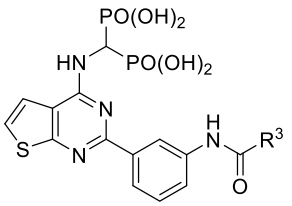

12a; R^3 = f1
12b; R^3 = f2
12c; R^3 = f3
12d; R^3 = f4
12e; R^3 = f5
12f; R^3 = f6
12g; R^3 = f7
12h; R^3 = f8
12i; R^3 = f9
12j; R^3 = f10
12k; R^3 = f11
12l; R^3 = f12
12m; R^3 = f13
12n; R^3 = f14
12o; R^3 = f15
12p; R^3 = f17
12q; R^3 = f18
12r; R^3 = f20
12s; R^3 = f22
12t; R^3 = f23
12u; R^3 = f24

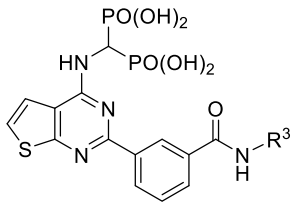

13a; R^3 = f1
13b; R^3 = f6
13c; R^3 = f8
13d; R^3 = f9
13e; R^3 = f10
13f; R^3 = f11
13g; R^3 = f12
13h; R^3 = f13

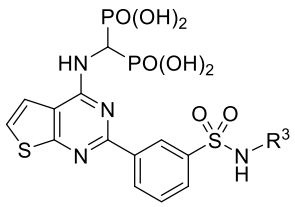

14a; R^3 = f8
14b; R^3 = f9
14c; R^3 = f10
14d; R^3 = f11
14e; R^3 = f12

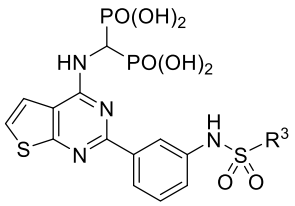

15a; R^3 = f8
15b; R^3 = f9
15c; R^3 = f10
15d; R^3 = f11
15e; R^3 = f12

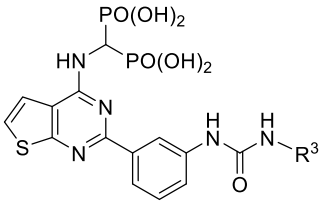

16a; R^3 = f8
16b; R^3 = f9
16c; R^3 = f10
16d; R^3 = f11
16e; R^3 = f12
16f; R^3 = f13
16g; R^3 = f15

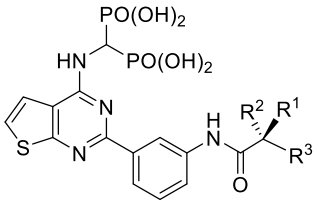

17a; $R^1 = R^2$ = H, R^3 = f1
17b; $R^1 = R^2$ = H, R^3 = f21
(S)-**17c**; R^1 = OMe, R^2 = H, R^3 = f1
(R)-**17c**; R^1 = H, R^2 = OMe, R^3 = f1
(S)-**17d**; R^1 = O*i*Pr, R^2 = H, R^3 = f1
(R)-**17d**; R^1 = H, R^2 = O*i*Pr, R^3 = f1
(S)-**17e**; R^1 = O*i*Pr, R^2 = H, R^3 = f8
(R)-**17e**; R^1 = H, R^2 = O*i*Pr, R^3 = f8
(R)-**17f**; R^1 = H, R^2 = Me, R^3 = f1
(R)-**17g**; R^1 = OMe, R^2 = CF_3, R^3 = f1

Figure 5. Examples of individual library members, analogues **12**−**17**.

Scheme 2. Synthesis of Chiral Mandelic Acid Derivatives 24, 25, and 28[a]

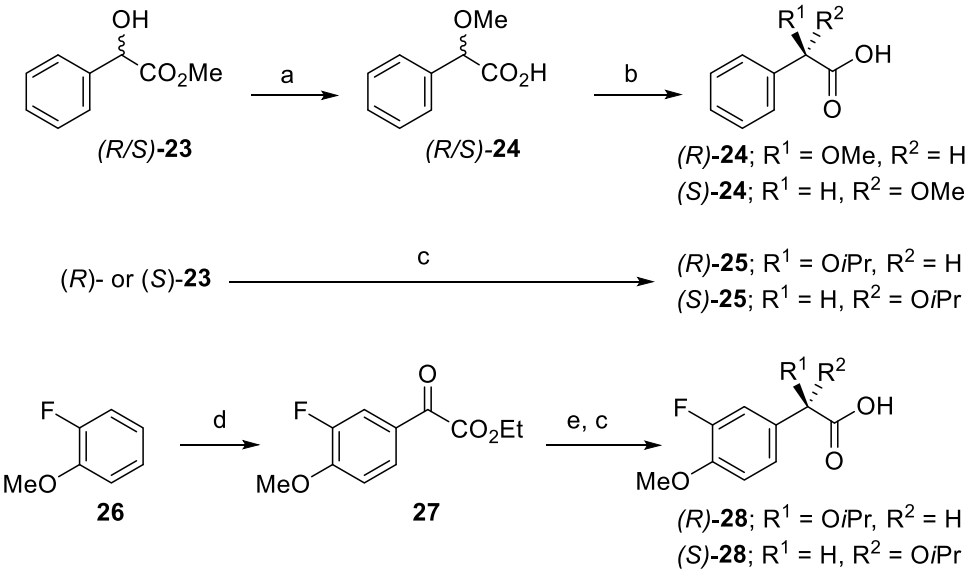

[a]Conditions: (a) NaH, MeI, THF, 0 °C; then H_2O, 62%; (b) (+)- or (-)-ephedrine, EtOH, or acetone, 25−30%; (c) *i*PrI, Ag_2O, 40 °C; then LiOH, MeOH/H_2O, RT, 48−59%; (d) ethyl oxalyl chloride, $AlCl_3$, DCM, RT, 92%; and (e) D- or L-tartaric acid, $NaBH_4$, THF, −20 °C, 18 h, 91% yield, 78% e.e.

https://doi.org/10.1021/acs.jmedchem.1c01913
J. Med. Chem. XXXX, XXX, XXX−XXX

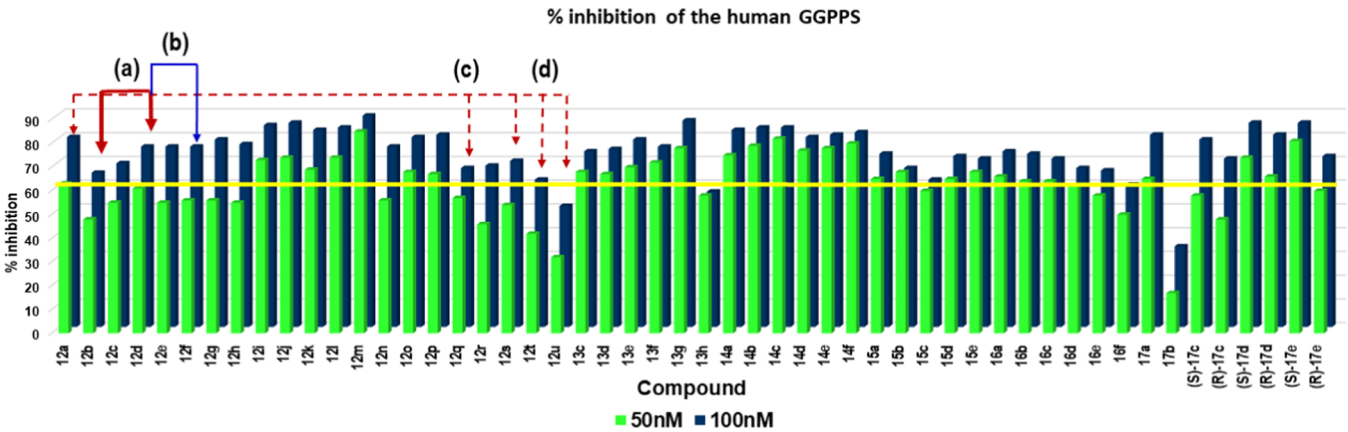

Figure 6. Examples of preliminary screening data of select library members at 50 and 100 nM (all assays were run in triplicate, and only values with standard deviation <10% are reported). Comparison of analogues **12** having different R^3 side chains: (a) *ortho vs meta vs para* tolyl moieties (*i.e.*, R^3 = f2, f3 or f4); (b) analogues of equivalent potency having a small substituent at the *para* position of a phenyl side chain (*i.e.*, R^3 = f4 *vs* f5 *vs* f6); (c) phenyl *vs* 2-pyridine *vs* cyclohexyl (*i.e.*, R^3 = f1, f18, f22); and (d) analogues with decreasing potency that seems to parallel the decreasing size of a lipophilic side chain (*i.e.*, R^3 = f22 *vs* f23 *vs* f24).

Finally, to explore the depth and volume of the enzyme pocket where the R^3 side chain is binding, we investigated derivatives of general structure **17** having an extended and branched linker (Figure 5). Synthesis of the (*R*)- and (*S*)-analogues **17c** and **17d** was achieved using the enantiomerically enriched building blocks **24** and **25**, respectively (Scheme 2). Racemic or enantioenriched (*R* or *S*) mandelate methyl ester **23** was alkylated at the Cα-hydroxyl moiety with an alkyl iodide under basic conditions or in the presence of Ag_2O, as previously reported (Scheme 2).[37] Chiral resolution of the carboxylic acids (*R*/*S*)-**24** was achieved by cocrystallization with either (1*R*,2*S*)-(−)- or (1*S*,2*R*)-(+)-ephedrine,[38] and their absolute stereochemistry and enantiomeric excess (% ee) were assigned by comparison of their optical rotations to those previously reported[39] and further confirmed by ^{1}H NMR of their corresponding diastereomeric menthol esters. Similarly, the enantiomeric excess of intermediates (*R*)- or (*S*)-**25** was confirmed by ^{1}H NMR of their corresponding diastereomeric menthol esters (Figure S1).

Inhibitors (*R*)- and (*S*)-**17e** were prepared starting from commercially available 2-fluoroanisole (**26**), which was treated with ethyl oxalyl chloride in the presence of $AlCl_3$ to give the α-keto ester intermediate **27** (Scheme 2).[40] Asymmetric reduction of the activated Cα carbonyl to either the *R*- or *S*-α-hydroxyl ethyl ester (in ∼78% ee; as confirmed by the chiral high-performance liquid chromatography (HPLC); Figure S6) was achieved using $NaBH_4$ in the presence of either L-(+)-tartaric acid or D-(-)-tartaric acid, respectively, as previously reported with minor modifications.[41] Alkylation of the hydroxyl moiety was subsequently achieved as previously described for building blocks **25**, the esters were saponified under basic conditions, and the carboxylic acids **28** and these compounds were crystallized as their sodium salts to obtain the (*R*)- and (*S*)-**28** in ≥97% ee, as confirmed by ^{1}H NMR of their corresponding diastereomeric menthol esters (Figure S2). Some analogues with general structure **17** were synthesized from commercially available building blocks; for example, analogues (*R*)-**17f** and (*R*)-**17g** were prepared from (*R*)-2-phenylpropanoic acid and (*R*)-3,3,3-trifluoro-2-methoxy-2-phenylpropanoic acid, respectively. The carboxylic acid building blocks were finally coupled to the aniline intermediate **21** using standard peptide coupling conditions.

Biological Activity of hGGPPS Inhibitors. To maximize our efficiency toward the identification of hGGPPS inhibitor(s) having all of the biopharmaceutical properties required for clinical development, approximately 150 new C2-ThP-BP derivatives were synthesized in a modular parallel mode and initially prescreened *in vitro* at two fixed concentrations of 50 and 100 nM using an optimized hGGPPS inhibition assay; an example of this prescreening evaluation is shown in Figure 6. For clarification, since our last report,[29] we modified our *in vitro* hGGPPS inhibition assay protocol to method 4 (M4) by slightly decreasing the concentration of the enzyme (from 20 to 12.5 nM) for higher sensitivity (in terms of the lowest measurable IC_{50}) and also adjusted the concentrations of the substrates (from 10 and 8.3 μM to 5 and 4.5 μM for FPP and IPP, respectively) to more closely align them with the reported K_m values.[42] Concentrations at (or near) the K_m values of the substrates are expected to provide the most reliable IC_{50} values when the inhibition modality is unknown,[43] whereas high substrate concentrations can increase the apparent IC_{50} of competitive inhibitors (thus making them appear less potent).[44] The assumption that our compounds are competitive inhibitors of hGGPPS is based on the fact that they are bisphosphonates, which typically bind to the allylic subpocket of the enzyme's active site, mimicking the FPP substrate. Consistent with this assumption, we also previously demonstrated that members of this class of inhibitors (*e.g.*, inhibitor **12o**) bind to the enzyme only in the presence of Mg^{2+} ions, which are essential for binding to the allylic subpocket of the active site.[29] Based on this assumption, it is not surprising that the IC_{50} of CML-07-119 (**13c**) was estimated to be 86 nM at high concentrations of substrates (M2 assay; FPP and IPP concentrations of 10 and 8.3 μM, respectively),[29] whereas, in our optimized M4 assay, the IC_{50} was determined to be 27 ± 2 nM (Table 1). Nonetheless, since hGGPPS also contains a large GGPP binding channel (presumed to participate in product feedback inhibition),[42] we cannot totally exclude the possibility that some members of our library could be binding in this channel and inhibiting the enzyme in a noncompetitive mechanism. It is noteworthy that several reported inhibition assays for hGGPPS contained varying amounts of enzymes and substrates, making direct comparison of reported IC_{50} values difficult; examples include

https://doi.org/10.1021/acs.jmedchem.1c01913
J. Med. Chem. XXXX, XXX, XXX−XXX

Table 1. Enzyme Inhibition (IC_{50}) and MTS Assay (EC_{50}) of Representative Analogues[d]

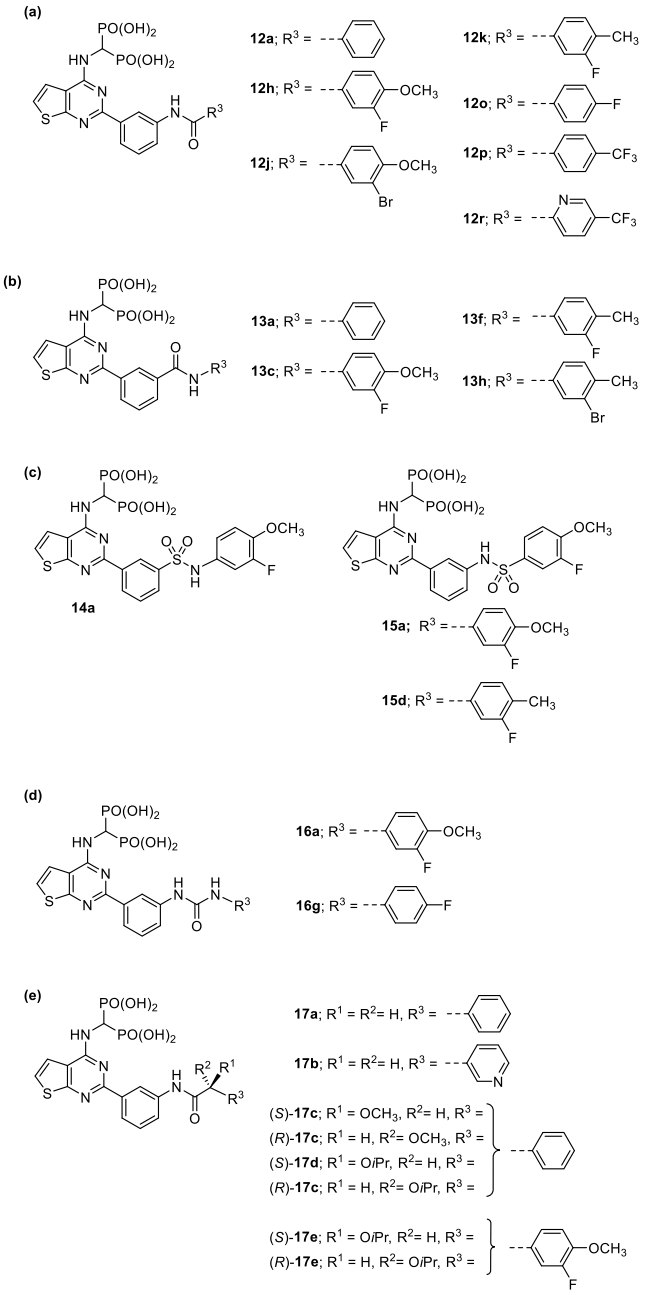

compound	hFPPS[a] IC_{50} (μM)	hGGPPS-M4 IC_{50} (nM)	RPMI-8226[b] EC_{50} (nM)
2	0.004		~11 000
DOX			130 ± 20[c]
18b	0.55	37	>10 000
12a	40%	19	>500
12h	60%	29	460
12j	40%	36	>500
12k	35%	21	290
12o	30%	25	700
12p	40%	18	710
12r	60%	52	21 300
13a	3.0	41	460
13c	1.3	27±2	90 ± 13[c]
13f	28%	31	130
13h	12%	15	161
14a	25%	23	5000
15a	40%	24	4700
15d	30%	23	7800
16a	nd	34	1300
16g	90%	41	4100
17a	55%	23	740
17b	60%	71	1200
(*S*)-**17c**	55%	38	390
(*R*)-**17c**	48%	39	920
(*S*)-**17d**	35%	21	135
(*R*)-**17d**	nd	23	910
(*S*)-**17e**	0.46	17	880
(*R*)-**17e**	0.73	20	>5000

[a]Compounds were initially screened at a single concentration of 1 μM ($n \geq 3$) with 10 min preincubation of the enzyme with each inhibitor, and the % inhibition observed at 1 μM is shown. The full dose–response inhibition curve (IC_{50}) was only carried out for select key compounds. IC_{50} values for both the hFPPS and hGGPPS inhibition assays were determined with 10 min preincubation of the enzyme with each inhibitor; the values shown are the average of $n \geq 3$ determinations with a standard deviation of ≤10%. [b]EC_{50} values were determined using an MTS assay after 72 h of incubation of the cells with or without an inhibitor; the values shown are the average of $n \geq 4$ determinations with a standard deviation of ≤10%; doxorubicin (DOX) was used as the positive control. [c]Reported values are the averages of 16 different assay determinations for inhibitor **13c** and 5 different assay determinations for doxorubicin (DOX) when tested in parallel with **13c**; all assays were run in quadruplicate. [d]nd, not determined.

assays run with 25 μM FPP, 21 μM IPP, and 100 nM hGGPPS,[45] or 10 μM FPP, 10 μM IPP, and 20 nM hGGPPS.[28]

In this report, method 4 (M4) of our *in vitro* hGGPPS inhibition assay was used to evaluate all members of our library. The basic ThP-BP scaffold **18a** (Figure 3) is totally inactive at 100 nM (IC_{50} > 1 μM), whereas the C-2 phenyl derivative **18b** was found to exhibit low nanomolar *in vitro* potency (Figure 3 and Table 1). However, compound **18b** has a relatively narrow window of selectivity in inhibiting hGGPPS *vs* hFPPS (~15-fold) and is completely inactive in blocking the proliferation of RPMI-8226 MM cells at the highest concentration tested of 10 μM. Therefore, our strategy focused on expanding the structural diversity of this series of inhibitors by first evaluating a focused library of analogues with structural variations on the linker moiety (*i.e.*, **X**) and the R^3 side chain of this chemotype (Figure 3).

The prescreening evaluation revealed very small differences in potency between analogues of all subseries **12**−**17** when having the same R^3 side chain (Figure 6), although some general trends were noted. For example, small substituents at the *ortho*, *meta*, and *para* positions of an R^3 phenyl moiety were well tolerated, with only marginal improvement in potency from the *ortho* to the *para* substitution (*e.g.*, **12b**/**c**/**d**; Figure 6a). Analogues with small substituents at the *para* position, such as methyl, ethyl, or methoxy, were all equivalent in potency (*e.g.*, **12d**/**e**/**f**; Figure 6b). Replacement of the phenyl ring with heteroaryl or cycloalkyl moieties of equivalent size (*e.g.*, **12a** *vs* **12q** *vs* **12s**; Figure 6c) did not have a significant effect, whereas replacement or R^3 with a smaller alkyl group led to a progressive decrease in potency that paralleled the decreasing size of this substituent (*e.g.*, **12s** *vs* **12t** *vs* **12u**; Figure 6d). Similar observations were

https://doi.org/10.1021/acs.jmedchem.1c01913
J. Med. Chem. XXXX, XXX, XXX−XXX

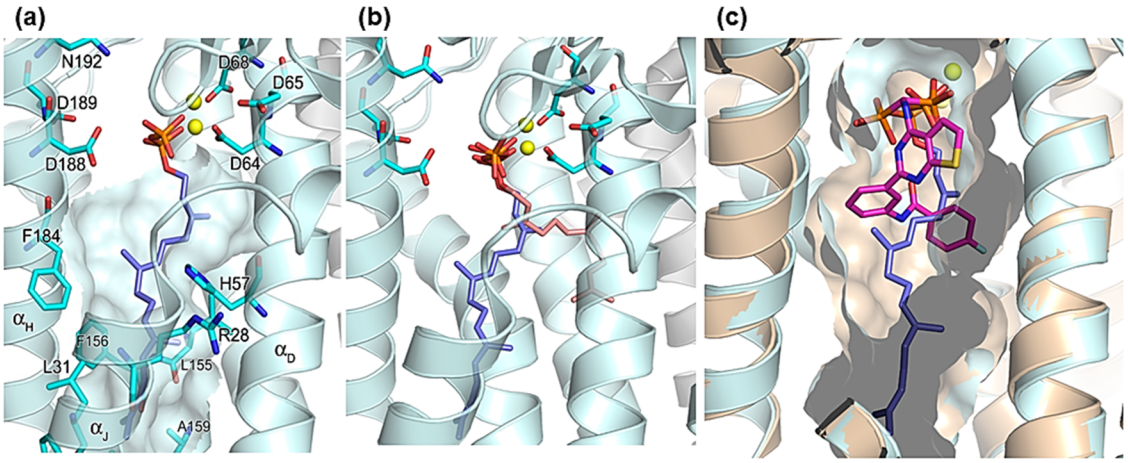

Figure 7. Structures of wild-type human (PDB: 2Q80), yeast GGPPS (PDB: 2E93), and mutant human GGPPS (PDB: 6C57). The sequence identity and similarity between the human and yeast GGPPS homologues are 44 and 61%, respectively. (a) Structure of the recombinant hGGPPS with the GGPP catalytic product from *E. coli* (PDB code: 2Q80). (b) Superposition of the human GGPPS−GGPP complex (2Q80) with the *S. cerevisiae* GGPPS−FPP complex (PDB code: 2E93) showing the bisphosphonate of GGPP bound to the allylic subpocket and its lipophilic tail extending into the product inhibition channel. (c) Superposition of the hGGPPS−GGPP complex (2Q80) with the Y246D hGGPPS mutant−**12o** complex (PDB code: 6C57). The protein structures of the wild-type hGGPPS and the Y246D hGGPPS mutants are highlighted in cyan and wheat colors, respectively. GGPP and FPP are highlighted in dark purple and red, respectively. Inhibitor **12o** is colored by atom, with the carbon skeleton highlighted in dark pink color and the Mg^{2+} ions highlighted as yellow spheres.

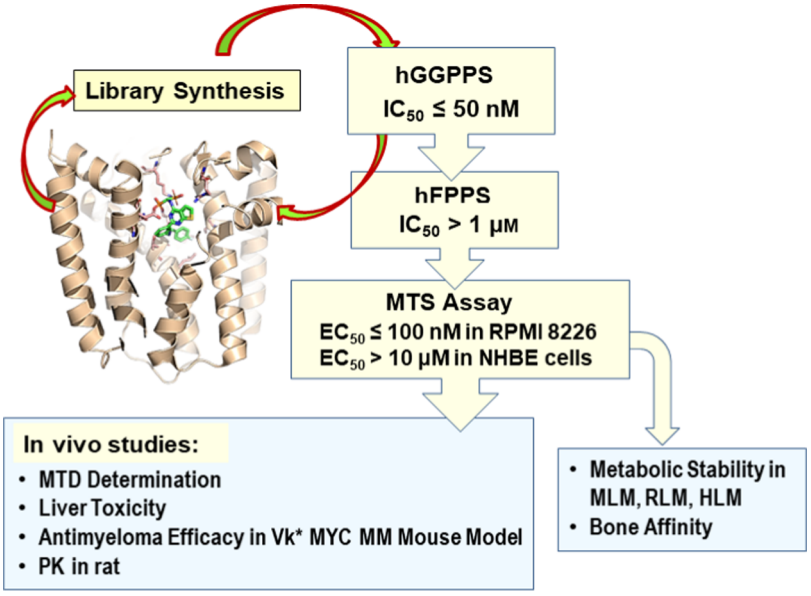

Figure 8. Screening progression and biological profiling of compounds.

made for the reversed amide analogues **13**, the sulfonamide derivatives **14** and **15**, and the urea analogues **16**.

In addition to analogues **12**−**16**, we also wanted to explore branched analogues of general structure **17** (Figures 3 and 5). Potent and selective inhibitors of hGGPPS have been previously reported to have a V-shaped molecular architecture;[27,46] examples include the isoprenoid derivative **10** (Figure 3). Crystallographic evidence has revealed that inhibitor **10** binds to the *Saccharomyces cerevisiae* GGPPS by simultaneously occupying both the FPP substrate subpocket of the enzyme's active site and the GGPP "product inhibition" channel (PDB code: 2z4w).[47] However, in the hGGPPS−GGPP cocrystal structure (PDB code: 2Q80),[42] the pyrophosphate moiety of GGPP is still bound to the DDXX(D/N) motifs of the allylic subpocket and only its hydrocarbon tail was found to extend into the mostly lipophilic product inhibition channel, which is located near the active site (Figure 7a,b). Additionally, multiple binding modes have been reported for several nonbranched, larger lipophilic bisphosphonate inhibitors bound to *S. cerevisiae* GGPPS (*e.g.*, PDB code: 2E93),[45b,47] which further supports the hypothesis that branched molecules may provide an advantage in terms of binding affinity for various GGPPSs.[48]

At the present time, the lack of high-resolution cocrystal structures of hGGPPS with potent and selective inhibitors bound to its active site hinders the rational structure-based design of potential human therapeutics targeting hGGPPS. Unfortunately, crystallization of the wild-type human GGPPS has proven to be very challenging. We previously presumed that a more readily crystallizable dimer of this enzyme, such as the Y246D hGGPPS mutant (PDB code: 6C56),[29] could overcome

https://doi.org/10.1021/acs.jmedchem.1c01913
J. Med. Chem. XXXX, XXX, XXX−XXX

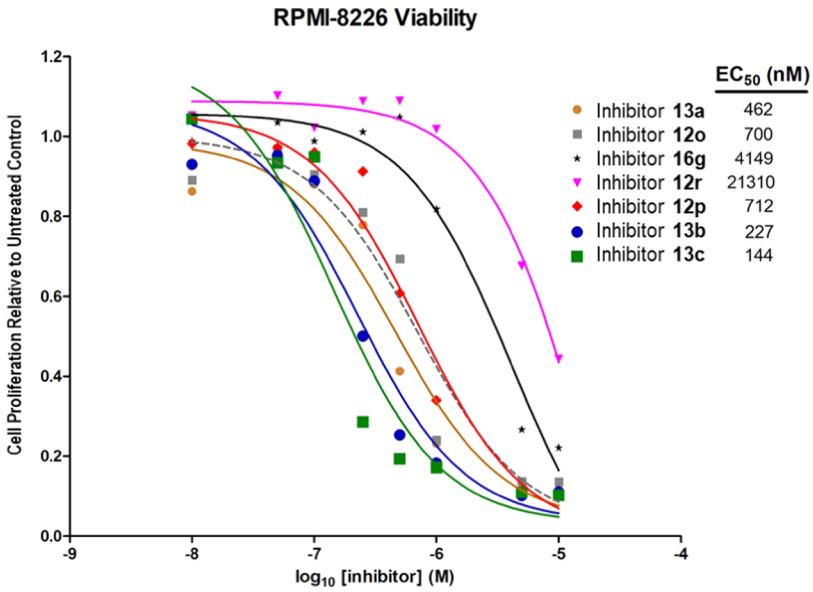

Figure 9. Examples of structurally diverse analogues within subseries **12**−**16** when tested in parallel in the MTS antiproliferation assay using MM RPMI-8226 cells.

this challenge. We were disappointed to see that a cocrystal structure of inhibitor **12o** bound to the active site of this mutant (PDB code: 6C57) could only be solved at a 3.5 Å resolution.[29] In this complex, the bisphosphonate of **12o** was clearly visible within the active site cavity and between the aspartate-rich motifs. Additionally, the fluorophenyl R^3 side chain appeared to be bound toward the FPP substrate binding site, whereas the thienopyrimidine scaffold occupied part of the IPP subpocket (although with less clarity due to weak electron density for these parts of the molecule). Superposition of the Y246D hGGPPS/**12o** complex with the original hGGPPS−GGPP structure (Figure 7c) suggested that the branching of our compounds at the linker moiety may lead to a novel subtype of thienopyrimidine-based inhibitors that could simultaneously bind to both the FPP binding subpocket and the GGPP product inhibition channel of hGGPPS (Figure 7c). Motivated by the available X-ray data and the binding mode of inhibitor **10** to the *S. cerevisiae* GGPPS, we synthesized a small number of compounds with general structure **17** to test our hypothesis (Figure 5). Interestingly, the extension of the amide linker of analogue **12a** (where R^3 = f1; Figure 4) by a methylene moiety (*i.e.*, analogue **17a**) did not affect the intrinsic potency of the new compounds (Figure 6 and Table 1). However, substitution of the R^3 phenyl with a pyridine gave analogue **17b**, which was found to be 3-fold less potent (**17a** *vs* **17b**; Figure 6 and Table 1). A similar 3- to 4-fold decrease in potency was also observed with analogues of subseries **12** when the R^3 phenyl-based group was replaced by a pyridine-based moiety, such as f18, f20, or f21 (*e.g.*, **12a** *vs* **12q** and **12r**; Figure 6). These observations may suggest that a pyridinium cation (which is likely to form under physiological conditions) is unfavorable in the binding interaction of the R^3 substituent with the enzyme. Alternatively, we cannot exclude the possibility that such zwitterionic compounds may suffer from aggregation effects in the assay buffer that disrupt their interactions with the enzyme. In contrast, small substituents at the R^1 and/or R^2 positions of **17**, such as a methoxy or an isopropoxy moiety (*e.g.*, *R*- or *S*-**17c**-**e**), were well tolerated, leading to inhibitors with IC_{50} values in the ∼20−40 nM range for both the *R*- and the *S*-enantiomers (Table 1).

Given the large number of compounds that required biological evaluation, a compound progression tree was also established (Figure 8) and used in conjunction with the prescreening data shown in Figure 6. Compounds exhibiting greater than 60% inhibition of hGGPPS at a concentration of 50 nM (Figure 6) were subsequently tested in a full dose−response assay to determine their IC_{50} values; some key examples within each subseries are shown in Table 1. An arbitrary threshold of *in vitro* potency (IC_{50}) below 50 nM was subsequently set for any compound that progressed through the profiling scheme shown in Figure 8. We also prioritized compounds with the best selectivity window between inhibiting hGGPPS *vs* hFPPS. Mindful of the more extensive biochemical consequences that the inhibition of hFPPS would have (both upstream and downstream; Figure 1) as compared to that of hGGPPS, it is reasonable to assume that a therapeutic agent that exhibits low selectivity in inhibiting hGGPPS *vs* hFPPS is more likely to also induce undesirable side effects. It should be mentioned that although our screening strategy does not provide a detailed structure−activity relationship (SAR) model (based on IC_{50} values), we believe that this is not an absolute requirement for lead optimization nor for the selection of a potential clinical candidate. In fact, given the numerous factors that influence the cell-based potency of compounds (*e.g.*, cell permeability, protein binding, binding to efflux pumps, metabolic stability, and the extent of intracellular target engagement), more often than not, comparison of the cell-based potency of compounds with their *in vitro* activity (IC_{50}) reveals poor correlation. In recent years, many pharmaceutical companies have relied on phenotypic assays for SAR and lead optimization, allowing the simultaneous optimization of potency and other druglike properties. Interestingly, recent FDA statistics revealed that over a 10 year period, 58 out of 75 new first-in-class drugs were discovered without relying on an *in vitro* activity-based SAR model.[49]

Following the investigations described above, several analogues were identified from all six subseries of compounds (**12**−**17**) with equivalent nanomolar potency in inhibiting

https://doi.org/10.1021/acs.jmedchem.1c01913
J. Med. Chem. XXXX, XXX, XXX−XXX

hGGPPS when having the same R^3 side chain, indicating that the linker did not affect the intrinsic potency of these compounds. For example, the IC_{50} values of analogues **12h**, **13c**, **14a**, **15a**, and **16a** (all having R^3 = f8) were found to be in the 20−35 nM range (Table 1). However, significant differences were observed when these compounds were tested in our antiproliferation assay (MTS) using MM cell lines, such as RPMI-8226. It is noteworthy that many compounds were once again prescreened in our MTS assay, using RPMI-8226 cells, at fixed concentrations of 100 nM, 500 nM, 1 μM, and 10 μM, and many of those that did not exhibit significant antiproliferation activity were not investigated any further. In all cases that we examined, the reversed amide analogues **13** were found to be consistently 2- to 4-fold more potent in blocking MM cell proliferation (EC_{50}) than the corresponding amides **12**. For example, analogues **12h** and **13c** (R^3 = f8) exhibited EC_{50} values of 460 and 90 nM, respectively. Similarly, analogues **12k** and **13f** (R^3 = f11) exhibited EC_{50} values of 290 and 130 nM, respectively. In contrast, the sulfonamide (**14**, **15**) and urea (**16**) analogues exhibited significantly lower cell-based potency in our antiproliferation assays. For example, the EC_{50} values of the amide inhibitor **12o** and its corresponding urea analogue **16g** (R^3 = f15) were determined to be 0.7 and 4.15 μM, respectively. The EC_{50} values of the reversed amide inhibitor **13c** and its urea analogue **16a** (R^3 = f8) were found to be 90 and 130 nM, respectively, whereas those of reversed amide **13f** and its corresponding sulfonamide **15d** (R^3 = f11) were 130 and ∼8 μM, respectively. In fact, all sulfonamide and urea analogues tested were found to have very poor potency in our cell-based assays. Analogues with a pyridine or substituted pyridine at the R^3 moiety were also substantially less potent than the corresponding phenyl analogues in blocking cell proliferation. For example, the EC_{50} values of the *para*-trifluoromethyl phenyl derivative **12p** (R^3 = f17) and its corresponding pyridyl derivative **12r** (R^3 = f20) were determined to be 0.7 and ∼21 μM, respectively (Table 1). For a direct comparison, representative examples from subseries **12**−**16** were tested in parallel and in the same assay (Figure 9).

Finally, preliminary evaluation of a few analogues **17** revealed very minor differences in intrinsic potency between the *R*- and the *S*-enantiomers, possibly suggesting a divergent SAR due to multiple (chirality-driven) binding modes for this series of compounds.[20c] However, within each pair of enantiomers, the (*S*)-enantiomer was found to be more potent in the MTS assay using RPMI-8226 cells than the (*R*)-enantiomers. For example, the EC_{50} value of the isopropyl ether derivative (*S*)-**17d** was found to be 135 nM, whereas that of the (*R*)-**17d** was 910 nM. Similarly, the EC_{50} value of analogue (*S*)-**17e** was found to be 0.88 μM, whereas (*R*)-**17e** exhibited only slight activity at the highest concentration tested of 10 μM. Inhibitors such as (*S*)-**17d** may represent a new "hit" of divergent SAR and be worthy of further investigation in the near future.

Estimation of the Relative Bone Affinity of C2-ThP-BP Inhibitors. Due to their biophysical properties, the current clinically validated N-BP compounds (*e.g.*, **1** and **2**) exhibit extremely low distribution in noncalcified tissues and most of the administered dose (that does not bind to the bone) is eliminated rapidly through the kidneys. The strength of their bone affinity has been largely attributed to the Cα-hydroxy bisphosphonate moiety, which allows the formation of a tridentate interaction with Ca^{2+} ions and the bone mineral hydroxyapatite (HAP).[17,51] Consistent with this assumption, the removal of the Cα-hydroxy group has been shown to decrease both the affinity of these compounds for bone and their potency in inhibiting the hFPPS enzyme.[17b] It is noteworthy that the inhibition of hFPPS in osteoclasts has been proposed as the primary mechanism by which this class of drugs decreases bone desorption.[50] However, biochemical studies have also proposed that the beneficial effect of N-BPs on bone resorption may be mainly indirect and the result of intracellular depletion of FPP, which leads to hGGPPS inhibition.[51] Given the intimate relationship between the human multiple myeloma (MM) cancer and lytic bone disease, it is reasonable to assume that a drug, which exhibits a good balance between bone affinity and direct antimyeloma toxicity, may provide an ideal set of biopharmaceutical properties for the treatment of MM. Consequently, in addition to evaluating the potency of our compounds in blocking MM cell proliferation, we routinely also evaluate the bone affinity of these compounds in comparison to the current N-BP drugs, such as ZOL (**1**) and RIS (**2**). The relative bone affinity of many drugs has been previously estimated using a simple ^{1}H NMR titration study in the presence of HAP and is shown to correlate well with the *in vivo* affinity of these compounds for the bone.[52] Although the N-BP drugs **1** and **2** exhibit higher affinity for the bone than the nonbisphosphonate allosteric inhibitors of hFPPS, compounds **4a**−**c** (Figure 2) also bind to the bone, demonstrating that a bisphosphonate moiety is not an absolute requirement for bone affinity.[53] Furthermore, even though **4a**−**c** are structurally very similar, analogue **4a** was reported to have a very weak bone affinity as compared to analogues **4b** and **4c** (the latter compounds exhibiting significant bone affinity).[53]

We were pleased to discover that in spite of having systemic exposure and *bona fide* antimyeloma activity *in vivo*,[29] inhibitor CML-07-119 (**13c**) exhibited equivalent affinity for HAP to ZOL (**1**) and slightly higher affinity than RIS (**2**).[29] In the present study, we employed the same ^{1}H NMR method to estimate the bone affinity of inhibitors from all subtypes **12**−**17** and having the same R^3 side chain (*e.g.*, R^3 = f8). We compared these molecules to RIS (**2**) and found that the relative affinity of our compounds was approximately 2.4-fold higher for urea **16a** (Figure S5), 1.9−2.1-fold higher for the amide/reversed amides **12h** and **13c** (Figure S3), 1.4-fold higher for sulfonamides **14a** and **15a** (Figure S4), and 1.2-fold higher for analogues (*S*)- and (*R*)-**17e** (Figure S5).

Preliminary Assessment of *In Vivo* Liver Toxicity and Toxicity to Healthy Bone Marrow Cells. A major challenge in the identification of a new therapeutic agent is the ability to reliably select a candidate compound that has a low probability of inducing liver injury, at the projected therapeutic doses.[54] As the "refinery" of the human body, drug-induced liver toxicity remains one of the most frequent causes of drug candidate failure during both preclinical and clinical development. In a recent report focusing on the preclinical properties of the hGGPPS inhibitors **11**,[55] liver toxicity was observed in mice after a single IV dose of 0.5 and 1.0 mg/kg that peaked at approximately 6−7 days post dosing, setting the maximum tolerated dose (MTD) for this compound at <1 mg/kg.[55] However, it was suggested that the hepatotoxicity was likely mechanism-based (*i.e.*, associated with the biological target) and proportional to the potency of the hGGPPS inhibitors. Such a possibility raises considerable concerns regarding the value of hGGPPS as a therapeutic target, and consequently, we anxiously examined the ability of CML-07-119 (**13c**) to induce liver injury at a range of concentrations in mice.

https://doi.org/10.1021/acs.jmedchem.1c01913
J. Med. Chem. XXXX, XXX, XXX−XXX

Table 2. Evaluation of Potential Liver Toxicity of CML-07-119 (13c) in Mice

I.V. Dose	MAV[a]	Vehicle			0.5 mg/kg			1.0 mg/kg			5.0 mg/kg			10.0 mg/kg		
Mouse ID		1742	1843	1844	1740	1847	1848	1744	1849	1850	1971	1968	1978	1974	1965	1975
Bil	2-15	8	7	14	14	6	11	7	4	4	8.7	7.7	10.3	4.1	7.0	9.7
ALT	28-132	72	50	78	64	55	171	54	45	46	43	29	103	30	43	109
AST	59-247	188	95	154	387[β]	69	241	105	67	92	204	98	327[β]	71	122	177
AP	62-209	133	87	63	83	86	87	135	99	94	74	60	123	82	107	108
GGT	-	<10	<10	<10	<10	<10	<10	<10	<10	<10	<10	<10	<10	<10	<10	<10
AM	1691-3615	1494	1879	1358	1734	1666	2074	1706	2078	1708	3187	1610	2159	2600	2058	2048

[a]Mouse average values (MAVs). [b]Serum samples were slightly hemolyzed, and since red cells have AST (but not ALT), it is likely that the slightly higher than normal levels of AST are due to the hemolysis and not liver toxicity.

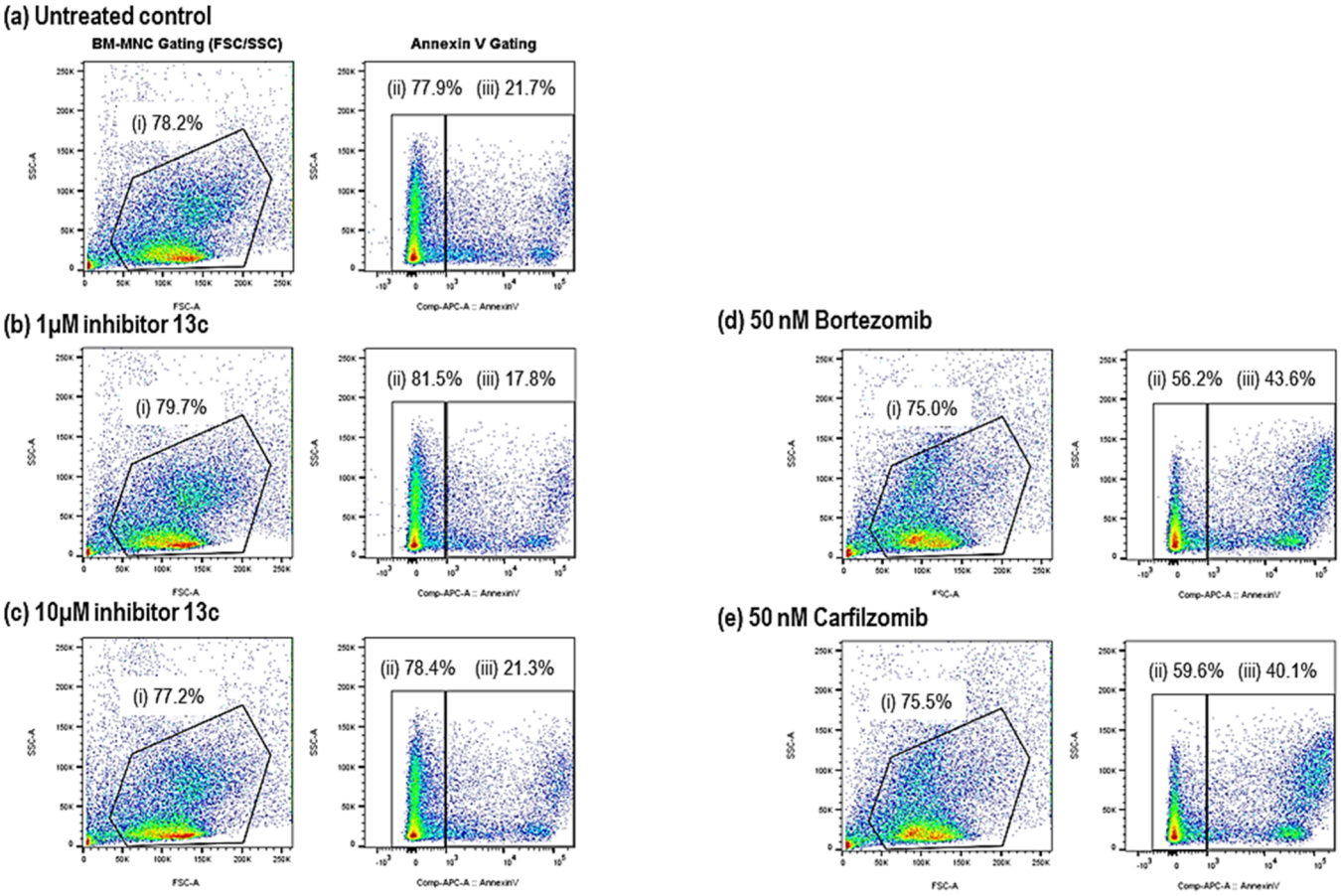

Figure 10. Evaluation of toxicity to healthy bone marrow mononuclear cells (BM-MNCs) *ex vivo* with hGGPPS inhibitor **13c** and clinically relevant proteasome inhibitors. Viability by flow cytometry is shown by Annexin V staining with (i) the total % amount of BM-MNCs in a sample; (ii) % of viable BM-MNCs post 72 h treatment with or without an inhibitor; and (iii) apoptotic BM-MNCs post 72 h treatment with or without the hGGPPS inhibitor **13c** or a proteasome inhibiting drug, as indicated.

A total of 21 mice (C57/bl/6; 7 female and 14 male) were bred and maintained in a pathogen-free standard animal facility with a light/dark cycle of 12 h and were provided with food and water *ad libitum*. The animals were divided into seven groups of three animals/group (one female and two male) and treated by IV dosing (tail vein injection) with a single dose of 0.1, 0.5, 1.0, 2.0, 5.0, and 10.0 mg/kg of inhibitor **13c** dissolved in PBS or with just vehicle (PBS) as the reference control (Table 2). The mice were observed daily for any signs of overt toxicity, such as significant weight loss, decreased mobility, skin lesions, inflammation at the site of injection, or morbidity, according to the Facility Animal Care Committees protocol number 2012−7242 from the Research Institute of McGill University Health Center (RI MUHC; Glen site) and in accordance with

https://doi.org/10.1021/acs.jmedchem.1c01913
J. Med. Chem. XXXX, XXX, XXX−XXX

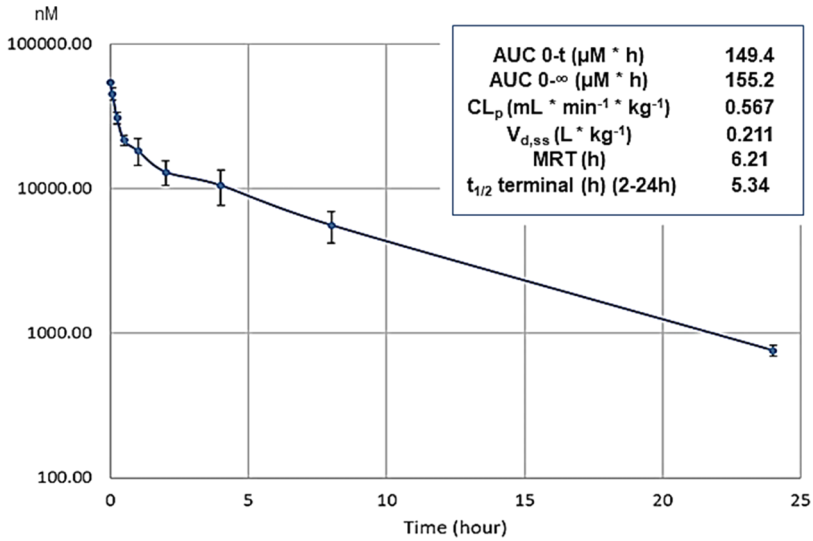

Figure 11. Measurements of CML-07-119 (**13c**) in rat plasma after IV injection at 3 mg/kg and determination of key pharmacokinetic parameters.

the Policies and Guidelines of the Canadian Council on Animal Care (CCAC). Seven days post dosing, none of the animals exhibited any obvious signs of toxicity, at which point, the study was terminated. Serum (from SST-clotted whole blood) was collected from all 21 animals and analyzed at the McGill University, Comparative Medicine Diagnostic Laboratory for select biomarkers indicative of liver toxicity (data shown in Table 2). Normal levels of bilirubin (Bil), alanine aminotransferase (ALT), aspartate aminotransferase (AST), alkaline phosphatase (AP), γ-glutamyl transferase (GGT), and amylase (AM) were observed, which were consistent with the known mouse average values (MAVs) of healthy animals. Therefore, the MTD dose for compound **13c** was determined to be higher than 10 mg/kg and no liver toxicity was observed up to 10 mg/kg, at least in mice.

Additionally, we evaluated the toxicity of compound **13c** on healthy bone marrow cells isolated from bone marrow aspirates of MM patients (following informed consent as per McGill University Health Center (MUHC) Ethics Board; ERB number 11−139-BMA). Treatment of *ex vivo* healthy bone marrow mononuclear cells (BM-MNC) with 1 and 10 μM of the hGGPPS inhibitor **13c** for 72 h showed similar levels of apoptosis to that of untreated controls and much lower levels of toxicity to BM-MNCs treated with the clinically validated proteasome inhibitors bortezomib or carfilzomib at a concentration of 50 nM (Figure 10). These findings indicate that inhibitor **13c** does not exert any significant toxicity on normal human BM-MNCs.

Given the above encouraging results, we proceeded to explore the pharmacokinetic properties of this compound in rat since rat PK is more reliable as a bridge to human PK than mouse PK. Male CD rats (n = 3) were purchased from Charles River and allowed a 5 day acclimatization period in the animal facility. The animals were dosed IV with 3 mg/kg (n = 3), and blood samples were collected in K3EDTA tubes at 5, 15, 30 min, 1, 2, 4, 8, and 24 h post dosing, to ensure an adequate description of the distribution and elimination phase of the compound (Figure 11). All samples were analyzed by LC/MS-MS with a predetermined limit of quantification (LOQ) at 38 nM (*i.e.*, 21 ng/mL). The pharmacokinetic parameters determined (Figure 11) indicated a mean residence time (MRT) of 6.21 h, an apparent volume of distribution at steady-state ($V_{d_{ss}}$) of 0.211 L/kg, a plasma clearance (CL_p) of 0.567 mL/(min kg), and a terminal half-life ($t_{1/2}$; 2−24 h) of 5.34 h.

■ CONCLUSIONS

Multiple myeloma (MM) is a mature B-cell neoplasm, characterized by the clonal expansion of malignant plasma cells in the bone marrow that secrete monoclonal immunoglobulins (M-proteins), giving rise to a constellation of target organ damage, including severe lytic bone disease. Inhibition of the human geranylgeranyl pyrophosphate synthase (hGGPPS) has been previously proposed as a potentially valuable mechanism for the treatment of MM; however, clinically validated inhibitors of hGGPPS are yet to be identified. We recently reported a new chemotype of C-2-substituted thienopyrimidine bisphosphonates (C2-ThP-BPs) that inhibit hGGPPS. We identified one compound within this series, CML-07-119 (**13c**), which exhibits EC_{50} of 90 ± 13 nM in blocking the proliferation of RPMI-8226 cells and 120−500 nM in antiproliferation MTS assays using other genetic variants of MM such as OPM1 (126 nM), KMS28PE (168 nM), KMS11 (205 nM), and JJN3 (507 nm) cells. Additionally, this compound has *bona fide* antimyeloma activity *in vivo* and binds to the bone mineral hydroxyapatite with equivalent affinity to the N-BP drug zoledronic acid (**1**)[29] and an ∼2-fold higher affinity than risedronic acid (**2**). In this study, we provide an in-depth discussion on the structural elements that modulate the MM antiproliferation activity within this class of compounds and additional preclinical profiling in the mouse and rat of CML-07-119 (**13c**). Given the unique disease biology of MM and its strong association with structural damage to bones, fractures, and spinal cord compression,[56] our efforts are directed toward the design of a human therapeutic agent with a novel mechanism of action and dual efficacy as a potent and direct antimyeloma agent and as osteoclast inhibitors. The preclinical data observed on CML-07-119 (**13c**) do not support a mechanism-based liver toxicity that is directly associated with the inhibition of hGGPPS. Furthermore, the combination of antimyeloma activity, metabolic stability, bone affinity, and pharmacokinetics observed with the current best C2-ThP-BP inhibitor (**13c**) is very encouraging in supporting our optimization efforts of this class of compounds as potential human therapeutics for multiple myeloma.

https://doi.org/10.1021/acs.jmedchem.1c01913
J. Med. Chem. XXXX, XXX, XXX−XXX

■ EXPERIMENTAL SECTION

General Chemistry. Chemicals and solvents were purchased from commercial suppliers and used without further purification. Normal phase column chromatography on silica gel was performed using a CombiFlash instrument, and the solvent gradients were indicated. The homogeneity of final inhibitors was confirmed to be ≥95% by C18 reversed-phase HPLC using a Waters ALLIANCE instrument (e2695 with 2489 UV detector, 3100 mass spectrometer, C18 5 μm column); solvent A: H_2O, 0.1% formic acid; solvent B: CH_3CN, 0.1% formic acid; mobile phase: linear gradient from 95% A and 5% B to 0% A and 100% B in 13 min. Inhibitors **16a−f** exhibited poor solubility in the H_2O:formic acid mobile phase (*i.e.*, extensive broadening of the peak was observed) and a different solvent system containing NH_4OAc had to be used: solvent A: H_2O, 0.2% NH_4OAc; solvent B: CH_3CN; mobile phase: linear gradient from 90% A and 10% B to 0% A and 100% B in 15 min.

All final compounds were fully characterized by ^1H, ^{13}C, ^{31}P NMR, and HRMS. Chemical shifts (δ) are reported in ppm relative to the internal deuterated solvent. The NMR spectra of all final bisphosphonate inhibitors were acquired in D_2O (either after conversion to their corresponding trisodium salt or by the addition of ∼2% ND_4OD or 0.5% NH_4OH) or in DMSO-d_6. In some cases, the Cα to the bisphosphonate moiety was very broad or overlapped with the solvent peak, as confirmed by HSQC NMR studies. The high-resolution MS spectra of final products were recorded using electrospray ionization ($ESI^{+/-}$) and Fourier transform ion cyclotron resonance mass analyzer (FTMS) and were acquired from their trisodium or ammonium salts.

*General Protocols for the Synthesis of Inhibitors **12−17**.* The synthesis of intermediates **19−21** and the deprotection of the phosphonate tetraethyl esters to the final bisphosphonic acid inhibitors were previously reported.[29]

General Protocol for the Amide Bond Formation. Three slightly different methods were used depending on the availability of commercial building blocks (*e.g.*, acid chlorides *vs* carboxylic acids) and the solubility of the starting materials. Methods A and B were previously reported.[29]

Method C: intermediate **19** was first treated with TFA to obtain the free carboxylic acid in an 85−90% yield. In a vial (10 mL), the thienopyrimidine scaffold bearing either the carboxylic acid of **19** or amine **21** (0.1 mmol) was dissolved in DCM (3 mL). The carboxylic acid or the amine to be coupled (0.12 mmol) was added, followed by DIPEA (34.8 μL, 0.2 mmol) and HATU (0.12 mmol, 45.6 mg), and the reaction mixture was stirred at RT overnight. Upon completion of the reaction, the mixture was dried under vacuum and the residue was purified by flash chromatography (typically, the product elutes at 5−10% MeOH in EtOAc); for some compounds, an additional purification was done using C18 reversed-phase chromatography using a CombiFlash instrument. Isolated yields varied from 11 to 68%.

*(((2-(3-Benzamidophenyl)thieno[2,3-d]pyrimidin-4-yl)amino)-methylene)bis(phosphonic Acid) (**12a**).* The synthesis and characterization of inhibitor **12a** were previously reported.[29]

*(((2-(3-(2-Methylbenzamido)phenyl)thieno[2,3-d]pyrimidin-4-yl)amino)methylene)bis(phosphonic Acid) (**12b**).* Intermediate **21** was reacted with *o*-toluoyl chloride under standard conditions to give the tetraethyl ester of inhibitor **12b**, a light yellow solid (74 mg, quantitative yield). ^1H NMR (500 MHz, DMSO-d_6) δ 10.47 (s, −NH), 8.88 (s, 1H), 8.63 (d, *J* = 9.7 Hz, −NH), 8.14−8.11 (m, 2H), 7.82 (d, *J* = 7.9 Hz, 1H), 7.64 (d, *J* = 6.0 Hz, 1H), 7.51−7.47 (m, 2H), 7.43−7.38 (m, 1H), 7.34−7.31 (m, 2H), 6.07 (td, *J* = 23.4, 9.7 Hz, 1H), 4.19−4.07 (m, 8H), 2.43 (s, 3H), 1.17 (t, *J* = 7.0 Hz, 6H), 1.12 (t, *J* = 7.0 Hz, 6H). ^{31}P NMR (203 MHz, DMSO-d_6) δ 17.01. MS [ESI^+] *m/z*: 647.1 $[M + H^+]^+$. Final inhibitor **12b** was isolated as a pale beige solid (43.1 mg, 87%). ^1H NMR (500 MHz, 2% ND_4OD in D_2O): δ 8.35 (s, 1H), 8.22 (d, *J* = 7.9 Hz, 1H), 7.98 (dd, *J* = 8.0, 1.2 Hz, 1H), 7.68 (t, *J* = 8.0 Hz, 1H), 7.64 (d, *J* = 6.0 Hz, 1H), 7.62 (d, *J* = 8.1 Hz, 1H), 7.53−7.50 (m, 2H), 7.44−7.39 (m, 2H), 5.11 (t, *J* = 19.0 Hz, 1H), 2.50 (s, 3H). ^{31}P NMR (203 MHz, 2% ND_4OD in D_2O) δ 13.77 (s). ^{13}C NMR (101 MHz, 2% ND_4OD in D_2O) δ 171.9, 165.5, 159.9, 157.0, 138.8, 137.3, 135.7, 135.5, 130.9, 130.6, 129.6, 126.9, 125.9, 125.4, 123.8, 123.0, 121.5, 119.0, 115.9, 18.6. C-α to the bisphosphonate was observed by HSQC. HSQC ($^1H-^{13}C$): ^1H at δ 5.11 correlates to ^{13}C-α at δ 49.8.

HRMS [ESI^-] calculated for $C_{21}H_{19}N_4O_7P_2S$ *m/z*, 533.04552; found 533.04567 $[M - H]^-$.

*(((2-(3-(3-Methylbenzamido)phenyl)thieno[2,3-d]pyrimidin-4-yl)amino)methylene)bis(phosphonic Acid) (**12c**).* The synthesis was carried out using *m*-toluoyl chloride, as previously reported.[29] The tetraethyl ester was isolated as a light yellow solid (74 mg, quant. yield). ^1H NMR (500 MHz, DMSO-d_6): δ 10.38 (br s, −NH), 8.85 (t, *J* = 1.8 Hz, 1H), 8.65 (d, *J* = 9.7 Hz, −NH), 8.12 (d, *J* = 7.9 Hz, 1H), 8.10 (d, *J* = 6.0 Hz, 1H), 7.92 (dd, *J* = 8.1, 1.1 Hz, 1H), 7.84 (s, 1H), 7.80 (d, *J* = 6.6 Hz, 1H), 7.64 (d, *J* = 6.0 Hz, 1H), 7.50 (t, *J* = 7.9 Hz, 1H), 7.45−7.41 (m, 2H), 6.06 (td, *J* = 23.4, 9.7 Hz, 1H), 4.18−4.07 (m, 8H), 2.42 (s, 3H), 1.19−1.10 (m, 12H). ^{31}P NMR (203 MHz, DMSO-d_6) δ 17.00 (s). MS [ESI^+] *m/z*: 647.2 $[M + H^+]^+$. Inhibitor **12c** was isolated as a pale beige solid (33.4 mg, 67%). ^1H NMR (500 MHz, 2% ND_4OD in D_2O) δ 8.39 (s, 1H), 8.21 (d, *J* = 7.9 Hz, 1H), 7.95 (d, *J* = 8.0 Hz, 1H), 7.82 (s, 1H), 7.78 (d, *J* = 7.3 Hz, 1H), 7.67 (t, *J* = 8.0 Hz, 1H), 7.64 (d, *J* = 6.0 Hz, 1H), 7.56−7.52 (m, 2H), 7.51 (d, *J* = 5.9 Hz, 1H), 5.11 (t, *J* = 19.0 Hz, 1H), 2.48 (s, 3H). ^{31}P NMR (203 MHz, 2% ND_4OD in D_2O) δ 13.80 (s). ^{13}C NMR (101 MHz, 2% ND_4OD in D_2O) δ 169.9, 165.3, 159.9, 157.0, 139.2, 138.7, 137.5, 134.0, 133.1, 129.6, 128.8, 127.9, 125.3, 124.5, 124.4, 122.9, 122.0, 119.1, 116.0, 20.5. C-α to the bisphosphonate was observed by HSQC. HSQC ($^1H-^{13}C$): ^1H at δ 5.11 correlates to ^{13}C-α at δ 50.1.

HRMS [ESI^-] calculated for $C_{21}H_{19}N_4O_7P_2S$ *m/z*, 533.04552; found 533.04553 $[M - H]^-$.

*(((2-(3-(4-Methylbenzamido)phenyl)thieno[2,3-d]pyrimidin-4-yl)amino)methylene)bis(phosphonic Acid) (**12d**).* The synthesis and characterization were previously reported.[29]

*(((2-(3-(4-Ethylbenzamido)phenyl)thieno[2,3-d]pyrimidin-4-yl)-amino)methylene)bis(phosphonic Acid) (**12e**).* The tetraethyl ester was isolated as a light brown solid (27 mg, 90%). ^1H NMR (500 MHz, DMSO-d_6): δ 10.36 (s, −NH), 8.86 (s, 1H), 8.66 (d, *J* = 9.7 Hz, −NH), 8.13−8.10 (m, 2H), 7.95 (d, *J* = 8.1 Hz, 2H), 7.91 (d, *J* = 9.1 Hz, 1H), 7.64 (d, *J* = 6.0 Hz, 1H), 7.50 (t, *J* = 7.9 Hz, 1H), 7.38 (d, *J* = 8.1 Hz, 2H), 6.07 (td, *J* = 23.4, 9.7 Hz, 1H), 4.18−4.09 (m, 8H), 2.69 (q, *J* = 7.6 Hz, 2H), 1.22 (t, *J* = 7.6 Hz, 3H), 1.19−1.10 (m, 12H). ^{31}P NMR (203 MHz, DMSO-d_6) δ 17.00 (s). MS [ESI^+] *m/z*: 661.2 $[M + H^+]^+$. Inhibitor **12e** was isolated as a light yellow solid (12.8 mg, 83%). ^1H NMR (500 MHz, 2% ND_4OD in D_2O): δ 8.39 (s, 1H), 8.21 (d, *J* = 7.9 Hz, 1H), 7.95−7.92 (m, 3H), 7.68−7.63 (m, 2H), 7.52−7.50 (m, 3H), 5.12 (t, *J* = 19.1 Hz, 2H), 2.79 (q, *J* = 7.6 Hz, 2H), 1.29 (t, *J* = 7.6 Hz, 3H). ^{31}P NMR (203 MHz, 2% ND_4OD in D_2O): δ 13.78 (s). ^{13}C NMR (126 MHz, 2% ND_4OD in D_2O): δ 169.6, 165.2, 160.0, 156.9, 149.8, 138.7, 137.5, 131.2, 129.5, 128.3, 127.7, 125.2, 124.4, 122.8, 122.0, 119.1, 115.9, 28.3, 14.6. C-α to the bisphosphonate was observed by HSQC. HSQC ($^1H-^{13}C$): ^1H at δ 5.12 correlates to ^{13}C-α at δ 50.5.

HRMS [ESI^-] calculated for $C_{22}H_{21}N_4O_7P_2S$ *m/z*, 547.06117; found 547.06190 $[M - H]^-$.

*(((2-(3-(4-Methoxybenzamido)phenyl)thieno[2,3-d]pyrimidin-4-yl)amino)methylene)bis(phosphonic Acid) (CML-06-149, **12f**).* The synthesis and characterization were previously reported.[29]

*(((2-(3-(4-Methoxy-3-methylbenzamido)phenyl)thieno[2,3-d]-pyrimidin-4-yl)amino)methylene)bis(phosphonic Acid) (**12g**).* The tetraethyl ester was isolated as an off-white solid (27.9 mg, 41%). ^1H NMR (800 MHz, $CDCl_3$) δ 8.41 (t, *J* = 1.9 Hz, 1H), 8.23 (dt, *J* = 7.8, 1.3 Hz, 1H), 8.18−8.13 (m, 1H), 8.05 (s, 1H), 7.80 (dd, *J* = 8.4, 2.4 Hz, 1H), 7.74 (dd, *J* = 2.4, 1.0 Hz, 1H), 7.50 (t, *J* = 7.9 Hz, 1H), 7.37−7.32 (m, 2H), 6.91 (d, *J* = 8.4 Hz, 1H), 5.97 (dd, *J* = 22.9, 13.8 Hz, 2H), 4.36−4.13 (m, 8H), 3.91 (s, 3H), 2.30 (s, 3H), 1.25 (t, *J* = 7.1 Hz, 6H), 1.24 (t, *J* = 7.0 Hz, 6H). ^{31}P NMR (203 MHz, $CDCl_3$) δ 16.74. ^{13}C NMR (201 MHz, $CDCl_3$) δ 165.69, 160.89, 158.87, 155.52, 138.79, 138.26, 129.77, 129.49, 127.23, 126.72, 126.68, 124.25, 124.20, 122.69, 119.49, 117.38, 115.44, 109.71, 64.03 (t, *J* = 3.0 Hz), 63.81 (t, *J* = 3.1 Hz), 55.67, 44.64 (t, *J* = 146.4 Hz), 16.52 (t, *J* = 2.9 Hz), 16.48, 16.46 (t, *J* = 2.9 Hz). MS [ESI^+] *m/z*: 677.5 $[M + H^+]^+$. Inhibitor **12g** was isolated as a white solid (18.5 mg, 79%). ^1H NMR (800 MHz, 0.5% NH_4OH in D_2O): δ 8.25 (s, 1H), 8.11 (d, *J* = 7.7 Hz, 1H), 7.74 (d, *J* =

https://doi.org/10.1021/acs.jmedchem.1c01913
J. Med. Chem. XXXX, XXX, XXX−XXX

8.0 Hz, 2H), 7.67 (s, 1H), 7.58 (d, J = 5.9 Hz, 1H), 7.55 (t, J = 7.9 Hz, 1H), 7.44 (d, J = 5.9 Hz, 1H), 7.01 (d, J = 8.4 Hz, 1H), 5.06 (t, J = 18.6 Hz, 1H), 3.83 (s, 3H), 2.20 (s, 3H). ^{31}P NMR (203 MHz, 0.5% NH_4OH in D_2O) δ 13.68. ^{13}C NMR (201 MHz, 0.5% NH_4OH in D_2O): δ 168.76, 165.34, 160.53, 159.79, 156.89, 138.47, 137.63, 129.85, 129.39, 127.23, 126.74, 125.46, 124.93, 124.10, 122.93, 121.52, 118.93, 115.89, 110.33, 55.57, 15.54. C-α to the bisphosphonate was observed by HSQC. HSQC (^{1}H−^{13}C): ^{1}H at δ 5.06 correlates to ^{13}C-α at δ 50.3. HRMS [ESI$^-$] calculated for $C_{22}H_{21}N_4O_8P_2S$ m/z, 563.0561; found 563.0563 [M − H]$^-$.

*(((2-(3-(3-Fluoro-4-methoxybenzamido)phenyl)thieno[2,3-d]-pyrimidin-4-yl)amino)methylene)bis(phosphonic Acid) (**12h**).* The tetraethyl ester was isolated as a pale beige solid (42.7 mg, 56%). ^{1}H NMR (800 MHz, $CDCl_3$): δ 8.43 (t, J = 1.9 Hz, 1H), 8.24 (dt, J = 7.9, 1.3 Hz, 1H), 8.18 (s, 1H), 8.11−8.08 (m, 1H), 7.75−7.70 (m, 2H), 7.49 (t, J = 7.9 Hz, 1H), 7.33 (d, J = 5.9 Hz, 1H), 7.30 (d, J = 5.9 Hz, 1H), 7.04 (t, J = 8.0 Hz, 1H), 6.03−5.91 (m, 2H), 4.29−4.14 (m, 8H), 3.96 (s, 3H), 1.25 (t, J = 7.1 Hz, 6H), 1.24 (t, J = 7.1 Hz, 6H). ^{31}P NMR (203 MHz, $CDCl_3$): δ 16.79. ^{13}C NMR (201 MHz, $CDCl_3$): δ 168.1, 164.4, 158.8, 155.5 (t, J = 3.6 Hz), 152.2 (d, J = 247.9 Hz), 150.9 (d, J = 10.9 Hz), 138.5, 138.4, 129.4, 127.8 (d, J = 5.3 Hz), 124.5, 124.2, 123.9 (d, J = 3.5 Hz), 122.7, 119.7, 117.3, 115.6 (d, J = 19.8 Hz), 115.4, 112.9, 64.0 (t, J = 3.1 Hz), 63.8 (t, J = 3.1 Hz), 56.5, 44.6 (t, J = 147.1 Hz), 16.5 (t, J = 2.9 Hz), 16.4 (t, J = 3.0 Hz). MS [ESI$^+$] m/z: 681.5 [M + H$^+$]$^+$. Inhibitor **12h** was isolated as a white solid (28.7 mg, 80%). ^{1}H NMR (800 MHz, 0.5% NH_4OH in D_2O): δ 8.18 (s, 1H), 8.04 (d, J = 7.7 Hz, 1H), 7.65 (d, J = 8.0 Hz, 1H), 7.61 (d, J = 8.4 Hz, 1H), 7.57 (d, J = 11.8 Hz, 1H), 7.53 (d, J = 5.9 Hz, 1H), 7.47 (t, J = 7.8 Hz, 1H), 7.40 (d, J = 5.8 Hz, 1H), 7.09 (t, J = 8.5 Hz, 1H), 5.06 (t, J = 18.6 Hz, 1H), 3.82 (s, 3H). ^{31}P NMR (203 MHz, 0.5% NH_4OH in D_2O): δ 13.68. ^{13}C NMR (201 MHz, 0.5% NH_4OH in D_2O): δ 167.0, 165.3, 159.6, 156.8, 151.2 (d, J = 243.7 Hz), 150.0 (d, J = 10.4 Hz), 138.3, 137.5, 129.3, 126.1 (d, J = 5.8 Hz), 124.9, 124.6, 123.7, 123.0, 121.1, 118.8, 115.8, 115.1 (d, J = 20.1 Hz), 113.1, 56.1. C-α to the bisphosphonate was observed by HSQC. HSQC (^{1}H−^{13}C): ^{1}H at δ 5.06 correlates to ^{13}C-α at δ 50.4. HRMS [ESI$^+$] calculated for $C_{21}H_{18}FN_4O_8P_2S$ m/z, 563.0310; found 563.0310 [M − H]$^-$.

*(((2-(3-(3-Chloro-4-methoxybenzamido)phenyl)thieno[2,3-d]-pyrimidin-4-yl)amino)methylene)bis(phosphonic Acid) (**12i**).* The tetraethyl ester was isolated as an off-white solid (39.9 mg, 57%). ^{1}H NMR (500 MHz, $CDCl_3$): δ 8.45 (t, J = 1.9 Hz, 1H), 8.25 (s, 1H), 8.23 (d, J = 8.0 Hz, 1H), 8.07 (d, J = 7.9 Hz, 1H), 7.99 (d, J = 2.3 Hz, 1H), 7.86 (dd, J = 8.5, 2.3 Hz, 1H), 7.47 (t, J = 7.9 Hz, 1H), 7.32 (d, J = 5.9 Hz, 1H), 7.29 (d, J = 6.0 Hz, 1H), 7.00 (d, J = 8.6 Hz, 1H), 6.07−5.90 (m, 2H), 4.32−4.12 (m, 9H), 3.96 (s, 3H), 1.24 (t, J = 7.1 Hz, 6H), 1.23 (t, J = 7.1 Hz, 7H). ^{31}P NMR (203 MHz, $CDCl_3$): δ 16.81. ^{13}C NMR (126 MHz, $CDCl_3$): δ 164.3, 158.8, 157.9, 155.5, 138.4, 129.6, 129.4, 128.0, 127.5, 124.4, 124.2, 123.0, 122.7, 119.8, 117.3, 115.4, 111.7, 64.0, 63.8, 56.5, 44.6 (t, J = 147.3 Hz), 16.5 (t, J = 2.7 Hz), 16.4 (t, J = 2.7 Hz). MS [ESI$^+$] m/z: 697.4 [M + H$^+$]$^+$. Inhibitor **12i** was isolated as a white solid (20.6 mg, 62%). ^{1}H NMR (500 MHz, 0.5% NH_4OH in D_2O): δ 8.21 (s, 1H), 8.07 (d, J = 7.7 Hz, 1H), 7.86 (s, 1H), 7.77 (d, J = 8.3 Hz, 1H), 7.69 (d, J = 8.0 Hz, 1H), 7.55 (d, J = 5.9 Hz, 1H), 7.50 (t, J = 7.9 Hz, 1H), 7.42 (d, J = 5.9 Hz, 1H), 7.09 (d, J = 8.4 Hz, 1H), 5.05 (t, J = 18.7 Hz, 1H), 3.84 (s, 3H). ^{31}P NMR (203 MHz, 0.5% NH_4OH in D_2O): δ 13.67. ^{13}C NMR (126 MHz, 0.5% NH_4OH in D_2O): δ 167.0, 165.3, 159.6, 157.2, 156.8, 138.4, 137.4, 129.4, 129.3, 128.0, 126.6, 124.9, 123.8, 122.9, 121.5, 121.2, 118.9, 115.9, 112.2, 56.3.

HRMS [ESI$^-$] calculated for $C_{21}H_{18}ClN_4O_8P_2S$ m/z, 583.0015; found 583.0021 [M − H]$^-$.

*(((2-(3-(3-Bromo-4-methoxybenzamido)phenyl)thieno[2,3-d]-pyrimidin-4-yl)amino)methylene)bis(phosphonic Acid) (**12j**).* The tetraethyl ester was isolated as an off-white solid (26.2 mg, 35.3%). ^{1}H NMR (500 MHz, $CDCl_3$): δ 8.45 (t, J = 1.9 Hz, 1H), 8.23 (dt, J = 7.9, 1.3 Hz, 1H), 8.18 (s, 1H), 8.16 (d, J = 2.2 Hz, 1H), 8.09 (ddd, J = 8.1, 2.3, 1.1 Hz, 1H), 7.91 (dd, J = 8.6, 2.3 Hz, 1H), 7.49 (t, J = 7.9 Hz, 1H), 7.36 (d, J = 6.0 Hz, 1H), 7.33 (d, J = 5.9 Hz, 1H), 6.97 (d, J = 8.6 Hz, 1H), 6.12 (s, 1H), 6.00 (td, J = 21.8, 9.8 Hz, 1H), 4.33−4.14 (m, 5H), 3.96 (s, 3H), 1.25 (t, J = 7.1 Hz, 6H), 1.24 (t, J = 7.1 Hz, 6H). ^{31}P NMR (203 MHz, $CDCl_3$): δ 16.79. ^{13}C NMR (126 MHz, $CDCl_3$): δ 164.2, 158.8, 155.5, 138.4, 132.7, 129.4, 128.5, 128.2, 124.5, 124.1, 122.7, 119.8, 117.5, 115.5, 112.0, 111.5, 64.1, 63.8, 56.6, 44.6 (t, J = 146.5 Hz), 16.5 (t, J = 2.8 Hz), 16.4 (t, J = 3.0 Hz). MS [ESI$^+$] m/z: 741.4 [M + H$^+$]$^+$. Inhibitor **12j** was isolated as an off-white solid (17.5 mg, 79%). ^{1}H NMR (500 MHz, 0.5% NH_4OH in D_2O): δ 8.25 (s, 1H), 8.11 (d, J = 7.7 Hz, 1H), 8.08 (s, 1H), 7.86 (d, J = 8.2 Hz, 1H), 7.74 (d, J = 7.9 Hz, 1H), 7.57 (d, J = 5.9 Hz, 1H), 7.54 (t, J = 7.9 Hz, 1H), 7.44 (d, J = 5.9 Hz, 1H), 7.11 (d, J = 8.4 Hz, 1H), 5.05 (t, J = 18.8 Hz, 1H), 3.88 (s, 3H). ^{31}P NMR (203 MHz, 0.5% NH_4OH in D_2O): δ 13.66. ^{13}C NMR (126 MHz, 0.5% NH_4OH in D_2O): δ 167.0, 165.3, 159.7, 158.2, 156.9, 138.4, 137.5, 132.5, 129.4, 128.7, 127.1, 125.0, 123.9, 122.9, 121.4, 118.9, 115.9, 112.1, 110.7, 56.4.

HRMS [ESI$^-$] calculated for $C_{21}H_{18}BrN_4O_8P_2S$ m/z, 626.9509; found 626.9516 [M − H]$^-$.

*(((2-(3-(3-Fluoro-4-methylbenzamido)phenyl)thieno[2,3-d]-pyrimidin-4-yl)amino)methylene)bis(phosphonic Acid) (**12k**).* The tetraethyl ester was isolated as an off-white solid (45.1 mg, 68%). ^{1}H NMR (800 MHz, $CDCl_3$): δ 8.43 (t, J = 2.0 Hz, 1H), 8.26 (dt, J = 7.8, 1.3 Hz, 1H), 8.15−8.07 (m, 2H), 7.63−7.60 (m, 2H), 7.51 (t, J = 7.9 Hz, 1H), 7.36 (d, J = 5.9 Hz, 1H), 7.33−7.31 (m, 2H), 6.06−5.87 (m, 2H), 4.33−4.15 (m, 8H), 2.36 (d, J = 1.8 Hz, 3H), 1.25 (t, J = 7.1 Hz, 6H), 1.25 (t, J = 7.0 Hz, 6H). ^{31}P NMR (203 MHz, $CDCl_3$) δ 16.75. ^{13}C NMR (201 MHz, $CDCl_3$): δ 166.4, 164.7, 161.5 (d, J = 246.5 Hz), 158.8, 155.5, 138.3, 134.6 (d, J = 6.8 Hz), 131.9 (d, J = 5.0 Hz), 129.5, 129.5 (d, J = 17.5 Hz), 124.6, 124.4, 122.7, 122.4, 122.4, 119.7, 117.3, 115.5, 114.4 (d, J = 23.8 Hz), 64.0 (t, J = 3.1 Hz), 63.8 (t, J = 3.1 Hz), 44.7 (t, J = 147.1 Hz), 16.5 (t, J = 2.9 Hz), 16.5 (t, J = 2.9 Hz), 14.9 (d, J = 3.1 Hz). MS [ESI$^+$] m/z: 665.5 [M + H$^+$]$^+$. Inhibitor **12k** was isolated as a white solid (31.6 mg, 84%). ^{1}H NMR (800 MHz, 0.5% NH_4OH in D_2O) δ 8.23 (s, 1H), 8.07 (d, J = 7.8 Hz, 1H), 7.69 (d, J = 7.8 Hz, 1H), 7.55−7.46 (m, 4H), 7.41 (d, J = 5.9 Hz, 1H), 7.31 (t, J = 7.8 Hz, 1H), 5.05 (t, J = 18.5 Hz, 1H), 2.20 (s, 3H). ^{31}P NMR (203 MHz, 0.5% NH_4OH in D_2O) δ 13.68.^{13}C NMR (201 MHz, 0.5% NH_4OH in D_2O) δ 167.7, 165.3, 160.7 (d, J = 243.6 Hz), 159.6, 156.9, 138.4, 137.4, 132.8 (d, J = 7.1 Hz), 131.9 (d, J = 5.1 Hz), 130.0 (d, J = 17.5 Hz), 129.4, 125.1, 124.0, 123.0, 123.0, 121.4, 118.9, 115.9, 113.9 (d, J = 24.2 Hz), 13.8 (d, J = 3.3 Hz). C-α to the bisphosphonate was observed by HSQC. HSQC (^{1}H−^{13}C): ^{1}H at δ 5.05 correlates to ^{13}C-α at δ 49.9. HRMS [ESI$^-$] calculated for $C_{21}H_{18}FN_4O_7P_2S$ m/z, 551.0361; found 551.0367 [M − H]$^-$.

*(((2-(3-(3-Chloro-4-methylbenzamido)phenyl)thieno[2,3-d]-pyrimidin-4-yl)amino)methylene)bis(phosphonic Acid) (**12l**).* The tetraethyl ester was isolated as an off-white solid (41.9 mg, 62%). ^{1}H NMR (800 MHz, $CDCl_3$): δ 8.44 (t, J = 1.9 Hz, 1H), 8.26 (dt, J = 7.8, 1.3 Hz, 1H), 8.11 (dt, J = 11.7, 2.8 Hz, 2H), 7.93 (d, J = 1.9 Hz, 1H), 7.73 (dd, J = 7.8, 1.9 Hz, 1H), 7.51 (t, J = 7.9 Hz, 1H), 7.39−7.35 (m, 2H), 7.32 (d, J = 5.9 Hz, 1H), 6.02−5.92 (m, 2H), 4.31−4.15 (m, 8H), 2.46 (s, 3H), 1.25 (t, J = 7.0 Hz, 6H), 1.25 (t, J = 7.1 Hz, 6H). ^{31}P NMR (203 MHz, $CDCl_3$) δ 16.76. ^{13}C NMR (201 MHz, $CDCl_3$) δ 164.6, 158.8, 155.5, 140.5, 138.3, 135.2, 134.2, 131.4, 129.5, 128.2, 125.3, 124.6, 124.3, 122.7, 119.7, 117.3, 115.5, 64.0 (t, J = 3.1 Hz), 63.8 (t, J = 3.2 Hz), 44.7 (t, J = 147.5 Hz), 20.4, 16.5 (t, J = 2.9 Hz), 16.5 (t, J = 3.0 Hz). MS [ESI$^+$] m/z: 681.5 [M + H$^+$]$^+$. Inhibitor **12l** was isolated as a white solid (26.6 mg, 76%). ^{1}H NMR (800 MHz, 0.5% NH_4OH in D_2O) δ 8.24 (s, 1H), 8.09 (d, J = 7.7 Hz, 1H), 7.81 (s, 1H), 7.72 (d, J = 7.9 Hz, 1H), 7.64 (d, J = 7.8 Hz, 1H), 7.55 (d, J = 5.9 Hz, 1H), 7.52 (t, J = 7.8 Hz, 1H), 7.42 (d, J = 5.9 Hz, 1H), 7.36 (d, J = 7.9 Hz, 1H), 5.06 (t, J = 18.5 Hz, 1H), 2.30 (s, 3H). ^{31}P NMR (203 MHz, 0.5% NH_4OH in D_2O) δ 13.68. ^{13}C NMR (201 MHz, 0.5% NH_4OH in D_2O) δ 167.6, 165.3, 159.7, 156.9, 140.9, 138.4, 137.3, 134.1, 132.6, 131.2, 129.4, 127.9, 125.7, 125.1, 124.0, 123.0, 121.4, 118.9, 115.9, 19.3. C-α to the bisphosphonate was observed by HSQC. HSQC (^{1}H−^{13}C): ^{1}H at δ 5.06 correlates to ^{13}C-α at δ 49.9. HRMS [ESI$^-$] calculated for $C_{21}H_{18}ClN_4O_7P_2S$ m/z, 567.0065; found 567.0069 [M − H]$^-$.

*(((2-(3-(3-Bromo-4-methylbenzamido)phenyl)thieno[2,3-d]-pyrimidin-4-yl)amino)methylene)bis(phosphonic Acid) (**12m**).* The tetraethyl ester was isolated as an off-white solid (41.9 mg, 62%). ^{1}H NMR (500 MHz, $CDCl_3$): δ 8.46 (t, J = 1.9 Hz, 1H), 8.27−8.21 (m, 2H), 8.11 (d, J = 1.9 Hz, 1H), 8.09−8.04 (m, 1H), 7.77 (dd, J = 7.9, 1.9 Hz, 1H), 7.47 (t, J = 7.9 Hz, 1H), 7.37−7.29 (m, 2H), 7.28 (d, J = 6.0

https://doi.org/10.1021/acs.jmedchem.1c01913
J. Med. Chem. XXXX, XXX, XXX−XXX

Hz, 1H), 5.98 (td, J = 21.7, 9.9 Hz, 1H), 5.90−5.85 (m, 1H), 4.33−4.12 (m, 6H), 2.45 (s, 3H), 1.24 (t, J = 7.2 Hz, 6H), 1.23 (t, J = 7.1 Hz, 6H). ^{31}P NMR (203 MHz, $CDCl_3$) δ 16.83. ^{13}C NMR (126 MHz, $CDCl_3$) δ 168.4, 164.4, 158.8, 155.5, 142.2, 138.6, 138.3, 134.3, 131.4, 131.1, 129.4, 126.1, 125.4, 124.6, 124.1, 122.6, 119.8, 117.3, 115.4, 64.0 (t, J = 3.2 Hz), 63.8 (t, J = 3.2 Hz), 44.6 (t, J = 147.5 Hz), 23.2, 16.5 (t, J = 3.0 Hz), 16.4 (t, J = 3.0 Hz). MS [ESI$^-$] m/z: 723.1 [M − H]$^-$. Inhibitor **12m** was isolated as a white solid (26.6 mg, 76%). ^{1}H NMR (800 MHz, 0.5% NH_4OH in D_2O): δ 8.20 (d, J = 2.1 Hz, 1H), 8.07 (d, J = 7.7 Hz, 1H), 7.92 (d, J = 1.9 Hz, 1H), 7.65 (dd, J = 7.9, 2.2 Hz, 1H), 7.62 (dd, J = 7.7, 1.9 Hz, 1H), 7.53 (d, J = 5.9 Hz, 1H), 7.48 (t, J = 7.8 Hz, 1H), 7.39 (d, J = 5.9 Hz, 1H), 7.28 (d, J = 7.9 Hz, 1H), 5.03 (t, J = 18.9 Hz, 1H), 2.25 (s, 3H). ^{31}P NMR (203 MHz, 0.5% NH_4OH in D_2O): δ 13.66. ^{13}C NMR (201 MHz, 0.5% NH_4OH in D_2O): δ 167.1, 165.3, 159.6, 156.9, 142.7, 138.4, 137.3, 132.5, 131.1, 130.9, 129.4, 126.3, 125.1, 124.4, 123.9, 123.0, 121.3, 118.9, 115.9, 50.3 (t, J = 124.8 Hz), 22.2. HRMS [ESI$^-$] calculated for $C_{21}H_{18}BrN_4O_7P_2S$ m/z, 610.9560; found 610.9577 [M − H]$^-$.

*(((2-(3-(4-((Trifluoromethyl)thio)benzamido)phenyl)thieno[2,3-d]pyrimidin-4-yl)amino)methylene)bis(phosphonic Acid) (**12n**).* The tetraethyl ester was isolated as an off-white solid (50.6 mg, 69%). ^{1}H NMR (800 MHz, $CDCl_3$): δ 8.47 (q, J = 2.0 Hz, 2H), 8.24 (dt, J = 7.9, 1.3 Hz, 1H), 8.11−8.07 (m, 1H), 8.04−7.97 (m, 2H), 7.79−7.75 (m, 2H), 7.47 (t, J = 7.9 Hz, 1H), 7.30 (d, J = 5.9 Hz, 1H), 7.28 (d, J = 5.9 Hz, 1H), 6.05−5.92 (m, 2H), 4.29−4.13 (m, 8H), 1.24 (t, J = 7.1 Hz, 6H), 1.23 (t, J = 7.1 Hz, 6H). ^{31}P NMR (203 MHz, $CDCl_3$) δ 16.82. ^{13}C NMR (201 MHz, $CDCl_3$): δ 168.1, 164.8, 158.7, 155.5 (t, J = 3.6 Hz), 138.5, 138.2, 137.3, 136.2, 129.5 (q, J = 308.3 Hz), 129.4, 128.6, 128.4, 124.8, 124.2, 122.8, 119.9, 117.3, 115.4, 64.0 (t, J = 3.2 Hz), 63.8 (t, J = 3.2 Hz), 44.7 (t, J = 147.1 Hz), 16.5 (t, J = 2.9 Hz), 16.4 (t, J = 2.9 Hz). MS [ESI$^-$] m/z: 731.4 [M − H]$^-$. Inhibitor **12n** was isolated as a white solid (26.6 mg, 76%). ^{1}H NMR (800 MHz, 0.5% NH_4OH in D_2O): δ 8.33 (s, 1H), 8.14 (d, J = 7.8 Hz, 1H), 7.95 (d, J = 7.9 Hz, 2H), 7.85 (d, J = 7.8 Hz, 2H), 7.81 (d, J = 7.9 Hz, 1H), 7.60−7.54 (m, 2H), 7.44 (d, J = 5.8 Hz, 1H), 5.04 (t, J = 18.6 Hz, 1H). ^{31}P NMR (203 MHz, 0.5% NH_4OH in D_2O): δ 13.65. ^{13}C NMR (201 MHz, 0.5% NH_4OH in D_2O): δ 168.14, 165.29, 159.76, 156.88, 138.59, 137.32, 136.04, 135.98, 129.51, 129.40 (q, J = 307.3 Hz), 128.47, 128.31, 125.29, 124.10, 122.96, 121.67, 118.99, 115.94. C-α to the bisphosphonate was observed by HSQC. HSQC (^{1}H−^{13}C): ^{1}H at δ 5.04 correlates to ^{13}C-α at δ 50.3. HRMS [ESI$^-$] calculated for $C_{21}H_{16}F_3N_4O_7P_2S$ m/z, 618.9893; found 618.9898 [M − H]$^-$.

*(((2-(3-(4-Fluorobenzamido)phenyl)thieno[2,3-d]pyrimidin-4-yl)-amino)methylene)bis(phosphonic Acid) (**12o**).* The synthesis and characterization were previously reported.[29]

*(((2-(3-(4-(Trifluoromethyl)benzamido)phenyl)thieno[2,3-d]-pyrimidin-4-yl)amino)methylene)bis(phosphonic Acid) (**12p**).* The tetraethyl ester was isolated as a light yellow solid (45.0 mg, 62%). ^{1}H NMR (500 MHz, $CDCl_3$): δ 8.47 (s, 1H), 8.43 (br_s, 1H), 8.27 (d, J = 7.8 Hz, 1H), 8.14 (d, J = 6.8 Hz, 1H), 8.06 (d, J = 8.0 Hz, 2H), 7.76 (d, J = 8.2 Hz, 2H), 7.50 (t, J = 7.9 Hz, 1H), 7.41 (d, J = 5.9 Hz, 1H), 7.32 (d, J = 6.0 Hz, 1H), 6.29 (br_s, 1H), 6.05 (br, 1H), 4.27−4.14 (m, 8H), 1.25−1.21 (m, 12H). ^{31}P NMR (203 MHz, $CDCl_3$) δ 16.95 (s). ^{13}C NMR (126 MHz, $CDCl_3$): δ 168.5, 164.8, 158.7, 155.5, 138.8, 138.5, 138.2, 133.7−133.1 (m), 129.5, 127.9, 125.9 (q, J = 3.6 Hz), 124.8, 124.0, 123.8 (q, J = 272.6 Hz), 122.6, 119.8, 117.7, 115.5, 64.1−63.9 (m), 44.4 (t, J = 148.8 Hz), 16.5−16.4 (m). MS [ESI$^+$] m/z: 701.3 [M + H$^+$]$^+$. Inhibitor **12p** was isolated as a light beige solid (24.5 mg, 73%) and converted to its trisodium salt by the addition of 3 equivalents of NaOH. ^{1}H NMR (500 MHz, D_2O): δ 8.36 (s, 1H), 8.18 (d, J = 7.9 Hz, 1H), 8.08 (d, J = 8.1 Hz, 2H), 7.91−7.90 (m, 3H), 7.63 (t, J = 8.0 Hz, 1H), 7.60 (d, J = 6.0 Hz, 1H), 7.48 (d, J = 6.0 Hz, 1H), 5.14 (t, J = 19.0 Hz, 1H). ^{31}P NMR (162 MHz, D_2O): δ 14.00 (s). ^{13}C NMR (126 MHz, D_2O): δ 168.5, 165.5, 159.8, 157.0, 138.7, 137.5, 137.3, 132.9 (q, J = 32.6 Hz), 129.5, 128.0, 125.8 (q, J = 3.7 Hz), 125.4, 124.2, 124.0 (q, J = 271.8 Hz), 123.1, 121.9, 119.0, 115.9. C-α to the bisphosphonate was observed by HSQC. HSQC (^{1}H−^{13}C): ^{1}H at δ 5.13 correlates to ^{13}C-α at δ 49.4. HRMS [ESI$^-$] calculated for $C_{21}H_{15}F_3N_4NaO_7P_2S$ m/z, 608.9992; found 608.9985 [M − H]$^-$.

*(((2-(3-(Picolinamido)phenyl)thieno[2,3-d]pyrimidin-4-yl)-amino)methylene)bis(phosphonic Acid) (**12q**).* The tetraethyl ester was isolated as a light yellow solid (74 mg, 95%). ^{1}H NMR (500 MHz, DMSO-d_6): δ 10.77 (s, −NH), 9.02 (t, J = 1.8 Hz, 1H), 8.77 (ddd, J = 4.8, 1.5, 0.9 Hz, 1H), 8.65 (d, J = 9.7 Hz, NH), 8.18 (d, J = 7.8 Hz, 1H), 8.15 (d, J = 7.9 Hz, 1H), 8.12−8.08 (m, 2H), 7.93 (ddd, J = 8.1, 2.0, 0.8 Hz, 1H), 7.70 (ddd, J = 7.5, 4.8, 1.2 Hz, 1H), 7.64 (d, J = 6.0 Hz, 1H), 7.51 (t, J = 7.9 Hz, 1H), 6.08 (td, J = 23.4, 9.7 Hz, 1H), 4.20−4.07 (m, 8H), 1.20−1.10 (m, 12H). ^{31}P NMR (203 MHz, DMSO-d_6): δ 17.00 (s). MS [ESI$^+$] m/z: 634.3 [M + H$^+$]$^+$. Inhibitor **12q** was isolated as a light yellow solid (42 mg, 79%). ^{1}H NMR (500 MHz, 2% ND_4OD in D_2O): δ 8.72 (d, J = 4.7 Hz, 1H), 8.48 (s, 1H), 8.17 (d, J = 7.9 Hz, 2H), 8.07 (td, J = 7.8, 1.5 Hz, 1H), 7.98 (d, J = 9.1 Hz, 1H), 7.68−7.63 (m, 2H), 7.60 (d, J = 5.9 Hz, 1H), 7.46 (d, J = 5.9 Hz, 1H), 5.06 (t, J = 9.1 Hz, 1H). ^{31}P NMR (203 MHz, 2% ND_4OD in D_2O): δ 13.68 (s). ^{13}C NMR (101 MHz, 2% ND_4OD in D_2O): δ 165.5, 165.3, 159.7, 156.9, 148.9, 148.7, 138.6, 138.4, 137.0, 129.5, 127.3, 125.2, 123.5, 123.1, 122.7, 121.2, 118.9, 115.8, 49.3 (t, J = 121.8 Hz).

HRMS [ESI$^-$] calculated for $C_{19}H_{16}N_5O_7P_2S$ m/z, 520.02511; found 520.02541 [M − H]$^-$.

*(((2-(3-(5-(Trifluoromethyl)picolinamido)phenyl)thieno[2,3-d]-pyrimidin-4-yl)amino)methylene)bis(phosphonic Acid) (**12r**).* The tetraethyl ester was isolated as a pale beige solid (64 mg, 88%). ^{1}H NMR (500 MHz, $CDCl_3$): δ 10.11 (s, 1H), 8.93 (s, 1H), 8.62 (s, 1H), 8.46 (d, J = 8.1 Hz, 1H), 8.29 (d, J = 7.9 Hz, 1H), 8.18 (dt, J = 8.1, 2.3 Hz, 2H), 7.54 (t, J = 7.9 Hz, 1H), 7.49 (d, J = 5.0 Hz, 1H), 7.36 (d, J = 5.9 Hz, 1H), 6.52 (br_s, 1H), 6.03 (td, J = 22.0, 9.8 Hz, 1H), 4.31−4.15 (m, 8H), 1.27 (t, J = 7.0 Hz, 6H), 1.22 (t, J = 7.1 Hz, 6H). ^{31}P NMR (203 MHz, $CDCl_3$): δ 16.85 (s). ^{13}C NMR (126 MHz, $CDCl_3$): δ 174.4, 160.7, 158.6, 155.5 (t, J = 3.6 Hz), 152.8, 145.2 (q, J = 3.8 Hz), 138.6, 137.6, 135.2 (q, J = 3.4 Hz), 129.4, 129.1 (q, J = 33.4 Hz), 124.7, 124.0, 123.1 (q, J = 272.7 Hz), 122.3, 121.9, 119.4, 117.8, 115.5, 64.0−63.8 (m), 44.4 (t, J = 147.6 Hz), 16.4−16.3 (m). MS [ESI$^+$] m/z: 702.1 [M + H$^+$]$^+$. Inhibitor **12r** was isolated as a pale beige solid (26 mg, 69%). ^{1}H NMR (500 MHz, 0.5% NH_4OH in D_2O) δ 9.06 (s, 1H), 8.49 (t, J = 2.0 Hz, 1H), 8.38 (dd, J = 8.4, 2.2 Hz, 1H), 8.33 (d, J = 8.3 Hz, 1H), 8.18 (d, J = 7.8 Hz, 1H), 7.99 (dd, J = 7.9, 1.6 Hz, 1H), 7.67−7.58 (m, 2H), 7.49 (d, J = 6.0 Hz, 1H), 5.20 (t, J = 18.9 Hz, 1H). ^{31}P NMR (203 MHz, 0.5% NH_4OH in D_2O) δ 13.86. ^{13}C NMR (201 MHz, 0.5% NH_4OH in D_2O) δ 165.6, 164.0, 159.8, 157.0, 152.2, 145.9 (q, J = 4.2 Hz), 138.7, 136.9, 135.9 (q, J = 3.2 Hz), 129.6, 128.7 (q, J = 32.9 Hz), 125.4, 123.6, 123.2, 123.2 (q, J = 272.1 Hz), 122.6, 121.5, 118.9, 115.8, 49.0 (t, J = 120.8 Hz). HRMS [ESI$^-$] calculated for $C_{20}H_{14}F_3N_5NaO_7P_2S$ m/z, 609.9944; found 609.9944 [M − H]$^-$.

*(((2-(3-(Cyclohexanecarboxamido)phenyl)thieno[2,3-d]-pyrimidin-4-yl)amino)methylene)bis(phosphonic Acid) (**12s**).* The tetraethyl ester was isolated as a light yellow solid (45.5 mg, 68%). ^{1}H NMR (500 MHz, DMSO-d_6): δ 9.97 (s, −NH), 8.68 (t, J = 1.8 Hz, 1H), 8.62 (d, J = 9.7 Hz, −NH), 8.09 (d, J = 6.0 Hz, 1H), 8.03 (d, J = 7.9 Hz, 1H), 7.71 (ddd, J = 8.1, 2.0, 0.9 Hz, 1H), 7.62 (d, J = 6.0 Hz, 1H), 7.42 (t, J = 7.9 Hz, 1H), 6.04 (td, J = 23.4, 9.7 Hz, 1H), 4.18−4.06 (m, 8H), 2.37 (tt, J = 11.6, 3.4 Hz, 1H), 1.78−1.65 (m, 5H), 1.48−1.20 (m, 5H), 1.19−1.09 (m, 12H). ^{31}P NMR (203 MHz, DMSO-d_6): δ 16.98 (s). MS [ESI$^+$] m/z: 639.2 [M + H$^+$]$^+$. Inhibitor **12s** was isolated as a light yellow solid (23.5 mg, 81%). ^{1}H NMR (500 MHz, 2% ND_4OD in D_2O): δ 8.25 (s, 1H), 8.14 (d, J = 7.9 Hz, 1H), 7.82 (d, J = 8.1 Hz, 1H), 7.64−7.59 (m, 2H), 7.50 (d, J = 5.9 Hz, 1H), 5.11 (t, J = 19.1 Hz, 1H), 2.49 (tt, J = 11.8, 3.3 Hz, 1H), 1.99−1.73 (m, 5H), 1.56−1.27 (m, 5H). ^{31}P NMR (203 MHz, 0.5% 2% ND_4OD in D_2O): δ 13.77 (s). ^{13}C NMR (101 MHz, 2% ND_4OD in D_2O): δ 179.1, 165.6, 159.9, 157.0, 138.6, 137.5, 129.5, 124.9, 123.8, 123.1, 121.4, 118.9, 115.8, 45.8, 29.1, 25.3, 25.2. C-α to the bisphosphonate was observed by HSQC. HSQC (^{1}H−^{13}C): ^{1}H at δ 5.11 correlates to ^{13}C-α at δ 49.0.

HRMS [ESI$^-$] calculated for $C_{20}H_{23}N_4O_7P_2S$ m/z, 525.07682; found 525.07638 [M − H]$^-$.

*(((2-(3-(3-Methylbutanamido)phenyl)thieno[2,3-d]pyrimidin-4-yl)amino)methylene)bis(phosphonic Acid) (**12t**).* The tetraethyl ester was isolated as an off-white solid (50.6 mg, 69%). ^{1}H NMR (800 MHz, $CDCl_3$): δ 8.31 (t, J = 2.0 Hz, 1H), 8.18 (d, J = 7.7 Hz, 1H), 8.05−7.99 (m, 1H), 7.76 (s, 1H), 7.42 (t, J = 7.9 Hz, 1H), 7.32 (d, J = 6.0 Hz, 1H),

https://doi.org/10.1021/acs.jmedchem.1c01913
J. Med. Chem. XXXX, XXX, XXX−XXX

7.29 (d, J = 5.9 Hz, 1H), 6.14−6.05 (m, 1H), 5.98 (td, J = 21.9, 9.8 Hz, 1H), 4.29−4.12 (m, 8H), 2.30−2.21 (m, 3H), 1.23 (t, J = 7.0 Hz, 6H), 1.22 (t, J = 7.0 Hz, 6H), 1.02 (d, J = 6.4 Hz, 6H). ^{31}P NMR (203 MHz, $CDCl_3$): δ 16.84. ^{13}C NMR (201 MHz, $CDCl_3$): δ 171.2, 168.2, 158.8, 155.4 (t, J = 3.7 Hz), 138.6, 138.3, 129.3, 124.0, 123.9, 122.2, 119.1, 117.4, 115.4, 64.0 (t, J = 3.0 Hz), 63.8 (t, J = 3.2 Hz), 47.1, 44.5 (t, J = 147.1 Hz), 26.4, 22.6, 16.5 (t, J = 2.9 Hz), 16.4 (t, J = 2.9 Hz). MS [ESI$^+$] m/z: 613.5 [M + H$^+$]$^+$. Inhibitor **12t** was isolated as a white solid (30.7 mg, 86%). ^{1}H NMR (800 MHz, 0.5% NH_4OH in D_2O): δ 8.18 (d, J = 2.0 Hz, 1H), 8.09 (d, J = 7.7 Hz, 1H), 7.71 (dd, J = 8.0, 2.2 Hz, 1H), 7.57 (d, J = 5.9 Hz, 1H), 7.53 (t, J = 7.9 Hz, 1H), 7.44 (d, J = 5.9 Hz, 1H), 5.03 (t, J = 18.6 Hz, 1H), 2.30 (d, J = 7.5 Hz, 2H), 2.11 (non, J = 6.8 Hz, 1H), 0.99 (d, J = 6.7 Hz, 6H). ^{31}P NMR (203 MHz, 0.5% NH_4OH in D_2O): δ 13.70. ^{13}C NMR (201 MHz, 0.5% NH_4OH in D_2O): δ 175.47, 165.37, 159.81, 156.89, 138.57, 137.25, 129.46, 124.96, 123.70, 122.98, 121.20, 118.94, 115.86, 45.70, 26.30, 21.55. C-α to the bisphosphonate was observed by HSQC. HSQC (^{1}H−^{13}C): ^{1}H at δ 5.03 correlates to ^{13}C-α at δ 49.9. HRMS [ESI$^-$] calculated for $C_{18}H_{21}N_4O_7P_2S$ m/z, 499.0612; found 499.0614 [M − H]$^-$.

*(((2-(3-(Cyclopropanecarboxamido)phenyl)thieno[2,3-d]pyrimidin-4-yl)amino)methylene)bis(phosphonic Acid) (**12u**).* The tetraethyl ester was isolated as a light yellow solid (52 mg, 84%). ^{1}H NMR (400 MHz, DMSO-d_6): δ 10.36 (s, −NH), 8.66 (s, 1H), 8.62 (d, J = 9.7 Hz, −NH), 8.09 (d, J = 6.0 Hz, 1H), 8.04 (d, J = 7.8 Hz, 1H), 7.72 (d, J = 9.0 Hz, 1H), 7.63 (d, J = 6.0 Hz, 1H), 7.43 (t, J = 7.9 Hz, 1H), 6.03 (td, J = 23.4, 9.7 Hz, 1H), 4.17−4.05 (m, 8H), 1.85−1.79 (m, 1H), 1.19−1.09 (m, 12H), 0.82−0.79 (m, 4H). ^{31}P NMR (203 MHz, DMSO-d_6): δ 16.98 (s). MS [ESI$^+$] m/z: 597.16 [M + H$^+$]$^+$. Inhibitor **12u** was isolated as a light yellow solid (25.7 mg, 75%). ^{1}H NMR (500 MHz, 2% ND_4OD in D_2O): δ 8.27 (s, 1H), 8.12 (d, J = 7.7 Hz, 1H), 7.82 (d, J = 8.1 Hz, 1H), 7.63 (d, J = 5.9 Hz, 1H), 7.59 (t, J = 8.0 Hz, 1H), 7.51 (d, J = 6.0 Hz, 1H), 5.13 (t, J = 19.0 Hz, 1H), 1.90−1.85 (m, 1H), 1.04−0.98 (m, 4H). ^{31}P NMR (203 MHz, 2% ND_4OD in D_2O): δ 13.81 (s). ^{13}C NMR (126 MHz, 2% ND_4OD in D_2O): δ 176.2, 165.2, 159.9, 156.8, 138.6, 137.7, 129.4, 124.5, 123.3, 122.7, 120.9, 119.1, 115.9, 50.5 (t, J = 125.0 Hz), 14.8, 7.4.

HRMS [ESI$^-$] calculated for $C_{17}H_{17}N_4O_7P_2S$ m/z, 483.02987; found 483.02977 [M − H]$^-$.

*(((2-(3-(Phenylcarbamoyl)phenyl)thieno[2,3-d]pyrimidin-4-yl)amino)methylene)bis(phosphonic Acid) (**13a**).* The synthesis and characterization were previously reported.[29]

*(((2-(3-((4-Methoxyphenyl)carbamoyl)phenyl)thieno[2,3-d]pyrimidin-4-yl)amino)methylene)bis(phosphonic Acid) (CML-07-90, **13b**).* The synthesis and characterization were previously reported.[29]

*(((2-(3-((3-Fluoro-4-methoxyphenyl)carbamoyl)phenyl)thieno[2,3-d]pyrimidin-4-yl)amino)methylene)bis(phosphonic Acid) (**13c**).* The synthesis and characterization were previously reported.[29]

*(((2-(3-((3-Chloro-4-methoxyphenyl)carbamoyl)phenyl)thieno[2,3-d]pyrimidin-4-yl)amino)methylene)bis(phosphonic Acid) (**13d**).* The tetraethyl ester was isolated as an off-white solid (49.9 mg, 72%). ^{1}H NMR (500 MHz, $CDCl_3$): δ 9.34 (s, 1H), 9.23 (s, 1H), 8.62 (dt, J = 7.8, 1.4 Hz, 1H), 8.16 (d, J = 7.7 Hz, 1H), 7.93 (dd, J = 8.8, 2.6 Hz, 1H), 7.87 (d, J = 2.6 Hz, 1H), 7.59 (t, J = 7.7 Hz, 1H), 7.41 (d, J = 6.0 Hz, 1H), 7.24 (d, J = 6.0 Hz, 1H), 6.91 (d, J = 8.9 Hz, 2H), 5.71−5.46 (m, 1H), 4.26−4.08 (m, 8H), 3.90 (s, 3H), 1.22 (t, J = 7.1 Hz, 12H). ^{31}P NMR (203 MHz, $CDCl_3$): δ 17.33. ^{13}C NMR (126 MHz, $CDCl_3$): δ 168.4, 165.3, 158.5, 155.8, 151.7, 138.0, 134.6, 132.8, 131.1, 130.3, 129.1, 126.9, 123.8, 122.9, 122.2, 120.3, 117.9, 115.5, 112.2, 63.9 (t, J = 3.3 Hz), 63.7 (t, J = 3.2 Hz), 56.5, 47.3 (t, J = 148.0 Hz), 16.5 (t, J = 3.1 Hz), 16.4 (t, J = 3.1 Hz). MS [ESI$^+$] m/z: 697.2 [M + H$^+$]$^+$. Inhibitor **13d** was isolated as a light yellow solid (40.1 mg, 95%). ^{1}H NMR (800 MHz, 0.5% NH_4OH in D_2O): δ 8.78 (t, J = 1.9 Hz, 1H), 8.55 (dt, J = 7.8, 1.3 Hz, 1H), 8.03 (dt, J = 7.9, 1.3 Hz, 1H), 7.76−7.70 (m, 2H), 7.64 (d, J = 5.9 Hz, 1H), 7.52−7.48 (m, 2H), 7.23 (d, J = 8.9 Hz, 1H), 5.17 (t, J = 18.8 Hz, 1H), 3.97 (s, 3H). ^{31}P NMR (203 MHz, 0.5% NH_4OH in D_2O): δ 13.70. ^{13}C NMR (201 MHz, 0.5% NH_4OH in D_2O): δ 167.9, 165.3, 159.3, 156.9, 151.3, 138.0, 133.6, 131.8, 130.8, 129.1, 129.1, 126.8, 123.4, 123.1, 121.7, 120.9, 118.8, 115.9, 112.6, 56.0, 50.0 (t, J = 124.5 Hz). HRMS [ESI$^-$] calculated for $C_{21}H_{18}ClN_4O_8P_2S$ m/z, 583.0015; found 583.0009 [M − H]$^-$.

*(((2-(3-((3-Bromo-4-methoxyphenyl)carbamoyl)phenyl)thieno[2,3-d]pyrimidin-4-yl)amino)methylene)bis(phosphonic Acid) (**13e**).* The tetraethyl ester was isolated as an off-white solid (50.9 mg, 69%). ^{1}H NMR (500 MHz, $CDCl_3$): δ 9.32 (s, 1H), 9.13 (s, 1H), 8.63 (dt, J = 7.9, 1.4 Hz, 1H), 8.17 (dt, J = 7.9, 1.5 Hz, 1H), 8.07−7.94 (m, 2H), 7.60 (t, J = 7.8 Hz, 1H), 7.39 (d, J = 6.0 Hz, 1H), 7.28 (d, J = 6.0 Hz, 1H), 6.90 (d, J = 8.8 Hz, 1H), 6.66 (s, 1H), 5.58 (td, J = 22.4, 8.4 Hz, 1H), 4.27−4.07 (m, 8H), 3.90 (s, 3H), 1.23 (t, J = 7.0z Hz, 6H), 1.22 (t, J = 7.1 Hz, 6H). ^{31}P NMR (203 MHz, $CDCl_3$): δ 17.26. ^{13}C NMR (126 MHz, $CDCl_3$): δ 165.2, 158.5, 155.8, 152.7, 134.7, 133.1, 131.2, 130.3, 129.1, 126.8, 125.9, 124.0, 121.1, 117.8, 115.5, 112.0, 111.3, 63.9 (t, J = 3.3 Hz), 63.8 (t, J = 3.3 Hz), 56.6, 47.3 (t, J = 149.0 Hz), 16.5 (t, J = 3.0 Hz), 16.5 (t, J = 3.0 Hz). MS [ESI$^+$] m/z: 741.1 [M + H$^+$]$^+$. Inhibitor **13e** was isolated as a light yellow solid (35 mg, 81%). ^{1}H NMR (500 MHz, 0.5% NH_4OH in D_2O): δ 8.75 (t, J = 1.9 Hz, 1H), 8.54 (dt, J = 7.8, 1.5 Hz, 1H), 8.01 (dt, J = 8.0, 1.4 Hz, 1H), 7.86 (d, J = 2.6 Hz, 1H), 7.72 (t, J = 7.8 Hz, 1H), 7.62 (d, J = 5.9 Hz, 1H), 7.53 (dd, J = 8.8, 2.6 Hz, 1H), 7.50 (d, J = 5.9 Hz, 1H), 7.17 (d, J = 8.9 Hz, 1H), 5.17 (t, J = 19.0 Hz, 1H), 3.94 (s, 3H). ^{31}P NMR (203 MHz, 0.5% NH_4OH in D_2O): δ 13.75. ^{13}C NMR (201 MHz, 0.5% NH_4OH in D_2O): δ 169.3, 165.6, 159.7, 157.1, 153.1, 138.3, 134.1, 132.1, 131.0, 129.4, 129.3, 127.9, 126.9, 123.8, 123.2, 118.9, 115.9, 112.9, 110.4, 56.4, 49.2 (t, J = 123.4 Hz). HRMS [ESI$^-$] calculated for $C_{21}H_{18}BrN_4O_8P_2S$ m/z, 626.9509; found 626.9527 [M − H]$^-$.

*(((2-(3-((3-Fluoro-4-methylphenyl)carbamoyl)phenyl)thieno[2,3-d]pyrimidin-4-yl)amino)methylene)bis(phosphonic Acid) (**13f**).* The tetraethyl ester was isolated as an off-white solid (33.9 mg, 51%). ^{1}H NMR (500 MHz, $CDCl_3$): δ 9.27 (s, 1H), 9.01 (s, 1H), 8.63 (dt, J = 7.8, 1.4 Hz, 1H), 8.15 (dt, J = 7.8, 1.6 Hz, 1H), 7.68 (dd, J = 11.7, 2.1 Hz, 1H), 7.60 (t, J = 7.8 Hz, 1H), 7.54 (dd, J = 8.3, 2.1 Hz, 1H), 7.39 (d, J = 6.0 Hz, 1H), 7.28 (d, J = 6.0 Hz, 1H), 7.14 (t, J = 8.4 Hz, 1H), 6.64 (s, 1H), 5.64 (td, J = 22.7, 8.8 Hz, 1H), 4.28−4.09 (m, 8H), 2.25 (d, J = 1.8 Hz, 3H), 1.23 (t, J = 7.1 Hz, 6H), 1.22 (t, J = 7.1 Hz, 6H). ^{31}P NMR (203 MHz, $CDCl_3$): δ 17.21. ^{13}C NMR (126 MHz, $CDCl_3$): δ 168.3, 165.2, 161.1 (d, J = 242.9 Hz), 158.4, 155.7, 137.9, 137.8, 134.7, 131.3−130.9 (m), 130.1, 129.0, 126.6, 123.9, 120.2 (d, J = 17.4 Hz), 117.7, 115.6 (d, J = 3.2 Hz), 115.4, 107.6 (d, J = 27.2 Hz), 63.7 (t, J = 3.2 Hz), 63.6 (t, J = 3.3 Hz), 46.7 (t, J = 149.2 Hz), 16.3 (dt, J = 6.3, 2.9 Hz), 14.1 (d, J = 3.1 Hz). MS [ESI$^+$] m/z: 665.2 [M + H$^+$]$^+$. Inhibitor **13f** was isolated as a pale yellow solid (21 mg, 75%). ^{1}H NMR (500 MHz, 0.5% NH_4OH in D_2O): δ 8.68 (t, J = 1.9 Hz, 1H), 8.46 (dt, J = 7.9, 1.4 Hz, 1H), 7.94 (dt, J = 8.0, 1.3 Hz, 1H), 7.65 (t, J = 7.8 Hz, 1H), 7.54 (d, J = 6.0 Hz, 1H), 7.41 (d, J = 6.0 Hz, 1H), 7.34 (dd, J = 11.3, 2.1 Hz, 1H), 7.25 (t, J = 8.4 Hz, 1H), 7.19 (dd, J = 8.2, 2.1 Hz, 1H), 5.05 (t, J = 19.0 Hz, 1H), 2.20 (d, J = 1.9 Hz, 3H). ^{31}P NMR (203 MHz, 0.5% NH_4OH in D_2O): δ 13.68. ^{13}C NMR (201 MHz, 0.5% NH_4OH in D_2O): δ 169.4, 165.5, 160.8 (d, J = 242.0 Hz), 159.8, 157.1, 138.3, 135.9 (d, J = 10.5 Hz; couple to ^{19}F) 134.3, 132.1, 131.7 (d, J = 6.4 Hz), 129.5, 129.3, 126.9, 123.2, 122.4 (d, J = 17.6 Hz), 119.0, 118.2 (d, J = 3.4 Hz), 115.9, 109.6 (d, J = 26.3 Hz), 49.4 (t, J = 123.0 Hz), 13.3 (d, J = 3.1 Hz). HRMS [ESI$^-$] calculated for $C_{21}H_{18}FN_4O_7P_2S$ m/z, 551.0361; found 567.0358 [M − H]$^-$.

*(((2-(3-((3-Chloro-4-methylphenyl)carbamoyl)phenyl)thieno[2,3-d]pyrimidin-4-yl)amino)methylene)bis(phosphonic Acid) (**13g**).* The tetraethyl ester was isolated as an off-white solid (39.4 mg, 58%). ^{1}H NMR (500 MHz, $CDCl_3$): δ 9.33 (s, 1H), 9.17 (s, 1H), 8.63 (dt, J = 7.8, 1.4 Hz, 1H), 8.17 (dt, J = 7.8, 1.5 Hz, 1H), 7.90 (d, J = 2.3 Hz, 1H), 7.80 (dd, J = 8.3, 2.2 Hz, 1H), 7.60 (t, J = 7.7 Hz, 1H), 7.40 (d, J = 6.0 Hz, 1H), 7.25 (d, J = 5.7 Hz, 1H), 7.19 (d, J = 8.3 Hz, 1H), 6.80 (s, 1H), 5.58 (td, J = 23.0, 22.4, 8.3 Hz, 1H), 4.28−4.09 (m, 8H), 2.35 (s, 3H), 1.23 (t, J = 7.1 Hz, 6H), 1.25−1.19 (m, 6H). ^{31}P NMR (203 MHz, $CDCl_3$): δ 17.29. ^{13}C NMR (126 MHz, $CDCl_3$): δ 168.4, 165.3, 158.5, 155.8, 138.0, 137.9, 134.7, 134.2, 131.6, 131.2, 131.0, 130.3, 129.1, 126.9, 123.9, 121.0, 118.9, 117.8, 115.5, 63.9 (t, J = 3.2 Hz), 63.7 (t, J = 3.3 Hz), 47.2 (t, J = 149.2 Hz), 19.6, 16.5 (t, J = 3.2 Hz), 16.4 (d, J = 3.0 Hz). MS [ESI$^-$] m/z: 679.2 [M − H]$^-$. Inhibitor **13g** was isolated as a pale yellow solid (30 mg, 91%). ^{1}H NMR (500 MHz, 0.5% NH_4OH in D_2O): δ 8.76 (t, J = 1.9 Hz, 1H), 8.55 (dt, J = 7.9, 1.4 Hz, 1H), 8.02 (dt, J = 8.0, 1.2 Hz, 1H), 7.73 (t, J = 7.8 Hz, 1H), 7.70 (d, J = 2.0 Hz, 1H), 7.62 (d, J = 6.0 Hz, 1H), 7.50 (d, J = 5.9 Hz, 1H), 7.43−7.37 (m,

https://doi.org/10.1021/acs.jmedchem.1c01913
J. Med. Chem. XXXX, XXX, XXX−XXX

2H), 5.15 (t, J = 19.0 Hz, 1H), 2.39 (s, 3H). ^{31}P NMR (203 MHz, 0.5% NH_4OH in D_2O): δ 13.64. ^{13}C NMR (201 MHz, 0.5% NH_4OH in D_2O): δ 168.7, 165.3, 159.6, 157.0, 138.2, 135.8, 134.1, 133.7, 133.3, 131.9, 131.2, 129.3, 129.3, 126.9, 123.0, 122.4, 120.7, 119.0, 116.0, 50.6 (t, J = 125.8 Hz), 18.7. HRMS [ESI$^-$] calculated for $C_{21}H_{18}ClN_4O_7P_2S$ m/z, 567.0065; found 567.0065 [M − H]$^-$.

*(((2-(3-((3-Bromo-4-methylphenyl)carbamoyl)phenyl)thieno[2,3-d]pyrimidin-4-yl)amino)methylene)bis(phosphonic Acid) (**13h**).* The tetraethyl ester was isolated as an off-white solid (40.4 mg, 56%). ^{1}H NMR (500 MHz, $CDCl_3$): δ 9.33 (s, 1H), 9.17 (s, 1H), 8.63 (dt, J = 7.8, 1.4 Hz, 1H), 8.17 (dt, J = 7.9, 1.5 Hz, 1H), 8.06 (d, J = 2.2 Hz, 1H), 7.86 (dd, J = 8.4, 2.2 Hz, 1H), 7.60 (t, J = 7.8 Hz, 1H), 7.40 (d, J = 6.0 Hz, 1H), 7.28−7.24 (m, 1H), 7.20 (d, J = 8.3 Hz, 1H), 6.79 (s, 1H), 5.70−5.48 (m, 1H), 4.28−4.08 (m, 8H), 2.37 (s, 3H), 1.23 (t, J = 7.1 Hz, 12H). ^{31}P NMR (203 MHz, $CDCl_3$): δ 17.29. ^{13}C NMR (126 MHz, $CDCl_3$): δ 168.5, 165.3, 158.5, 155.8, 138.0, 137.9, 134.6, 133.4, 131.2, 130.8, 130.3, 129.1, 126.8, 124.6, 124.2, 123.9, 119.6, 117.8, 115.5, 63.9 (t, J = 3.3 Hz), 63.7 (t, J = 3.3 Hz), 47.2 (t, J = 148.1 Hz), 22.4, 16.5 (t, J = 3.0 Hz), 16.5 (t, J = 3.1 Hz). MS [ESI$^-$] m/z: 723.2 [M − H]$^-$. Inhibitor **13h** was isolated as a light yellow solid (24 mg, 70%). ^{1}H NMR (500 MHz, 0.5% NH_4OH in D_2O): δ 8.61 (s, 1H), 8.45 (d, J = 7.5 Hz, 1H), 7.90 (d, J = 7.8 Hz, 1H), 7.76 (s, 1H), 7.63 (t, J = 8.0 Hz, 1H), 7.54 (d, J = 6.0 Hz, 1H), 7.44 (d, J = 6.0 Hz, 1H), 7.33 (d, J = 8.3 Hz, 1H), 7.22 (d, J = 8.4 Hz, 1H), 5.16 (t, J = 19.0 Hz, 1H), 2.26 (s, 3H). ^{31}P NMR (203 MHz, 0.5% NH_4OH in D_2O): δ 13.66. ^{13}C NMR (201 MHz, 0.5% NH_4OH in D_2O) δ 168.5, 165.5, 159.4, 156.9, 138.1, 135.8, 135.0, 133.8, 132.0, 130.8, 129.3, 129.2, 126.9, 125.3, 123.9, 123.2, 121.1, 118.8, 115.9, 49.4 (t, J = 118.4 Hz), 21.5. HRMS [ESI$^-$] calculated for $C_{21}H_{18}BrN_4O_7P_2S$ m/z, 610.9560; found 610.9558 [M − H]$^-$.

*General Procedure for Synthesis of Sulfonamides **14a−e**.* Step 1: In a culture tube, the required substituted aniline (0.15 mmol) and pyridine (60.4 μL, 0.75 mmol) were dissolved in anhydrous DCM (1.4 mL), and intermediate **22** (61.2 mg, 0.1 mmol) was added. The reaction mixtures were stirred at RT overnight, and the completion of the coupling was confirmed by TLC and LCMS. Each reaction mixture was evaporated to dryness under vacuum, and the residues were purified on silica gel by flash chromatography (using 1−3% MeOH in $CHCl_3$ as the eluent) to give the sulfonamide derivatives **14** as their tetraesters in a 16−57% isolated yield.

Step 2: Deprotection of the phosphonate tetraethyl esters with TMSBr followed by methanolysis was carried out as previously reported[29] to give inhibitors **14a−e**.

*(((2-(3-(N-(3-Fluoro-4-methoxyphenyl)sulfamoyl)phenyl)thieno-[2,3-d]pyrimidin-4-yl)amino)methylene)bis(phosphonic Acid) (**14a**).* The tetraethyl ester was isolated as a light yellow solid (40.9 mg, 57%). ^{1}H NMR (500 MHz, $CDCl_3$): δ 9.00 (t, J = 1.8 Hz, 1H), 8.58 (dt, J = 7.9, 1.4 Hz, 1H), 8.50−8.46 (m, 1H), 7.83 (ddd, J = 7.8, 2.0, 1.1 Hz, 1H), 7.49 (t, J = 7.8 Hz, 1H), 7.37 (d, J = 6.0 Hz, 1H), 7.26 (d, J = 5.9 Hz, 1H), 6.97 (dd, J = 12.1, 2.5 Hz, 1H), 6.90 (ddd, J = 8.8, 2.6, 1.4 Hz, 1H), 6.77 (t, J = 9.0 Hz, 1H), 6.39 (d, J = 9.7 Hz, 1H), 5.95 (td, J = 22.3, 9.7 Hz, 1H), 4.33−4.14 (m, 8H), 1.26 (t, J = 7.1 Hz, 6H), 1.24 (t, J = 7.1 Hz, 6H). ^{31}P NMR (162 MHz, $CDCl_3$): δ 16.9. ^{13}C NMR (126 MHz, $CDCl_3$): δ 168.3, 157.4, 155.7 (t, J = 4.0 Hz), 152.2 (d, J = 246.7 Hz), 145.4 (d, J = 10.7 Hz), 139.8, 139.2, 132.2, 130.3 (d, J = 8.7 Hz), 129.0, 128.8, 127.1, 124.3, 118.1 (d, J = 3.6 Hz), 118.0, 115.8, 113.8 (d, J = 2.7 Hz), 111.2, 111.0, 64.1 (t, J = 3.3 Hz), 64.0 (t, J = 3.2 Hz), 56.5, 45.0 (t, J = 147.7 Hz), 16.5 (t, J = 2.8 Hz), 16.4 (t, J = 2.9 Hz). MS [ESI$^+$] m/z: 717.4 [M + H$^+$]$^+$. Inhibitor **14a** was isolated as a white solid (16.4 mg, 48%). ^{1}H NMR (500 MHz, 0.5% NH_4OH in D_2O): δ 8.57 (s, 1H), 8.55 (d, J = 8.1 Hz, 1H), 7.88 (dt, J = 7.9, 1.5 Hz, 1H), 7.66 (t, J = 7.8 Hz, 1H), 7.61 (d, J = 6.0 Hz, 1H), 7.49 (d, J = 6.0 Hz, 1H), 6.97−6.89 (m, 1H), 6.80 (dd, J = 13.6, 2.6 Hz, 1H), 6.69 (ddd, J = 8.9, 2.6, 1.4 Hz, 1H), 5.08 (t, J = 18.9 Hz, 1H), 3.78 (s, 3H). ^{31}P NMR (203 MHz, 0.5% NH_4OH in D_2O): δ 13.67. ^{13}C NMR (201 MHz, 0.5% NH_4OH in D_2O): δ 165.4, 159.5, 157.0, 152.1 (d, J = 242.8 Hz), 143.1, 141.2 (d, J = 11.0 Hz), 140.1 (d, J = 8.5 Hz), 138.6, 131.6, 129.5, 128.1, 125.6, 123.1, 119.0, 118.5 (d, J = 2.9 Hz), 116.0, 114.9 (d, J = 2.7 Hz), 110.9 (d, J = 19.0 Hz), 56.8. C-α to the bisphosphonate was observed by HSQC. HSQC (^{1}H−^{13}C): ^{1}H at δ 5.08 correlates to ^{13}C-α at δ 50.3. HRMS [ESI$^-$] calculated for $C_{20}H_{18}FN_4O_9P_2S_2$ m/z, 602.9980; found 602.9958 [M − H]$^-$.

*(((2-(3-(N-(3-Chloro-4-methoxyphenyl)sulfamoyl)phenyl)thieno-[2,3-d]pyrimidin-4-yl)amino)methylene)bis(phosphonic Acid) (**14b**).* The tetraethyl ester was isolated as a light yellow solid (28.3 mg, 38.6%). ^{1}H NMR (500 MHz, $CDCl_3$): δ 9.00 (t, J = 1.8 Hz, 1H), 8.58 (dt, J = 7.9, 1.4 Hz, 1H), 8.35 (s, 1H), 7.80 (ddd, J = 7.8, 2.0, 1.1 Hz, 1H), 7.49 (t, J = 7.8 Hz, 1H), 7.38 (d, J = 6.0 Hz, 1H), 7.27 (d, J = 6.0 Hz, 1H), 7.18 (d, J = 2.6 Hz, 1H), 7.07 (dd, J = 8.8, 2.6 Hz, 1H), 6.75 (d, J = 8.9 Hz, 1H), 6.34 (dt, J = 9.7, 1.8 Hz, 1H), 5.94 (td, J = 22.2, 9.7 Hz, 1H), 4.33−4.13 (m, 8H), 3.80 (s, 3H), 1.25 (t, J = 7.1 Hz, 6H), 1.24 (t, J = 7.1 Hz, 6H). ^{31}P NMR (162 MHz, $CDCl_3$): δ 16.91. ^{13}C NMR (126 MHz, $CDCl_3$): δ 168.3, 157.4, 155.7 (t, J = 3.8 Hz), 152.9, 139.8, 139.2, 132.3, 130.4, 129.0, 128.8, 127.1, 124.8, 124.4, 122.7, 122.1, 117.9, 115.8, 112.4, 64.1 (t, J = 3.2 Hz), 64.0 (t, J = 3.3 Hz), 56.4, 46.2, 45.0, 16.5 (t, J = 2.8 Hz), 16.5 (t, J = 3.0 Hz). MS [ESI$^+$] m/z: 733.4 [M + H$^+$]$^+$. Inhibitor **14b** was isolated as a white solid (14.7 mg, 61%). ^{1}H NMR (500 MHz, 0.5% NH_4OH in D_2O): δ 8.59−8.54 (m, 2H), 7.87 (dt, J = 8.0, 1.5 Hz, 1H), 7.66 (t, J = 7.9 Hz, 1H), 7.61 (d, J = 6.0 Hz, 1H), 7.49 (d, J = 6.0 Hz, 1H), 7.04 (d, J = 2.6 Hz, 1H), 6.93 (d, J = 8.9 Hz, 1H), 6.85 (dd, J = 8.9, 2.6 Hz, 1H), 5.07 (t, J = 18.8 Hz, 1H), 3.79 (s, 3H). ^{31}P NMR (203 MHz, 0.5% NH_4OH in D_2O): δ 13.70. ^{13}C NMR (201 MHz, 0.5% NH_4OH in D_2O) δ 165.41, 159.44, 156.97, 149.05, 142.99, 140.00, 138.57, 131.60, 129.44, 128.02, 125.53, 124.58, 123.17, 122.52, 121.49, 119.01, 116.01, 113.79, 56.50. C-α to the bisphosphonate was observed by HSQC. HSQC (^{1}H−^{13}C): ^{1}H at δ 5.07 correlates to ^{13}C-α at δ 50.0. HRMS [ESI$^-$] calculated for $C_{20}H_{18}ClN_4O_9P_2S_2$ m/z, 618.9684; found 618.9700 [M − H]$^-$.

*(((2-(3-(N-(3-Bromo-4-methoxyphenyl)sulfamoyl)phenyl)thieno-[2,3-d]pyrimidin-4-yl)amino)methylene)bis(phosphonic Acid) (**14c**).* The tetraethyl ester was isolated as a light yellow solid (23.6 mg, 30.4%). ^{1}H NMR (500 MHz, $CDCl_3$): δ 9.00 (t, J = 1.8 Hz, 1H), 8.59 (dt, J = 7.9, 1.4 Hz, 1H), 8.26 (s, 1H), 7.79 (ddd, J = 7.8, 2.0, 1.1 Hz, 1H), 7.49 (t, J = 7.8 Hz, 1H), 7.37 (d, J = 6.0 Hz, 1H), 7.34 (d, J = 2.6 Hz, 1H), 7.28 (d, J = 6.0 Hz, 1H), 7.13 (dd, J = 8.8, 2.6 Hz, 1H), 6.73 (d, J = 8.9 Hz, 1H), 6.31 (d, J = 9.7 Hz, 1H), 5.94 (td, J = 22.2, 9.7 Hz, 1H), 4.33−4.14 (m, 8H), 3.79 (s, 3H), 1.25 (t, J = 7.1 Hz, 6H), 1.25 (t, J = 7.1 Hz, 6H). ^{31}P NMR (162 MHz, $CDCl_3$): δ 16.91. ^{13}C NMR (126 MHz, $CDCl_3$): δ 168.3, 157.4, 155.7, 153.8, 139.7, 139.2, 132.3, 130.7, 129.0, 128.8, 127.8, 127.1, 124.4, 122.9, 117.9, 115.8, 112.2, 111.7, 64.1 (t, J = 3.2 Hz), 64.0 (t, J = 3.2 Hz), 56.5, 45.0 (t, J = 147.7 Hz), 16.5 (t, J = 3.0 Hz), 16.5 (t, J = 3.0 Hz). MS [ESI$^+$] m/z: 777.4 [M + H$^+$]$^+$. Inhibitor **14c** was isolated as a white solid (11.6 mg, 57%). ^{1}H NMR (500 MHz, 0.5% NH_4OH in D_2O): δ 8.58−8.53 (m, 2H), 7.86 (d, J = 7.8 Hz, 1H), 7.66 (t, J = 7.8 Hz, 1H), 7.61 (d, J = 6.0 Hz, 1H), 7.49 (d, J = 5.9 Hz, 1H), 7.22 (d, J = 2.1 Hz, 1H), 6.91 (d, J = 2.5 Hz, 2H), 5.10 (t, J = 18.6 Hz, 1H), 3.78 (s, 3H). ^{31}P NMR (203 MHz, 0.5% NH_4OH in D_2O): δ 13.69. ^{13}C NMR (201 MHz, 0.5% NH_4OH in D_2O): δ 165.5, 159.4, 157.0, 150.2, 142.7, 139.9, 138.5, 131.7, 129.4, 128.0, 127.7, 125.5, 123.4, 123.3, 118.9, 116.0, 113.6, 110.7, 56.6. C-α to the bisphosphonate was observed by HSQC. HSQC (^{1}H−^{13}C): ^{1}H at δ 5.10 correlates to ^{13}C-α at δ 49.4. HRMS [ESI$^-$] calculated for $C_{20}H_{18}BrN_4O_9P_2S_2$ m/z, 662.9179; found 662.9207 [M − H]$^-$.

*(((2-(3-(N-(3-Fluoro-4-methylphenyl)sulfamoyl)phenyl)thieno-[2,3-d]pyrimidin-4-yl)amino)methylene)bis(phosphonic Acid) (**14d**).* The tetraethyl ester was isolated as a light yellow solid (10.9 mg, 16%). ^{1}H NMR (500 MHz, $CDCl_3$): δ 9.01 (t, J = 1.8 Hz, 1H), 8.57 (dt, J = 7.9, 1.4 Hz, 1H), 8.45 (s, 1H), 7.89 (ddd, J = 7.7, 2.0, 1.1 Hz, 1H), 7.50 (t, J = 7.8 Hz, 1H), 7.29 (d, J = 6.0 Hz, 1H), 7.25 (d, J = 6.0 Hz, 1H), 6.98 (td, J = 8.3, 0.9 Hz, 1H), 6.91 (dd, J = 10.9, 2.2 Hz, 1H), 6.86 (dd, J = 8.2, 2.2 Hz, 1H), 6.31−6.25 (m, 1H), 5.94 (td, J = 22.3, 9.7 Hz, 1H), 4.33−4.14 (m, 8H), 2.13 (d, J = 1.8 Hz, 3H), 1.25 (t, J = 7.1 Hz, 6H), 1.25 (t, J = 7.1 Hz, 6H). ^{31}P NMR (162 MHz, $CDCl_3$): δ 16.97. ^{13}C NMR (126 MHz, $CDCl_3$): δ 168.3, 161.3 (d, J = 245.0 Hz), 157.3, 155.6 (t, J = 3.8 Hz), 139.9, 139.2, 136.4 (d, J = 10.1 Hz), 132.3, 131.8 (d, J = 6.3 Hz), 129.0, 128.9, 127.0, 124.4, 121.1 (d, J = 17.4 Hz), 117.8, 116.1 (d, J = 3.3 Hz), 115.8, 108.0 (d, J = 26.1 Hz), 64.2 (t, J = 3.3 Hz), 63.9 (t, J = 3.3 Hz), 45.0 (t, J = 148.2 Hz), 16.5 (t, J = 3.6 Hz), 16.4 (t, J = 2.9 Hz), 14.1 (d, J = 3.0 Hz). MS [ESI$^+$] m/z: 701.5 [M + H$^+$]$^+$. Inhibitor **14d** was isolated as a white solid (2 mg, 22%). ^{1}H NMR (800

https://doi.org/10.1021/acs.jmedchem.1c01913
J. Med. Chem. XXXX, XXX, XXX−XXX

MHz, 0.5% NH_4OH in D_2O): δ 8.61 (s, 1H), 8.58 (d, J = 7.8 Hz, 1H), 7.91 (d, J = 7.8 Hz, 1H), 7.67 (t, J = 7.8 Hz, 1H), 7.62 (d, J = 5.9 Hz, 1H), 7.50 (d, J = 5.9 Hz, 1H), 7.03 (t, J = 8.7 Hz, 1H), 6.71 (dd, J = 12.3, 2.2 Hz, 1H), 6.68 (dd, J = 8.2, 2.2 Hz, 1H), 5.14 (t, J = 19.0 Hz, 1H), 2.10 (s, 3H). ^{31}P NMR (203 MHz, 0.5% NH_4OH in D_2O): δ 13.87. ^{13}C NMR (201 MHz, 0.5% NH_4OH in D_2O): δ 165.6, 161.2 (d, J = 241.5 Hz), 159.4, 157.0, 144.3, 142.6, 138.7, 131.9, 131.4 (d, J = 6.7 Hz), 129.5, 128.1, 125.6, 123.3, 118.9, 117.9 (d, J = 2.7 Hz), 117.5 (d, J = 17.1 Hz), 115.9, 108.8 (d, J = 23.6 Hz), 12.8 (d, J = 3.2 Hz). C-α to the bisphosphonate was observed by HSQC. HSQC (^{1}H−^{13}C): ^{1}H at δ 5.14 correlates to ^{13}C-α at δ 49.4. HRMS [ESI$^-$] calculated for $C_{20}H_{18}FN_4O_8P_2S_2$ m/z, 587.0031; found 587.0040 [M − H]$^-$.

*(((2-(3-(N-(3-Chloro-4-methylphenyl)sulfamoyl)phenyl)thieno-[2,3-d]pyrimidin-4-yl)amino)methylene)bis(phosphonic Acid) (**14e**).* The tetraethyl ester was isolated as a light yellow solid (21.2 mg, 30%). ^{1}H NMR (500 MHz, $CDCl_3$): δ 9.01 (t, J = 1.8 Hz, 1H), 8.70 (s, 1H), 8.57 (dt, J = 7.9, 1.4 Hz, 1H), 7.89 (ddd, J = 7.8, 2.0, 1.1 Hz, 1H), 7.50 (t, J = 7.8 Hz, 1H), 7.33 (d, J = 6.1 Hz, 1H), 7.24 (d, J = 6.0 Hz, 1H), 7.19 (t, J = 1.2 Hz, 1H), 7.03 (d, J = 1.6 Hz, 2H), 6.36 (d, J = 9.7 Hz, 1H), 5.96 (td, J = 22.3, 9.7 Hz, 1H), 4.33−4.14 (m, 8H), 2.22 (s, 3H), 1.25 (t, J = 7.1 Hz, 6H), 1.25 (t, J = 7.1 Hz, 6H). ^{31}P NMR (203 MHz, $CDCl_3$): δ 16.99. ^{13}C NMR (126 MHz, $CDCl_3$): δ 168.3, 157.3, 155.6, 139.9, 139.2, 136.2, 134.7, 132.4, 132.3, 131.4, 129.1, 128.8, 127.1, 124.3, 121.5, 119.2, 117.9, 115.8, 64.2 (t, J = 3.2 Hz), 64.0 (t, J = 3.2 Hz), 45.0 (t, J = 147.8 Hz), 19.5, 16.5 (t, J = 2.8 Hz), 16.5 (t, J = 2.8 Hz). MS [ESI$^+$] m/z: 717.3 [M + H$^+$]$^+$. Inhibitor **14e** was isolated as a white solid (7.5 mg, 42%). ^{1}H NMR (500 MHz, 0.5% NH_4OH in D_2O): δ 8.60 (t, J = 1.8 Hz, 1H), 8.57 (dt, J = 7.8, 1.5 Hz, 1H), 7.90 (ddd, J = 7.8, 1.9, 1.1 Hz, 1H), 7.67 (t, J = 7.8 Hz, 1H), 7.61 (d, J = 6.0 Hz, 1H), 7.48 (d, J = 5.9 Hz, 1H), 7.07 (dd, J = 8.2, 0.8 Hz, 1H), 7.00 (d, J = 2.3 Hz, 1H), 6.80 (dd, J = 8.2, 2.4 Hz, 1H), 5.06 (t, J = 18.8 Hz, 1H), 2.20 (s, 3H). ^{31}P NMR (203 MHz, 0.5% NH_4OH in D_2O): δ 13.66. ^{13}C NMR (201 MHz, 0.5% NH_4OH in D_2O): δ 165.34, 159.47, 156.96, 145.13, 143.16, 138.63, 133.69, 131.66, 131.11, 129.50, 128.20, 128.04, 125.49, 123.10, 122.41, 121.00, 119.05, 116.04, 18.15. C-α to the bisphosphonate was observed by HSQC. HSQC (^{1}H−^{13}C): ^{1}H at δ 5.06 correlates to ^{13}C-α at δ 49.7. HRMS [ESI$^-$] calculated for $C_{20}H_{18}ClN_4O_8P_2S_2$ m/z, 602.9735; found 602.9759 [M − H]$^-$.

*General Procedure for Synthesis of Sulfonamides **15a−e**.* Intermediate **21** (52.8 mg, 0.1 mmol) and pyridine (60 μL, 0.75 mmol) were dissolved in DCM (1.4 mL) in a sample vial. Arylsulfonyl chloride (0.12 mmol) was added, and the mixture was stirred at RT and monitored by TLC and LCMS. Upon completion of the reaction, the mixture was dried under vacuum and the residue was purified on silica gel by flash chromatography (typically, the products eluted at 5−10% MeOH in EtOAc); in some cases, a second purification was required, which was carried out on C18 reversed-phase silica using a CombiFlash instrument. Isolated yields ranged from 32 to 55%.

*(((2-(3-((3-Fluoro-4-methoxyphenyl)sulfonamido)phenyl)thieno-[2,3-d]pyrimidin-4-yl)amino)methylene)bis(phosphonic Acid) (**15a**).* The tetraethyl ester was isolated as a light yellow solid (35.0 mg, 49%). ^{1}H NMR (500 MHz, $CDCl_3$): δ 8.23 (s, 1H), 8.19 (t, J = 1.7 Hz, 0H), 8.18 (t, J = 1.9 Hz, 0H), 7.68 (ddd, J = 8.6, 2.2, 1.1 Hz, 1H), 7.63 (dd, J = 10.4, 2.3 Hz, 1H), 7.42 (d, J = 6.0 Hz, 1H), 7.37−7.28 (m, 3H), 6.95 (t, J = 8.3 Hz, 1H), 6.22 (d, J = 10.0 Hz, 1H), 6.02 (td, J = 22.1, 9.9 Hz, 1H), 4.35−4.14 (m, 8H), 3.86 (s, 3H), 1.24 (t, J = 6.9 Hz, 6H), 1.23 (t, J = 6.9 Hz, 6H). ^{31}P NMR (203 MHz, $CDCl_3$): δ 16.90. ^{13}C NMR (126 MHz, $CDCl_3$): δ 168.5, 158.5, 155.5, 151.7 (d, J = 251.1 Hz), 151.6 (d, J = 10.2 Hz), 139.2, 137.4, 131.5 (d, J = 5.7 Hz), 129.5, 125.0 (d, J = 3.7 Hz), 124.7, 124.0, 122.1, 120.2, 117.8, 115.5, 115.5 (d, J = 21.4 Hz), 112.8, 64.1 (t, J = 3.2 Hz), 63.9 (t, J = 3.3 Hz), 56.4, 44.5 (t, J = 147.1 Hz), 16.5−16.4 (m). MS [ESI$^+$] m/z: 717.2 [M + H$^+$]$^+$. Inhibitor **15a** was isolated as a white solid (26 mg, 88%). ^{1}H NMR (500 MHz, 0.5% NH_4OH in D_2O): δ 7.91 (dt, J = 7.9, 1.4 Hz, 1H), 7.72 (t, J = 2.0 Hz, 1H), 7.65−7.60 (m, 2H), 7.58 (d, J = 6.0 Hz, 1H), 7.46 (d, J = 6.0 Hz, 1H), 7.35 (t, J = 7.9 Hz, 1H), 7.21 (t, J = 8.6 Hz, 1H), 7.11 (ddd, J = 8.1, 2.3, 1.0 Hz, 1H), 5.08 (t, J = 18.9 Hz, 1H), 3.91 (s, 3H). ^{31}P NMR (203 MHz, 0.5% NH_4OH in D_2O): δ 13.83. ^{13}C NMR (201 MHz, 0.5% NH_4OH in D_2O): δ 165.6, 160.4, 157.0, 151.4 (d, J = 247.2 Hz), 149.8 (d, J = 10.3 Hz), 144.9, 138.5, 134.4 (d, J = 5.3 Hz), 129.5, 123.9, 123.9 (d, J = 3.5 Hz), 122.9, 121.7, 121.6, 118.9, 115.6, 114.4 (d, J = 21.0 Hz), 113.6, 56.3, 49.2 (t, J = 121.6 Hz). HRMS [ESI$^-$] calculated for $C_{20}H_{18}FN_4O_9P_2S_2$ m/z, 602.9980; found 602.9964 [M − H]$^-$.

*(((2-(3-((3-Chloro-4-methoxyphenyl)sulfonamido)phenyl)thieno-[2,3-d]pyrimidin-4-yl)amino)methylene)bis(phosphonic Acid) (**15b**).* The tetraethyl ester was isolated as a light yellow solid (39.6 mg, 54%). ^{1}H NMR (500 MHz, $CDCl_3$): δ 9.26 (s, 1H), 8.31 (d, J = 2.2 Hz, 1H), 8.24−8.15 (m, 1H), 7.95 (d, J = 2.2 Hz, 1H), 7.84 (dd, J = 8.7, 2.3 Hz, 1H), 7.50 (d, J = 6.0 Hz, 1H), 7.35−7.30 (m, 2H), 7.27−7.20 (m, 1H), 6.89 (d, J = 8.8 Hz, 1H), 6.51 (d, J = 9.9 Hz, 1H), 6.10 (td, J = 22.3, 9.9 Hz, 1H), 4.37−4.15 (m, 8H), 3.85 (s, 3H), 1.25 (t, J = 7.0 Hz, 6H), 1.22 (t, J = 7.1 Hz, 6H). ^{31}P NMR (203 MHz, $CDCl_3$): δ 16.94. ^{13}C NMR (126 MHz, $CDCl_3$): δ 168.5, 158.6, 158.4, 155.6 (t, J = 3.7 Hz), 139.2, 137.7, 132.1, 129.4, 129.3, 128.2, 124.3, 123.7, 123.2, 121.8, 119.9, 118.2, 115.6, 111.6, 64.2 (t, J = 3.2 Hz), 64.0 (t, J = 3.3 Hz), 56.5, 44.4 (t, J = 147.5 Hz), 16.5−16.4 (m). MS [ESI$^+$] m/z: 733.2 [M + H$^+$]$^+$. Inhibitor **15b** was isolated as a light yellow solid (18 mg, 54%). ^{1}H NMR (800 MHz, 0.5% NH_4OH in D_2O): δ 7.90−7.87 (m, 2H), 7.75 (dd, J = 8.7, 2.3 Hz, 1H), 7.70 (d, J = 2.1 Hz, 1H), 7.57 (d, J = 5.9 Hz, 1H), 7.44 (d, J = 5.9 Hz, 1H), 7.33 (t, J = 7.9 Hz, 1H), 7.15 (d, J = 8.8 Hz, 1H), 7.08 (dd, J = 8.0, 2.3 Hz, 1H), 5.03 (t, J = 18.9 Hz, 1H), 3.90 (s, 3H). ^{31}P NMR (203 MHz, 0.5% NH_4OH in D_2O): δ 13.62. ^{13}C NMR (201 MHz, 0.5% NH_4OH in D_2O): δ 165.5, 160.4, 156.9, 156.8, 145.6, 138.5, 135.3, 129.5, 128.3, 127.1, 124.0, 122.8, 121.9, 121.6, 121.4, 118.9, 115.7, 112.6, 56.4, 49.6 (t, J = 123.0 Hz). HRMS [ESI$^-$] calculated for $C_{20}H_{18}ClN_4O_9P_2S_2$ m/z, 618.9684; found 618.9669 [M − H]$^-$.

*(((2-(3-((3-Bromo-4-methoxyphenyl)sulfonamido)phenyl)thieno-[2,3-d]pyrimidin-4-yl)amino)methylene)bis(phosphonic Acid) (**15c**).* The tetraethyl ester was isolated as a light yellow solid (34.0 mg, 44%). ^{1}H NMR (500 MHz, $CDCl_3$): δ 8.86 (s, 1H), 8.27 (q, J = 1.5 Hz, 1H), 8.17 (ddd, J = 5.3, 3.3, 1.5 Hz, 1H), 8.10 (d, J = 2.3 Hz, 1H), 7.86 (dd, J = 8.7, 2.3 Hz, 1H), 7.46 (d, J = 6.0 Hz, 1H), 7.32 (dd, J = 5.1, 1.4 Hz, 2H), 7.27 (d, J = 6.0 Hz, 1H), 6.86 (d, J = 8.8 Hz, 1H), 6.37 (d, J = 9.9 Hz, 1H), 6.06 (td, J = 22.2, 9.9 Hz, 1H), 4.35−4.13 (m, 8H), 3.86 (s, 3H), 1.25 (t, J = 7.1 Hz, 6H), 1.23 (t, J = 7.0 Hz, 6H). ^{31}P NMR (203 MHz, $CDCl_3$): δ 16.93. ^{13}C NMR (126 MHz, $CDCl_3$) δ 168.5, 159.3, 158.6, 155.6, 139.2, 137.6, 132.5, 132.5, 129.4, 128.9, 124.5, 123.8, 121.9, 120.0, 118.1, 115.6, 112.1, 111.4, 64.1 (t, J = 3.2 Hz), 64.0 (t, J = 3.3 Hz), 56.6, 44.4 (t, J = 147.3 Hz), 16.5−16.4 (m). MS [ESI$^+$] m/z: 777.2 [M + H$^+$]$^+$. Inhibitor **15c** was isolated as a pale yellow solid (15 mg, 52%). ^{1}H NMR (500 MHz, 0.5% NH_4OH in D_2O): δ 8.05 (d, J = 2.3 Hz, 1H), 7.91 (d, J = 7.7 Hz, 1H), 7.80 (dd, J = 8.7, 2.3 Hz, 1H), 7.68 (t, J = 2.0 Hz, 1H), 7.58 (d, J = 6.0 Hz, 1H), 7.46 (d, J = 6.0 Hz, 1H), 7.35 (t, J = 7.9 Hz, 1H), 7.14 (d, J = 8.8 Hz, 1H), 7.09 (ddd, J = 8.1, 2.4, 1.0 Hz, 1H), 5.07 (t, J = 19.0 Hz, 1H), 3.91 (s, 3H). ^{31}P NMR (203 MHz, 0.5% NH_4OH in D_2O): δ 13.82. ^{13}C NMR (201 MHz, 0.5% NH_4OH in D_2O): δ 165.6, 160.4, 157.8, 156.9, 145.3, 138.5, 135.6, 131.4, 129.5, 127.9, 124.1, 122.9, 121.6 (2C), 118.9, 115.6, 112.5, 110.9, 56.5. C-α to the bisphosphonate was observed by HSQC. HSQC (^{1}H−^{13}C): ^{1}H at δ 5.07 correlates to ^{13}C-α at δ 49.2. HRMS [ESI$^-$] calculated for $C_{20}H_{18}BrN_4O_9P_2S_2$ m/z, 662.9179; found 662.9156 [M − H]$^-$.

*(((2-(3-((3-Fluoro-4-methylphenyl)sulfonamido)phenyl)thieno-[2,3-d]pyrimidin-4-yl)amino)methylene)bis(phosphonic Acid) (**15d**).* The tetraethyl ester was isolated as a light yellow solid (25.4 mg, 36%). ^{1}H NMR (500 MHz, $CDCl_3$): δ 8.78 (s, 1H), 8.26 (s, 1H), 8.20−8.15 (m, 1H), 7.59 (ddd, J = 19.0, 8.5, 1.8 Hz, 2H), 7.45 (d, J = 6.1 Hz, 1H), 7.36−7.30 (m, 2H), 7.27 (d, J = 6.0 Hz, 1H), 7.21 (t, J = 7.6 Hz, 1H), 6.34 (d, J = 9.9 Hz, 1H), 6.05 (td, J = 22.2, 9.9 Hz, 1H), 4.36−4.13 (m, 8H), 2.23 (d, J = 2.0 Hz, 3H), 1.25 (t, J = 7.0 Hz, 6H), 1.22 (t, J = 7.0 Hz, 6H). ^{31}P NMR (203 MHz, $CDCl_3$): δ 16.92. ^{13}C NMR (126 MHz, $CDCl_3$): δ 168.5, 160.8 (d, J = 249.6 Hz), 158.5, 155.6, 139.2, 138.8 (d, J = 6.8 Hz), 137.5, 132.0 (d, J = 5.0 Hz), 130.8 (d, J = 17.3 Hz), 129.4, 124.6, 123.8, 123.2 (d, J = 3.6 Hz), 122.0, 120.2, 118.0, 115.5, 114.4 (d, J = 25.6 Hz), 64.1 (t, J = 3.2 Hz), 63.9 (t, J = 3.2 Hz), 44.4 (t, J = 147.3 Hz), 16.5−16.4 (m), 14.8 (d, J = 3.4 Hz). MS [ESI$^+$] m/z: 701.3 [M + H$^+$]$^+$. Inhibitor **15d** was isolated as a light yellow solid (8 mg, 38%). ^{1}H NMR (500 MHz, 0.5% NH_4OH in D_2O):

https://doi.org/10.1021/acs.jmedchem.1c01913
J. Med. Chem. XXXX, XXX, XXX−XXX

δ 7.89 (d, J = 7.7 Hz, 1H), 7.71 (d, J = 2.1 Hz, 1H), 7.60−7.50 (m, 3H), 7.45 (d, J = 5.9 Hz, 1H), 7.39 (t, J = 7.7 Hz, 1H), 7.33 (t, J = 7.8 Hz, 1H), 7.08 (dd, J = 7.9, 2.3 Hz, 1H), 5.05 (t, J = 19.0 Hz, 1H), 2.28 (d, J = 1.8 Hz, 3H). ^{31}P NMR (203 MHz, 0.5% NH_4OH in D_2O): δ 13.82. ^{13}C NMR (201 MHz, 0.5% NH_4OH in D_2O): δ 165.5, 160.6 (d, J = 246.5 Hz), 160.5, 156.9, 145.9, 141.7 (d, J = 6.3 Hz), 138.5, 132.1 (d, J = 5.2 Hz), 129.5, 129.3 (d, J = 17.4 Hz), 123.9, 122.8, 122.1 (d, J = 3.4 Hz), 121.6, 121.3, 118.9, 115.6, 113.2 (d, J = 25.0 Hz), 49.5 (t, J = 121.7 Hz), 13.7 (d, J = 3.1 Hz). HRMS [ESI$^-$] calculated for $C_{20}H_{18}FN_4O_8P_2S_2$ m/z, 587.0031; found 587.0017 [M − H]$^-$.

*(((2-(3-((3-Chloro-4-methylphenyl)sulfonamido)phenyl)thieno-[2,3-d]pyrimidin-4-yl)amino)methylene)bis(phosphonic Acid) (**15e**).* The tetraethyl ester was isolated as a pale yellow solid (22.5 mg, 31.4%). ^{1}H NMR (500 MHz, $CDCl_3$): δ 8.69 (s, 1H), 8.25 (q, J = 1.5 Hz, 1H), 8.18 (pd, J = 4.3, 1.6 Hz, 1H), 7.89 (d, J = 1.9 Hz, 1H), 7.69 (dd, J = 8.0, 1.9 Hz, 1H), 7.43 (d, J = 6.0 Hz, 1H), 7.35−7.30 (m, 2H), 7.27 (d, J = 6.1 Hz, 1H), 6.29 (d, J = 9.9 Hz, 1H), 6.04 (td, J = 22.2, 9.9 Hz, 1H), 4.36−4.14 (m, 8H), 2.33 (s, 3H), 1.25 (t, J = 7.1 Hz, 6H), 1.22 (t, J = 7.1 Hz, 6H). ^{31}P NMR (203 MHz, $CDCl_3$): δ 16.92. ^{13}C NMR (126 MHz, $CDCl_3$): δ 168.5, 158.5, 155.5, 141.7, 139.2, 138.6, 137.4, 135.2, 131.4, 129.4, 128.0, 125.8, 124.6, 123.9, 122.1, 120.3, 118.0, 115.5, 64.2 (t, J = 3.2 Hz), 63.9 (t, J = 3.2 Hz), 44.5 (t, J = 147.7 Hz), 20.4, 16.5 (t, J = 3.2 Hz), 16.5 (t, J = 3.2 Hz). MS [ESI$^+$] m/z: 717.2 [M + H$^+$]$^+$. Inhibitor **15e** was isolated as a light yellow solid (7 mg, 37%). ^{1}H NMR (500 MHz, 0.5% NH_4OH in D_2O): δ 7.90 (d, J = 7.8 Hz, 1H), 7.85 (d, J = 1.9 Hz, 1H), 7.69 (t, J = 2.0 Hz, 1H), 7.65 (dd, J = 8.0, 1.9 Hz, 1H), 7.58 (d, J = 6.0 Hz, 1H), 7.46 (d, J = 6.0 Hz, 1H), 7.43 (d, J = 8.1 Hz, 1H), 7.33 (t, J = 7.9 Hz, 1H), 7.08 (ddd, J = 8.1, 2.3, 1.0 Hz, 1H), 5.07 (t, J = 19.0 Hz, 1H), 2.38 (s, 3H). ^{31}P NMR (203 MHz, 0.5% NH_4OH in D_2O): δ 13.82. ^{13}C NMR (201 MHz, 0.5% NH_4OH in D_2O): δ 165.6, 160.4, 157.0, 145.6, 141.4, 140.4, 138.5, 134.3, 131.5, 129.5, 126.8, 124.9, 124.0, 122.9, 121.5, 118.9, 115.6, 19.2. C-α to the bisphosphonate was observed by HSQC. HSQC (^{1}H−^{13}C): ^{1}H at δ 5.07 correlates to ^{13}C-α at δ 49.2. HRMS [ESI$^-$] calculated for $C_{20}H_{18}BrN_4O_9P_2S_2$ m/z, 602.9735; found 602.9722 [M − H]$^-$.

*General Procedure for Synthesis of Urea Inhibitors **16a−g**.* Inhibitors **16a−g** were synthesized using a previously reported protocol with minor modifications.[36] Substituted anilines representing building blocks from Figure 4 (0.11 mmol) and triethylamine (46 μL, 0.33 mmol) were dissolved in DCM (0.7 mL). Triphosgene (11.87 mg, 0.04 mmol) was added, and the mixture was stirred for 1 h while monitoring the reaction by TLC. When all of the starting material had been consumed, a solution of intermediate **21** (52.8 mg, 0.1 mmol) in DCM (0.7 mL) was added, and stirring was continued for an additional 30 min. Upon completion of the reaction (as indicated by TLC and LC/MS), the mixture was evaporated to dryness under vacuum and purified on silica gel by flash chromatography (5−15% MeOH in EtOAc). Isolated yields ranged from 38 to 72%.

*(((2-(3-(3-(3-Fluoro-4-methoxyphenyl)ureido)phenyl)thieno[2,3-d]pyrimidin-4-yl)amino)methylene)bis(phosphonic Acid) (**16a**).* The tetraethyl ester was isolated as a light yellow solid (31.1 mg, 45%). ^{1}H NMR (800 MHz, DMSO-d_6): δ 8.85 (s, 1H), 8.67 (s, 1H), 8.64 (d, J = 9.7 Hz, 1H), 8.59 (t, J = 1.9 Hz, 1H), 8.10 (d, J = 6.0 Hz, 1H), 8.00 (dt, J = 7.7, 1.3 Hz, 1H), 7.63 (d, J = 5.9 Hz, 1H), 7.56−7.52 (m, 1H), 7.48 (ddd, J = 8.0, 2.3, 1.1 Hz, 1H), 7.41 (t, J = 7.8 Hz, 1H), 7.12−7.06 (m, 2H), 6.06 (td, J = 23.3, 9.8 Hz, 1H), 4.25−4.00 (m, 8H), 3.80 (s, 2H), 1.17 (t, J = 7.1 Hz, 6H), 1.10 (t, J = 7.0 Hz, 6H). ^{31}P NMR (203 MHz, DMSO-d_6): δ 16.98. ^{13}C NMR (201 MHz, DMSO): δ 167.6, 158.1, 155.8, 152.6, 151.2 (d, J = 241.3 Hz), 142.0 (d, J = 11.0 Hz), 139.9, 138.1, 133.3 (d, J = 9.4 Hz), 128.9, 123.3, 121.3, 120.3, 120.2, 117.6, 115.3, 114.3 (d, J = 2.9 Hz), 114.2 (d, J = 3.3 Hz), 107.0 (d, J = 22.8 Hz), 63.0−62.9 (m), 62.8−62.7 (m), 56.3, 16.2−15.9 (m). MS [ESI$^+$] m/z: 696.3 [M + H$^+$]$^+$. Inhibitor **16a** was isolated as a white solid (10 mg, 38%). ^{1}H NMR (500 MHz, 0.5% NH_4OH in D_2O): δ 7.97 (d, J = 7.8 Hz, 1H), 7.78 (s, 1H), 7.49 (d, J = 8.2 Hz, 1H), 7.43 (d, J = 6.0 Hz, 1H), 7.32 (d, J = 6.7 Hz, 2H), 7.25 (d, J = 13.2 Hz, 1H), 7.11−7.05 (m, 2H), 5.02 (t, J = 19.1 Hz, 1H), 3.85 (s, 3H). ^{31}P NMR (203 MHz, 0.5% NH_4OH in D_2O): δ 13.90. ^{13}C NMR (201 MHz, 0.5% NH_4OH in D_2O): δ 164.80, 158.84, 156.31, 155.69, 151.54 (d, J = 240.8 Hz), 142.65 (d, J = 11.7 Hz), 138.65, 137.28, 132.56 (d, J = 9.3 Hz), 128.94, 122.36, 122.26, 120.47, 118.18, 117.53, 117.13, 115.94, 114.25, 110.07 (d, J = 22.5 Hz), 56.57, 50.23 (t, J = 126.2 Hz). HRMS [ESI$^-$] calculated for $C_{21}H_{19}FN_5O_8P_2S$ m/z, 582.0419; found 582.0410 [M − H]$^-$.

*(((2-(3-(3-(3-Chloro-4-methoxyphenyl)ureido)phenyl)thieno[2,3-d]pyrimidin-4-yl)amino)methylene)bis(phosphonic Acid) (**16b**).* The tetraethyl ester was isolated as a white solid (26.4 mg, 19%). ^{1}H NMR (800 MHz, DMSO-d_6): δ 8.88 (s, 1H), 8.67−8.62 (m, 2H), 8.57 (t, J = 2.0 Hz, 1H), 8.09 (d, J = 6.0 Hz, 1H), 8.00 (d, J = 7.7 Hz, 1H), 7.71 (d, J = 2.6 Hz, 1H), 7.63 (dd, J = 5.9, 0.7 Hz, 1H), 7.52−7.48 (m, 1H), 7.42 (t, J = 7.8 Hz, 1H), 7.28 (dd, J = 8.8, 2.6 Hz, 1H), 7.09 (d, J = 8.9 Hz, 1H), 6.05 (td, J = 23.3, 9.7 Hz, 1H), 4.18−4.08 (m, 8H), 3.82 (s, 3H), 1.17 (t, J = 7.0 Hz, 6H), 1.11 (t, J = 7.0 Hz, 6H). ^{31}P NMR (203 MHz, DMSO-d_6): δ 16.99. ^{13}C NMR (201 MHz, DMSO-d_6): δ 167.6, 158.1, 155.8, 152.6, 149.7, 139.9, 138.1, 133.5, 128.9, 123.3, 121.3, 120.8, 120.3, 120.2, 120.1, 118.3, 117.6, 115.3, 113.1, 62.9−62.9 (m), 62.8−62.7 (m), 56.2, 16.2−16.1 (m). MS [ESI$^+$] m/z: 712.2 [M + H$^+$]$^+$. Inhibitor **16b** was isolated as a light beige solid (14 mg, 62%). ^{1}H NMR (800 MHz, 0.5% NH_4OH in D_2O): δ 7.94 (d, J = 7.7 Hz, 1H), 7.58 (s, 1H), 7.47 (d, J = 2.5 Hz, 1H), 7.36−7.25 (m, 4H), 7.19 (t, J = 7.8 Hz, 1H), 7.05 (d, J = 8.8 Hz, 1H), 5.30 (t, J = 19.2 Hz, 1H), 3.89 (s, 3H). ^{31}P NMR (203 MHz, 0.5% NH_4OH in D_2O): δ 14.27. ^{13}C NMR (201 MHz, 0.5% NH_4OH in D_2O): δ 165.1, 159.1, 156.4, 155.4, 150.2, 138.5, 137.4, 132.5, 128.9, 122.8, 122.6, 122.5, 121.1, 120.9, 120.8, 118.2, 117.7, 115.8, 113.1, 56.4, 49.4 (t, J = 123.4 Hz). HRMS [ESI$^-$] calculated for $C_{21}H_{19}ClN_5O_8P_2S$ m/z, 598.0124; found 598.0125 [M − H]$^-$.

*(((2-(3-(3-(3-Bromo-4-methoxyphenyl)ureido)phenyl)thieno[2,3-d]pyrimidin-4-yl)amino)methylene)bis(phosphonic Acid) (**16c**).* The tetraethyl ester was isolated as a white solid (40.1 mg, 27%). ^{1}H NMR (800 MHz, DMSO-d_6): δ 8.87 (s, 1H), 8.66−8.62 (m, 2H), 8.55 (t, J = 2.0 Hz, 1H), 8.09 (d, J = 5.9 Hz, 1H), 7.99 (dt, J = 7.7, 1.4 Hz, 1H), 7.86 (d, J = 2.6 Hz, 1H), 7.63 (d, J = 5.9 Hz, 1H), 7.50 (ddd, J = 8.0, 2.3, 1.1 Hz, 1H), 7.42 (t, J = 7.8 Hz, 1H), 7.33 (dd, J = 8.8, 2.6 Hz, 1H), 7.06 (d, J = 8.9 Hz, 1H), 6.05 (td, J = 23.2, 9.6 Hz, 1H), 4.18−4.06 (m, 8H), 3.81 (s, 3H), 1.17 (t, J = 7.0 Hz, 6H), 1.11 (t, J = 7.0 Hz, 6H). ^{31}P NMR (203 MHz, DMSO-d_6): δ 16.99. ^{13}C NMR (201 MHz, DMSO-d_6): δ 167.6, 158.1, 155.8, 152.7, 150.6, 139.9, 138.1, 133.8, 128.9, 123.3, 123.1, 121.3, 120.3, 120.3, 119.0, 117.6, 115.3, 112.9, 110.3, 63.0−62.9 (m), 62.8−62.7 (m), 56.3, 16.2−16.1 (m). MS [ESI$^+$] m/z: 756.3 [M + H$^+$]$^+$. Inhibitor **16c** was isolated as a beige solid (16 mg, 49%). ^{1}H NMR (800 MHz, 0.5% NH_4OH in D_2O): δ 7.94 (d, J = 7.6 Hz, 1H), 7.64 (s, 1H), 7.57 (s, 1H), 7.38−7.25 (m, 4H), 7.19 (t, J = 7.8 Hz, 1H), 7.04 (d, J = 8.8 Hz, 1H), 5.28 (t, J = 19.2 Hz, 1H), 3.89 (d, J = 3.0 Hz, 3H). ^{31}P NMR (203 MHz, 0.5% NH_4OH in D_2O): δ 14.25. ^{13}C NMR (201 MHz, 0.5% NH_4OH in D_2O): δ 165.0, 159.0, 156.4, 155.4, 151.1, 138.5, 137.4, 132.8, 128.9, 125.8, 122.5, 122.4, 121.7, 120.8, 118.2, 117.7, 115.7, 112.9, 110.3, 56.5, 49.5 (t, J = 122.7 Hz). HRMS [ESI$^-$] calculated for $C_{21}H_{19}BrN_5O_8P_2S$ m/z, 641.9618; found 641.9622 [M − H]$^-$.

*(((2-(3-(3-(3-Fluoro-4-methylphenyl)ureido)phenyl)thieno[2,3-d]pyrimidin-4-yl)amino)methylene)bis(phosphonic Acid) (**16d**).* The tetraethyl ester was isolated as a white solid (45.5 mg, 33%). ^{1}H NMR (800 MHz, DMSO-d_6): δ 8.93 (s, 1H), 8.83 (s, 1H), 8.64 (d, J = 9.7 Hz, 1H), 8.61 (t, J = 2.0 Hz, 1H), 8.10 (d, J = 6.0 Hz, 1H), 8.00 (dt, J = 7.7, 1.4 Hz, 1H), 7.63 (d, J = 5.9 Hz, 1H), 7.51−7.46 (m, 2H), 7.42 (t, J = 7.8 Hz, 1H), 7.17 (t, J = 8.6 Hz, 1H), 7.04 (dd, J = 8.2, 2.1 Hz, 1H), 6.06 (td, J = 23.3, 9.7 Hz, 1H), 4.19−4.05 (m, 8H), 2.17 (s, 3H), 1.17 (t, J = 7.0 Hz, 6H), 1.10 (t, J = 7.1 Hz, 6H). ^{31}P NMR (203 MHz, DMSO-d_6): δ 16.97. ^{13}C NMR (201 MHz, DMSO-d_6): δ 167.6, 160.5 (d, J = 240.0 Hz), 158.1, 155.8, 152.5, 139.8, 139.2 (d, J = 11.0 Hz), 138.1, 131.3 (d, J = 6.7 Hz), 128.9, 123.3, 121.4, 120.3, 120.2, 117.6, 116.8 (d, J = 17.5 Hz), 115.3, 113.8 (d, J = 2.9 Hz), 104.9 (d, J = 27.3 Hz), 62.9 (m), 62.7 (m), 16.2−16.1 (m), 13.55 (d, J = 2.8 Hz). MS [ESI$^+$] m/z: 680.4 [M + H$^+$]$^+$. Inhibitor **16d** was isolated as a beige solid (13 mg, 55%). ^{1}H NMR (800 MHz, 0.5% NH_4OH in D_2O): δ 7.97 (d, J = 7.7 Hz, 1H), 7.45 (s, 1H), 7.37−7.27 (m, 3H), 7.27−7.15 (m, 3H), 7.14−7.11 (m, 1H), 5.30 (t, J = 18.8 Hz, 1H), 2.22 (s, 3H). ^{31}P NMR (203 MHz, 0.5% NH_4OH in D_2O): δ 14.35. ^{13}C NMR (201 MHz, 0.5% NH_4OH in D_2O): δ 165.0, 160.8 (d, J = 240.5 Hz), 158.8, 156.3, 155.4,

https://doi.org/10.1021/acs.jmedchem.1c01913
J. Med. Chem. XXXX, XXX, XXX−XXX

138.4, 137.7 (d, J = 10.9 Hz), 137.2, 131.2 (d, J = 6.4 Hz), 128.9, 122.6, 122.5, 120.6, 119.4 (d, J = 16.7 Hz), 118.1, 117.3, 116.4, 115.8, 107.7 (d, J = 26.6 Hz), 49.8 (t, J = 123.5 Hz), 13.1 (d, J = 3.3 Hz). HRMS [ESI$^-$] calculated for $C_{21}H_{19}FN_5O_7P_2S$ m/z, 566.0470; found 566.0451 [M − H]$^-$.

*(((2-(3-(3-(3-Chloro-4-methylphenyl)ureido)phenyl)thieno[2,3-d]pyrimidin-4-yl)amino)methylene)bis(phosphonic Acid) (**16e**).* The tetraethyl ester was isolated as a white solid (83.9 mg, 60%). ^{1}H NMR (500 MHz, DMSO-d_6): δ 8.91 (s, 1H), 8.77 (s, 1H), 8.64 (d, J = 9.7 Hz, 1H), 8.58 (t, J = 2.0 Hz, 1H), 8.10 (d, J = 6.0 Hz, 1H), 8.01 (dt, J = 7.7, 1.4 Hz, 1H), 7.74 (d, J = 2.1 Hz, 1H), 7.63 (d, J = 6.0 Hz, 1H), 7.49 (ddd, J = 8.1, 2.3, 1.1 Hz, 1H), 7.42 (t, J = 7.9 Hz, 1H), 7.28−7.18 (m, 2H), 6.05 (td, J = 23.3, 9.7 Hz, 1H), 4.20−4.05 (m, 8H), 2.27 (s, 3H), 1.17 (t, J = 7.1 Hz, 6H), 1.11 (t, J = 7.0 Hz, 6H). ^{31}P NMR (203 MHz, DMSO-d_6): δ 16.98. ^{13}C NMR (201 MHz, DMSO-d_6): δ 167.6, 158.1, 155.8, 152.5, 139.8, 138.9, 138.1, 133.1, 131.1, 128.9, 128.2, 123.3, 121.4, 120.3, 120.3, 118.1, 117.6, 117.0, 115.3, 63.0−62.8 (m), 62.8−62.7 (m), 18.8, 16.2−16.1 (m). MS [ESI$^+$] m/z: 696.2 [M + H$^+$]$^+$. Inhibitor **16e** was isolated as a beige solid (29 mg, 72%). ^{1}H NMR (800 MHz, 0.5% NH_4OH in D_2O): δ 7.94 (d, J = 7.6 Hz, 1H), 7.53 (s, 1H), 7.47 (s, 1H), 7.34−7.28 (m, 3H), 7.23 (s, 2H), 7.18 (t, J = 7.8 Hz, 1H), 2.31 (s, 3H). ^{31}P NMR (203 MHz, 0.5% NH_4OH in D_2O): δ 14.27. ^{13}C NMR (201 MHz, D_2O): δ 165.1, 164.9, 158.9, 156.4, 155.2, 138.3, 137.4, 137.3, 133.4, 130.9, 130.7, 128.9, 122.7, 122.5, 120.8, 119.2, 118.2, 117.6, 115.7, 49.2 (t, J = 122.8 Hz), 18.5. HRMS [ESI$^-$] calculated for $C_{21}H_{19}ClN_5O_7P_2S$ m/z, 582.0174; found 582.0162 [M − H]$^-$.

*(((2-(3-(3-(3-Bromo-4-methylphenyl)ureido)phenyl)thieno[2,3-d]pyrimidin-4-yl)amino)methylene)bis(phosphonic Acid) (**16f**).* The tetraethyl ester was isolated as a white solid (83.6 mg, 56%). ^{1}H NMR (800 MHz, DMSO-d_6): δ 8.93 (s, 1H), 8.79 (s, 1H), 8.64 (d, J = 9.7 Hz, 1H), 8.57 (t, J = 2.0 Hz, 1H), 8.10 (d, J = 6.0 Hz, 1H), 8.00 (dt, J = 7.7, 1.3 Hz, 1H), 7.91 (d, J = 1.9 Hz, 1H), 7.63 (d, J = 5.9 Hz, 1H), 7.50 (ddd, J = 8.0, 2.2, 1.0 Hz, 1H), 7.42 (t, J = 7.8 Hz, 1H), 7.28−7.23 (m, 2H), 6.05 (td, J = 23.2, 9.6 Hz, 1H), 4.18−4.07 (m, 8H), 2.29 (s, 3H), 1.17 (t, J = 7.1 Hz, 6H), 1.11 (t, J = 7.0 Hz, 6H). ^{31}P NMR (203 MHz, DMSO-d_6): δ 16.98. ^{13}C NMR (201 MHz, DMSO-d_6): δ 165.5, 156.0, 153.7, 150.4, 137.7, 136.8, 136.0, 128.8, 127.9, 126.8, 121.8, 121.2, 119.3, 119.1, 118.18, 118.17, 115.5, 115.4, 113.1, 60.8−60.7 (m), 60.7−60.6 (m), 19.5, 14.1−14.0 (m). MS [ESI$^+$] m/z: 738.2 [M + H$^+$]$^+$. Inhibitor **16f** was isolated as a beige solid (17 mg, 43%). ^{1}H NMR (800 MHz, 0.5% NH_4OH in D_2O): δ 7.96 (d, J = 7.7 Hz, 1H), 7.69 (s, 1H), 7.54−7.52 (m, 1H), 7.34 (d, J = 5.9 Hz, 1H), 7.30 (d, J = 6.0 Hz, 1H), 7.26 (d, J = 7.6 Hz, 1H), 7.20 (t, J = 7.8 Hz, 1H), 5.27 (t, J = 17.7 Hz, 1H), 2.35 (s, 3H). ^{31}P NMR (203 MHz, 0.5% NH_4OH in D_2O): δ 14.27. ^{13}C NMR (201 MHz, D_2O): δ 165.0, 159.0, 156.4, 155.3, 138.4, 137.5, 137.4, 132.6, 130.7, 128.9, 124.2, 123.8, 122.7, 122.5, 120.8, 120.1, 118.2, 117.7, 115.8, 21.3. C-α to the bisphosphonate was observed by HSQC. HSQC (^{1}H−^{13}C): ^{1}H at δ 5.27 correlates to ^{13}C-α at δ 49.7. HRMS [ESI$^-$] calculated for $C_{21}H_{19}BrN_5O_7P_2S$ m/z, 625.9669; found 625.9668 [M − H]$^-$.

*(((2-(3-(3-(4-Fluorophenyl)ureido)phenyl)thieno[2,3-d]pyrimidin-4-yl)amino)methylene)bis(phosphonic Acid) (**16g**).* The tetraethyl ester was isolated as a yellow solid (45 mg, 71%). ^{1}H NMR (500 MHz, $CDCl_3$) δ 8.12−8.01 (m, 4H), 7.79 (br_s, 1H), 7.42−7.37 (m, 3H), 7.28 (d, J = 7.8 Hz, 1H), 7.21 (d, J = 5.6 Hz, 1H), 6.91 (t, J = 8.7 Hz, 2H), 6.74 (br_s, 1H), 6.20 (t, J = 25.8 Hz, 1H), 4.32−4.20 (m, 8H), 1.29−1.24 (m, 12H). ^{31}P NMR (203 MHz, $CDCl_3$) δ 17.14 (s). MS [ESI$^+$] m/z: 666.2 [M + H$^+$]$^+$. Inhibitor **16g** was isolated as a light yellow solid (26 mg, 74%). ^{1}H NMR (500 MHz, DMSO-d$_6$): δ 8.91 (br_s, 1H), 8.76 (br_s, 1H), 8.34 (s, 1H), 8.05 (d, J = 7.6 Hz, 1H), 7.92 (br_s, two overlapping protons), 7.73 (d, J = 8.1 Hz, 1H), 7.57 (d, J = 5.3 Hz, 1H), 7.50−7.47 (m, 2H), 7.41 (t, J = 7.9 Hz, 1H), 7.12 (t, J = 8.7 Hz, 2H), 5.66 (br, 1H). ^{31}P NMR (162 MHz, DMSO-d$_6$): δ 13.98 (s). ^{13}C NMR (126 MHz, DMSO-d$_6$): δ 167.1, 158.6, 157.8 (d, J = 238.0 Hz), 156.7, 153.2, 140.3, 138.7, 136.5 (d, J = 2.3 Hz), 129.2, 123.2, 122.4, 120.7, 120.6, 120.5 (d, J = 7.7 Hz), 118.1, 115.9, 115.7 (d, J = 22.1 Hz). C-α to the bisphosphonate was observed by HSQC. HSQC (^{1}H−^{13}C): ^{1}H at δ 5.66 correlates to ^{13}C-α at δ 47.9. HRMS [ESI$^-$] calculated for $C_{20}H_{16}FN_5NaO_7P_2S$ m/z, 574.0133; found 574.0146 [M − H]$^-$.

*(((2-(3-(2-Phenylacetamido)phenyl)thieno[2,3-d]pyrimidin-4-yl)-amino)methylene)bis(phosphonic Acid) (**17a**).* The tetraethyl ester was isolated as an off-white solid (39.2 mg, 61%). ^{1}H NMR (800 MHz, $CDCl_3$): δ 8.19 (t, J = 1.9 Hz, 1H), 8.17 (dt, J = 7.7, 1.3 Hz, 1H), 7.94 (dt, J = 7.9, 1.8 Hz, 1H), 7.52 (s, 1H), 7.44−7.36 (m, 5H), 7.36−7.29 (m, 3H), 6.00 (s, 1H), 5.93 (td, J = 21.7, 9.8 Hz, 1H), 4.31−4.12 (m, 8H), 3.78 (s, 2H), 1.24 (t, J = 7.1 Hz, 6H), 1.22 (t, J = 7.0 Hz, 6H). ^{31}P NMR (203 MHz, $CDCl_3$): δ 16.74. ^{13}C NMR (201 MHz, $CDCl_3$): δ 169.3, 167.9, 158.8, 155.5 (t, J = 3.7 Hz), 138.2, 134.6, 129.7, 129.3, 127.8, 124.4, 124.2, 122.4, 119.3, 117.4, 115.4, 64.0 (t, J = 3.0 Hz), 63.8 (t, J = 3.0 Hz), 45.0, 44.6 (t, J = 147.1 Hz), 16.5 (t, J = 2.8 Hz), 16.4 (t, J = 2.8 Hz). MS [ESI$^+$] m/z: 647.5 [M + H$^+$]$^+$. Inhibitor **17a** was isolated as a pale yellow solid (6 mg, 18%). ^{1}H NMR (800 MHz, 0.5% NH_4OH in D_2O): δ 8.20 (s, 1H), 8.10 (d, J = 7.8 Hz, 1H), 7.73 (d, J = 8.0 Hz, 1H), 7.59 (d, J = 6.0 Hz, 1H), 7.53 (t, J = 7.9 Hz, 1H), 7.48−7.42 (m, 5H), 7.38 (t, J = 7.0 Hz, 1H), 5.17 (t, J = 19.0 Hz, 1H), 3.83 (s, 2H). ^{31}P NMR (162 MHz, 0.5% NH_4OH in D_2O): δ 13.60. ^{13}C NMR (201 MHz, 0.5% NH_4OH in D_2O): δ 173.4, 165.6, 159.8, 157.0, 138.5, 137.3, 135.0, 129.5, 129.3, 129.0, 127.3, 125.1, 123.6, 123.2, 121.2, 118.9, 115.8, 49.0 (t, J = 121.3 Hz), 43.1. HRMS [ESI$^-$] calculated for $C_{21}H_{19}N_4O_7P_2S$ m/z, 533.0455; found 533.0463 [M − H]$^-$.

*(((2-(3-(2-(Pyridin-3-yl)acetamido)phenyl)thieno[2,3-d]-pyrimidin-4-yl)amino)methylene)bis(phosphonic Acid) (**17b**).* The synthesis was carried out using commercially available 2-(pyridin-3-yl)acetic acid hydrochloride. The tetraethyl ester was isolated as a light brown oil (40 mg, 68%). ^{1}H NMR (500 MHz, $CDCl_3$): δ 8.61 (s, 1H), 8.55 (d, J = 4.2 Hz, 1H), 8.37 (s, 1H), 8.25 (d, J = 7.8 Hz, 1H), 8.07 (d, J = 7.2 Hz, 1H), 7.71−7.89 (m, 2H), 7.46 (t, J = 8.0 Hz, 1H), 7.42−7.31 (m, 3H), 6.10−5.99 (brm, 1H), 5.91 (brm, 1H), 4.26−4.14 (m, 8H), 3.78 (s, 2H), 1.26 (t, J = 7.1 Hz, 6H), 1.20 (t, J = 7.0 Hz, 6H). ^{31}P NMR (202 MHz, $CDCl_3$): δ 16.98. MS [ESI$^+$] m/z: 648.4 [M + H$^+$]$^+$. Inhibitor **17b** was isolated as an off-white solid (20 mg, 67%). ^{1}H NMR (500 MHz, DMSO-d_6): δ 10.52 (s, 1H), 8.64 (brm, 1H), 8.49 (s, 1H), 8.15 (d, J = 6.4 Hz, 1H), 8.04 (brm, 2H), 7.94 (brm, 1H), 7.87 (brm, 2H), 7.59 (brm, 1H), 7.49−7.43 (m, 2H), 5.71−5.61 (m, 1H), 3.85 (s, 2H). ^{31}P NMR (202 MHz, DMSO-d_6): δ 13.92. ^{13}C NMR (125 MHz, DMSO-d_6): δ 168.6, 167.2, 158.6, 156.8, 148.0, 145.7, 140.8, 139.5, 139.0, 133.5, 129.1, 124.9, 123.9, 122.8, 121.4, 120.8, 119.0, 115.9, 47.8, 31.2. HRMS [ESI$^-$] calculated for $C_{20}H_{18}N_5O_7P_2S$ m/z, 534.0408; found 534.0421 [M − H]$^-$.

*(((2-(3-(2-Methoxy-2-phenylacetamido)phenyl)thieno[2,3-d]-pyrimidin-4-yl)amino)methylene)bis(phosphonic Acid) [(S)- and (R)-**17c**].* The tetraethyl esters were isolated as light yellow solids (68.5 mg, 67% for the (S)-enantiomer; 47.4 mg, 46% for the (R)-enantiomer). ^{1}H NMR (800 MHz, $CDCl_3$): δ 8.75 (s, 1H), 8.42 (t, J = 1.9 Hz, 1H), 8.19 (dt, J = 7.8, 1.3 Hz, 1H), 7.99 (ddd, J = 8.0, 2.2, 1.0 Hz, 1H), 7.48−7.45 (m, 2H), 7.43−7.39 (m, 2H), 7.38−7.34 (m, 2H), 7.33−7.30 (m, 1H), 7.28 (d, J = 5.9 Hz, 1H), 6.42 (d, J = 9.8 Hz, 1H), 5.98 (td, J = 22.0, 9.8 Hz, 1H), 4.76 (s, 1H), 4.30−4.07 (m, 8H), 3.46 (s, 3H), 1.24 (t, J = 7.1 Hz, 3H), 1.23 (t, J = 7.1 Hz, 3H), 1.19 (t, J = 6.9 Hz, 3H), 1.17 (t, J = 7.0 Hz, 3H). ^{31}P NMR (203 MHz, $CDCl_3$): δ 16.87. ^{13}C NMR (201 MHz, $CDCl_3$): δ 168.7, 168.2, 158.8, 155.5 (t, J = 3.7 Hz), 138.6, 137.7, 136.7, 129.3, 128.7, 128.6, 127.2, 124.3, 123.8, 121.8, 119.1, 117.7, 115.4, 84.0, 63.9 (t, J = 3.2 Hz), 63.7 (t, J = 3.2 Hz), 57.4, 44.4 (t, J = 147.2 Hz), 16.4−16.3 (m). MS [ESI$^+$] m/z: 677.4 [M + H$^+$]$^+$. Inhibitors (S)-**17c** and (R)-**17c** were both isolated as white solids. (S)-**17c:** 36.7 mg, 64% yield, 97%ee; (R)-**17c:** 25.4 mg, 64% yield, 86%ee. ^{1}H NMR (800 MHz, 0.5% NH_4OH in D_2O): δ 8.24 (t, J = 2.0 Hz, 1H), 8.13 (d, J = 7.8 Hz, 1H), 7.70 (dd, J = 8.1, 2.3 Hz, 1H), 7.58−7.52 (m, 4H), 7.51−7.42 (m, 4H), 5.10 (t, J = 18.9 Hz, 1H), 4.99 (s, 1H), 3.49 (s, 3H). ^{31}P NMR (203 MHz, 0.5% NH_4OH in D_2O): δ 13.79. ^{13}C NMR (201 MHz, 0.5% NH_4OH in D_2O): δ 172.0, 165.5, 159.7, 156.9, 138.6, 136.4, 136.3, 129.5, 129.3, 129.1, 127.5, 125.5, 124.1, 123.1, 121.7, 118.8, 115.8, 83.4, 57.1, 49.3 (t, J = 124.0 Hz). HRMS [ESI$^-$] calculated for $C_{22}H_{21}N_4O_8P_2S$ m/z, 563.0561; found 523.0548 [M − H]$^-$.

(((2-(3-(2-Isopropoxy-2-phenylacetamido)phenyl)thieno[2,3-d]-pyrimidin-4-yl)amino)methylene)bis(phosphonic Acid) [(S)- and

https://doi.org/10.1021/acs.jmedchem.1c01913
J. Med. Chem. XXXX, XXX, XXX−XXX

*(R)-**17d**].* The tetraethyl esters were isolated as light yellow solids (53.6 mg, 50% isolated yield of the (*S*); 31 mg, 29% isolated yield of the (*R*)). ^{1}H NMR (800 MHz, $CDCl_3$): δ 8.75 (s, 1H), 8.42 (t, *J* = 1.9 Hz, 1H), 8.19 (dt, *J* = 7.8, 1.3 Hz, 1H), 7.99 (ddd, *J* = 8.0, 2.2, 1.0 Hz, 1H), 7.48−7.45 (m, 2H), 7.43−7.39 (m, 2H), 7.38−7.34 (m, 2H), 7.33−7.30 (m, 1H), 7.28 (d, *J* = 5.9 Hz, 1H), 6.42 (d, *J* = 9.8 Hz, 1H), 5.98 (td, *J* = 22.0, 9.8 Hz, 1H), 4.76 (s, 1H), 4.30−4.07 (m, 8H), 3.46 (s, 3H), 1.24 (t, *J* = 7.1 Hz, 3H), 1.23 (t, *J* = 7.1 Hz, 3H), 1.19 (t, *J* = 6.9 Hz, 3H), 1.17 (t, *J* = 7.0 Hz, 3H). ^{31}P NMR (203 MHz, $CDCl_3$): δ 16.87. ^{13}C NMR (201 MHz, $CDCl_3$) δ 168.7, 168.2, 158.8, 155.5 (t, *J* = 3.7 Hz), 138.6, 137.7, 136.7, 129.3, 128.7, 128.6, 127.2, 124.3, 123.8, 121.8, 119.1, 117.7, 115.4, 84.0, 63.9 (t, *J* = 3.2 Hz), 63.7 (t, *J* = 3.2 Hz), 57.4, 44.4 (t, *J* = 147.2 Hz), 16.4−16.3 (m). MS [ESI$^+$] *m/z*: 677.4 [M + H$^+$]$^+$. Inhibitors (*S*)-**17d** and (*R*)-**17d** were both isolated as white solids. (*S*)-**17d:** 16.4 mg, 36% yield, 89%ee; (*R*)-**17d:** 9.5 mg, 36% yield, 88% ee. ^{1}H NMR (800 MHz, 0.5% NH_4OH in D_2O): δ 8.25 (t, *J* = 2.0 Hz, 1H), 8.18 (d, *J* = 7.8 Hz, 1H), 7.70 (dd, *J* = 8.0, 2.1 Hz, 1H), 7.62−7.56 (m, 4H), 7.52−7.44 (m, 4H), 5.23 (s, 1H), 5.06 (t, *J* = 18.8 Hz, 1H), 3.93 (hept, *J* = 6.2 Hz, 1H), 1.33 (d, *J* = 6.1 Hz, 3H), 1.27 (d, *J* = 6.1 Hz, 3H). ^{31}P NMR (203 MHz, 0.5% NH_4OH in D_2O): δ 13.74. ^{13}C NMR (201 MHz, 0.5% NH_4OH in D_2O): δ 173.0 165.4, 159.9, 157.0, 138.8, 137.1, 136.4, 129.5, 129.2, 129.1, 127.6, 125.8, 124.5, 123.1, 122.0, 119.0, 115.9, 79.5, 72.4, 21.4, 21.1. C-α to the bisphosphonate was observed by HSQC. HSQC (^{1}H−^{13}C): ^{1}H at δ 5.07 correlates to ^{13}C-α at δ 49.6. HRMS [ESI$^-$] calculated for $C_{24}H_{25}N_4O_8P_2S$ *m/z*, 591.0874; found 591.0876 [M − H]$^-$.

*(((2-(3-(2-Isopropoxy-2-phenylacetamido)phenyl)thieno[2,3-d]-pyrimidin-4-yl)amino)methylene)bis(phosphonic Acid) [(S)- and (R)-**17e**].* The syntheses inhibitors (*R*)- and (*S*)-**17e** were carried out using the general procedures described, with the addition of HOBt·H_2O (1.2 equiv) for the amide coupling reaction. The tetraethyl esters were both isolated as white solids (62 mg, 68% of the (*S*)-enantiomer; 64 mg, 70% for the (*R*)-enantiomer). ^{1}H NMR (800 MHz, $CDCl_3$): δ 8.67 (s, 1H), 8.42 (t, *J* = 1.9 Hz, 1H), 8.21 (dt, *J* = 7.8, 1.4 Hz, 1H), 7.94 (ddd, *J* = 8.1, 2.3, 1.1 Hz, 1H), 7.43 (t, *J* = 7.9 Hz, 1H), 7.35 (d, *J* = 5.9 Hz, 1H), 7.29 (d, *J* = 6.0 Hz, 1H), 7.27−7.22 (m, 2H), 6.96 (t, *J* = 8.4 Hz, 1H), 5.91 (td, *J* = 21.7, 9.8 Hz, 1H), 5.74 (d, *J* = 9.8 Hz, 1H), 4.90 (s, 1H), 4.30−4.14 (m, 8H), 3.88 (s, 3H), 3.82 (hept, *J* = 6.1 Hz, 1H), 1.33 (d, *J* = 6.1 Hz, 3H), 1.29 (d, *J* = 6.1 Hz, 3H), 1.27 (t, *J* = 7.1 Hz, 3H), 1.26 (t, *J* = 7.1 Hz, 3H), 1.24 (t, *J* = 7.1 Hz, 3H), 1.23 (t, *J* = 7.1 Hz, 3H). ^{31}P NMR (162 MHz, $CDCl_3$): δ 16.79. ^{19}F NMR (377 MHz, $CDCl_3$): δ −134.51. ^{13}C NMR (201 MHz, $CDCl_3$): δ 169.3, 168.7, 159.2, 155.7 (t, *J* = 3.7 Hz), 152.8 (d, *J* = 247.1 Hz), 148.0 (d, *J* = 10.8 Hz), 139.0, 137.9, 131.4 (d, *J* = 5.5 Hz), 129.3, 124.6, 124.1, 123.1 (d, *J* = 3.5 Hz), 122.0, 119.4, 117.2, 115.5, 114.9 (d, *J* = 19.3 Hz), 114.1, 79.3, 71.9, 63.9 (t, *J* = 3.2 Hz), 63.7 (t, *J* = 3.0 Hz), 56.7, 45.1 (t, *J* = 147.1 Hz), 23.0, 22.0, 16.5−16.4 (m). MS [ESI$^+$] *m/z*: 753.5 [M + H$^+$]$^+$. Inhibitors (*S*)-**17e** and (*R*)-**17e** were both isolated as white solids. (*R*)-**17e:** 17 mg, 55% yield, 98% ee; (*S*)-**17e:** 13 mg, 45% yield, 97% ee. ^{1}H NMR (500 MHz, 0.5% NH_4OH in D_2O): δ 8.25 (t, *J* = 2.0 Hz, 1H), 8.19 (dt, *J* = 8.0, 1.3 Hz, 1H), 7.74 (dt, *J* = 8.4, 1.3 Hz, 1H), 7.64−7.56 (m, 2H), 7.49 (d, *J* = 6.0 Hz, 1H), 7.42−7.33 (m, 2H), 7.22 (t, *J* = 8.6 Hz, 1H), 5.19 (s, 1H), 5.12 (t, *J* = 19.0 Hz, 1H), 3.94 (s, 3H), 3.93 (hept, *J* = 6.1 Hz, 1H), 1.32 (d, *J* = 6.1 Hz, 3H), 1.27 (d, *J* = 6.1 Hz, 3H). ^{19}F NMR (471 MHz, 0.5% NH_4OH in D_2O): δ −135.43. ^{31}P NMR (203 MHz, 0.5% NH_4OH in D_2O): δ 13.79.

^{13}C NMR (201 MHz, 0.5% NH_4OH in D_2O): δ 172.6, 165.5, 159.8, 157.0, 151.9 (d, *J* = 244.0 Hz), 147.3 (d, *J* = 10.4 Hz), 138.7, 136.3, 130.3 (d, *J* = 5.9 Hz), 129.5, 125.9, 124.4, 124.1 (d, *J* = 3.3 Hz), 123.1, 121.9, 118.9, 115.8, 115.0 (d, *J* = 19.2 Hz), 114.1, 78.5, 72.3, 56.2, 49.3 (t, *J* = 122.0 Hz), 21.4, 21.1. HRMS [ESI$^-$] calculated for $C_{25}H_{26}FN_4O_9P_2S$ *m/z*, 639.0885; found 639.0879 [M − H]$^-$.

*(R)-(((2-(3-(2-Phenylpropanamido)phenyl)thieno[2,3-d]-pyrimidin-4-yl)amino)methylene)bis(phosphonic Acid) [(R)-**17f**].* The synthesis was carried out using commercially available (*R*)-2-phenylpropanoic acid. The tetraethyl ester was isolated as a slightly yellow solid (25 mg, 40%). ^{1}H NMR (500 MHz, $CDCl_3$): δ 8.19 (d, *J* = 7.4 Hz, 2H), 7.97 (d, *J* = 7.7 Hz, 1H), 7.46−7.41 (m, 4H), 7.37−7.33 (m, 2H), 7.30 (d, *J* = 6.1 Hz, 2H), 7.25 (m, 1H), 5.95 (td, J_1 = 21.8 Hz, J_2 = 9.9 Hz, 1H), 5.73 (d, *J* = 9.4 Hz, 1H), 4.30−4.20 (m, 8H), 3.79 (q, *J* = 7.0 Hz, 1H), 1.65 (d, *J* = 7.1 Hz, 3H), 1.26 (td, J_1 = 7.0 Hz, J_2 = 2.7 Hz, 12H). ^{31}P NMR (202 MHz, $CDCl_3$): δ 16.78. MS [ESI$^+$] *m/z*: 661.5 [M + H$^+$]$^+$. Inhibitor (*R*)-**17f** was isolated as an off-white solid (8 mg, 57%). ^{1}H NMR (500 MHz, DMSO-d_6): δ 10.26 (s, 1H), 8.48 (s, 1H), 8.13 (d, *J* = 7.5 Hz, 1H), 7.90 (d, *J* = 7.9 Hz, 2H), 7.56 (brs, 1H), 7.44 (d, *J* = 7.6 Hz, 3H), 7.35 (t, *J* = 7.6 Hz, 2H), 7.25 (t, *J* = 7.3 Hz, 1H), 5.69-5.59 (m, 2H), 3.89 (q, *J* = 6.8 Hz, 1H), 1.45 (d, *J* = 7.0 Hz, 3H). ^{31}P NMR (202 MHz, DMSO-d_6): δ 14.04. ^{13}C NMR (125 MHz, DMSO-d_6): δ 172.8, 167.3, 158.6, 156.7, 142.4, 139.8, 138.8, 129.1, 128.9, 127.8, 127.2, 123.7, 123.0, 121.3, 120.6, 118.7, 110.0, 46.4, 40.9, 19.1. HRMS [ESI$^+$] calculated for $C_{20}H_{22}N_4NaO_7P_2S$ *m/z*, 571.0577; found 571.0575 [M + Na]$^+$.

*(R)-(((2-(3-(3,3,3-Trifluoro-2-methoxy-2-phenylpropanamido)-phenyl)thieno[2,3-d]pyrimidin-4-yl)amino)methylene)bis-(phosphonic Acid) [(R)-**17g**].* The synthesis was carried out using commercially available (*S*)-3,3,3-trifluoro-2-methoxy-2-phenylpropanoyl chloride. The tetraethyl ester was isolated as a slightly yellow semisolid (51 mg, 71%). ^{1}H NMR (500 MHz, $CDCl_3$): δ 8.75 (s, 1H), 8.48 (s, 1H), 8.27 (d, *J* = 7.9 Hz, 1H), 8.02 (dd, J_1 = 8.0 Hz, J_2 = 1.3 Hz, 1H), 7.64−7.63 (m, 2H), 7.51−7.45 (m, 4H), 7.39 (d, *J* = 6.0 Hz, 1H), 7.32 (d, *J* = 4.6 Hz, 1H), 5.97 (dt, J_1 = 21.7 Hz, J_2 = 9.8 Hz, 1H), 5.77 (brm, 1H), 4.30−4.19 (m, 8H), 3.57 (d, *J* = 1.1 Hz, 3H), 1.70 (d, *J* = 8.4 Hz, 2H), 1.30-1.23 (m, 12H). ^{31}P NMR (202 MHz, $CDCl_3$): δ 16.73. MS [ESI$^+$] *m/z*: 745.5 [M + H$^+$]$^+$. Inhibitor (*R*)-**17g** was isolated as an off-white solid (8 mg, 57%). ^{1}H NMR (500 MHz, DMSO-d_6): δ 10.39 (s, 1H), 8.66 (s, 1H), 8.24 (d, *J* = 7.7 Hz, 1H), 8.06 (brs, 1H), 7.96 (brs, 1H), 7.87 (d, *J* = 8.2 Hz, 1H), 7.63 (d, *J* = 7.3 Hz, 2H), 7.56 (brm, 1H), 7.47−7.53 (m, 4H), 5.66 (td, J_1 = 21.6 Hz, J_2 = 8.4 Hz, 1H), 3.60 (s, 3H). ^{31}P NMR (202 MHz, DMSO-d_6): δ 14.17. ^{13}C NMR (125 MHz, DMSO-d_6): δ 167.3, 165.2, 158.5, 156.8, 138.9, 138.2, 133.6, 130.1, 129.0, 127.6, 125.5, 125.1, 123.2, 123.1, 128.8, 115.9, 84.5 (d), 55.8. HRMS [ESI$^+$] calculated for $C_{20}H_{21}F_3N_4NaO_8P_2S$ *m/z*, 655.0400; found 655.0404 [M + Na]$^+$.

*Tetraethyl (((2-(3-(Chlorosulfonyl)phenyl)thieno[2,3-d]pyrimidin-4-yl)amino)methylene)bis(phosphonate) (**22**).* Synthesis of intermediate **22** was achieved as previously reported with minor modifications.[34] In a round-bottom flask, H_2O (2 mL) was added, briefly degassed, and filled with argon. The flask was cooled in an ice/NaCl bath to approximately −5 °C, and $SOCl_2$ (595 mg, 365 μL, 5 equiv, 5.00 mmol) was added dropwise. The resulting solution was allowed to warm to RT and stirred for 4 h under argon. In a second flask, intermediate **21** (529 mg, 1 equiv, 1.00 mmol) was dissolved in 12 M HCl (1.1 mL) and the resulting solution was also cooled in an ice/NaCl bath (at approximately −5 °C), before a solution of sodium nitrite (79.3 mg, 1.15 equiv, 1.15 mmol) in H_2O (0.9 mL, cooled to −5 °C) was added dropwise and the mixture was stirred for another 30 min at −5 °C to give the diazonium species. To the flask containing SO_2 (forms *in situ* from $SOCl_2$ in H_2O), Cu(I)Cl (14.8 mg, 0.15 equiv, 150 μmol) was quickly added under a flow of argon and the flask was cooled again to −5 °C. The aqueous diazonium solution of intermediate **21** was added dropwise to the SO_2/Cu(I)Cl solution at −5 °C. The reaction mixture was stirred at −5 to 0 °C for 20 min and then allowed to warm to RT for 40 min, at which point the conversion was completed as confirmed by LCMS. The reaction mixture was partitioned between water and EtOAc and quickly extracted three times with EtOAc and dried over anhydrous Na_2SO_4, and the solvent was removed under vacuum to give the desired intermediate **22** (524 mg, 85.6%) in >90% purity by ^{1}H and ^{31}P NMR and LCMS, which was used directly in the next step without further purification.

^{1}H NMR (500 MHz, DMSO-d_6): δ 8.79 (d, *J* = 9.7 Hz, 1H), 8.66 (t, *J* = 1.8 Hz, 1H), 8.31 (dt, *J* = 7.8, 1.3 Hz, 1H), 8.10 (d, *J* = 6.0 Hz, 1H), 7.72 (dt, *J* = 7.6, 1.5 Hz, 1H), 7.65 (d, *J* = 6.0 Hz, 1H), 7.49 (t, *J* = 7.7 Hz, 1H), 6.02 (td, *J* = 23.3, 9.5 Hz, 1H), 4.19−3.99 (m, 8H), 1.19 (t, *J* = 7.0 Hz, 6H), 1.10 (t, *J* = 7.0 Hz, 6H).

^{13}C NMR (126 MHz, DMSO-d_6): δ 166.8, 157.7, 155.9, 148.7, 136.6, 128.1, 127.6, 127.6, 125.1, 123.7, 120.3, 115.4, 63.0 (t, *J* = 3.1 Hz), 62.9 (t, *J* = 3.1 Hz), 44.1 (t, *J* = 147.6 Hz), 16.2−16.1 (m).

^{31}P NMR (203 MHz, DMSO-d_6): δ 16.85.

https://doi.org/10.1021/acs.jmedchem.1c01913
J. Med. Chem. XXXX, XXX, XXX−XXX

MS [ESI$^-$] m/z: 592.2 [RSO_3]$^-$; the LCMS of this intermediate gave the molecular ion of the sulfonic acid (the decomposition product of the sulfonyl chloride).

*Synthesis of Chiral Mandelic Acid Derivatives **24**, **25**, and **28**. (R/S)-2-Methoxy-2-phenylacetic Acid (**24**).* The racemic intermediate **24** was synthesized as previously reported.[57] ^{1}H NMR (500 MHz, DMSO-d_6) δ 12.83 (s, 1H), 7.49−7.20 (m, 5H), 4.77 (s, 1H), 3.31 (s, 3H). ^{13}C NMR (126 MHz, DMSO-d_6) δ 171.8, 137.2, 128.4, 128.3, 127.1, 81.6, 56.7, 40.0, 39.9, 39.7, 39.5, 39.4, 39.2, 39.0.

*(R)-2-Methoxy-2-phenylacetic Acid ((R)-**24**).* Chiral resolution of R/S-**24** was achieved as previously reported.[38] The (R)-enantiomer was isolated in a 33% recovery (55 mg) and in 86% ee based on its reported optical rotation; observed: $[\alpha]_D^{20}$ = −123.32 (c 5.0, EtOH).[39]

Intermediate (S)-**24** was obtained in a similar way in a 36% recovery (60 mg) and 97% ee, based on its optical rotation; observed: $[\alpha]_D^{20}$ = −139.8 (c 1.0, EtOH).

*R- and S-2-Isopropoxy-2-phenylacetic Acid (**25**).* Enantiomerically enriched (R)- and (S)-**25** were prepared as previously reported.[37]

^{1}H NMR (500 MHz, $CDCl_3$) δ 7.47−7.43 (m, 2H), 7.40−7.33 (m, 3H), 4.99 (s, 1H), 3.74 (hept, J = 6.1 Hz, 1H), 1.26 (d, J = 6.1 Hz, 3H), 1.20 (d, J = 6.2 Hz, 3H).

^{13}C NMR (126 MHz, $CDCl_3$) δ 174.3, 136.4, 129.0, 128.8, 127.3, 78.0, 71.5, 22.6, 21.7.

Both enantiomers were isolated as white solids; the (R)-**25** in 88%ee, as determined by the ^{1}H NMR of its menthol ester derivative (Figure S1a) and further confirmed by its optical rotation; observed:$[\alpha]_D^{20}$ = −108.87 (c 10.0, $CHCl_3$).

Similarly, the (S)-**25** was obtained in 89% ee, as determined by the ^{1}H NMR of its menthol ester derivative (Figure S1b) and further confirmed by its optical rotation; observed: $[\alpha]_D^{20}$ = +107.96 (c 10.0, $CHCl_3$).

*Ethyl 2-(3-Fluoro-4-methoxyphenyl)-2-oxoacetate (**27**).* Intermediate **27** was prepared as previously reported,[40] with minor modifications. A suspension of $AlCl_3$ (10 g, 75 mmol) in dry DCM (24 mL) was cooled to 0 °C before ethyl oxalyl chloride (10 g, 8.2 mL, 73 mmol) was added dropwise. The initial suspension became a clear, light yellow solution before 2-fluoroanisole (6.24 g, 5.6 mL, 49.5 mmol) dissolved in dry DCM (6 mL) was slowly added dropwise, while the solution was maintained at 0 °C. After 90 min, ^{1}H NMR suggested that all of the starting material was converted to a product and the mixture was partitioned between H_2O:EtOAc (100 mL:50 mL) and further extracted twice with EtOAc (∼50 mL). The combined organic extracts were washed with brine, dried over anhydrous Na_2SO_4, concentrated, and purified on silica gel using flash column chromatography (isocratic 10% EtOAc in hexanes) to give pure ethyl 2-(3-fluoro-4-methoxyphenyl)-2-oxoacetate (10.3 g, 92%) as a yellow oil. ^{1}H NMR (500 MHz, $CDCl_3$): δ 7.85 (ddd, J = 8.6, 2.1, 1.1 Hz, 1H), 7.79 (dd, J = 11.5, 2.1 Hz, 1H), 7.03 (dd, J = 8.6, 7.9 Hz, 1H), 4.44 (q, J = 7.2 Hz, 2H), 3.98 (s, 3H), 1.42 (t, J = 7.1 Hz, 3H). ^{19}F NMR (377 MHz, $CDCl_3$) δ −133.17.

*2-(3-Fluoro-4-methoxyphenyl)-2-isopropoxyacetic Acid [(S)- and (R)-**28**].* Step 1: Asymmetric reduction of the prochiral α-keto ester intermediate **27** was achieved using $NaBH_4$ and either L-(+)- or D-(−)-tartaric acid, as previously reported.[41] A solution of D- or L-tartaric acid (3 g, 20 mmol) and $NaBH_4$ (757 mg, 20 mmol) in dry THF (50 mL) was heated at 70 °C in a sealed round-bottom flask under argon while stirring. After 2 h, the vial was cooled to −40 °C, and intermediate **27** (1.13 g, 1 mmol) was added. The mixture was then stirred at −20 °C, and after 18 h, all starting material was consumed, as indicated by TLC. The mixture was partitioned between EtOAc and saturated aqueous NH_4Cl, extracted twice with EtOAc, and then the combined organic layers were extracted with brine and dried over anhydrous Na_2SO_4. The mixture was evaporated to dryness under vacuum and purified on silica gel by flash column chromatography (using a solvent gradient from 10 to 50% EtOAc in hexanes. (S)- and (R)-ethyl 2-(3-fluoro-4-methoxyphenyl)-2-hydroxyacetate eluted at ∼30% EtOAc) as a colorless oil in a 90% yield (1.03 g) and 78% ee, as determined by chiral HPLC on a Chiralpak AD column, using hexanes/i-PrOH (95:5) at a flow rate of 1 mL/min; retention time of (R)-enantiomer: 19.13 min; retention time of (S)-enantiomer: 16.64 min.

The corresponding racemic α-hydroxy ester was also prepared from the α-keto ester **27** by simple $NaBH_4$ (38 mg, 1 mmol) reduction in THF. ^{1}H NMR (500 MHz, $CDCl_3$): δ 7.18−7.12 (m, 2H), 6.94 (t, J = 8.6 Hz, 1H), 5.08 (d, J = 5.5 Hz, 1H), 4.27 (dq, J = 10.8, 7.1 Hz, 1H), 4.19 (dq, J = 10.8, 7.1 Hz, 1H), 3.89 (s, 3H), 3.44 (d, J = 5.5 Hz, 1H), 1.24 (t, J = 7.1 Hz, 3H). ^{13}C NMR (126 MHz, $CDCl_3$): δ 173.6, 152.4 (d, J = 246.3 Hz), 147.8 (d, J = 10.6 Hz), 131.4 (d, J = 6.0 Hz), 122.5 (d, J = 3.6 Hz), 114.5 (d, J = 19.6 Hz), 113.4 (d, J = 2.2 Hz), 72.1 (d, J = 1.6 Hz), 62.6, 56.4, 14.2. ^{19}F NMR (471 MHz, $CDCl_3$): δ −134.55.

Step 2: Alkylation of the above α-hydroxyl ester intermediates (S)- and (R)-ethyl 2-(3-fluoro-4-methoxyphenyl)-2-hydroxyacetate was achieved as previously reported,[37] and crude products formed (as confirmed by MS and ^{1}H NMR) were carried forward to the saponification step without further purification.

Step 3: Saponification of the ethyl esters was achieved under basic (LiOH) conditions following well-established protocols.

The (R)- and (S)-2-(3-fluoro-4-methoxyphenyl)-2-isopropoxyacetic acids (**28**) were isolated as colorless oils in 59% (648 mg) and 48% (523 mg) yields, respectively (over the two steps).

Intermediates (R)- and (S)-**28** were further crystallized as their corresponding Na^+ salts in MeOH/MeCN to obtain the (R)-enantiomer in 98% ee and the (S)-enantiomer in 97% ee, as confirmed by ^{1}H NMR of their corresponding menthol ester derivatives.

^{1}H NMR (500 MHz, $CDCl_3$): δ 7.20−7.12 (m, 2H), 6.96 (t, J = 8.6 Hz, 1H), 4.91 (s, 1H), 3.89 (s, 3H), 3.76 (hept, J = 6.2 Hz, 1H), 1.26 (d, J = 6.1 Hz, 3H), 1.22 (d, J = 6.1 Hz, 3H). ^{13}C NMR (101 MHz, $CDCl_3$): δ 173.7, 152.5 (d, J = 247.2 Hz), 148.2 (d, J = 10.7 Hz), 129.2 (d, J = 5.9 Hz), 123.3 (d, J = 3.6 Hz), 115.0 (d, J = 19.5 Hz), 113.5 (d, J = 2.2 Hz), 77.1, 71.7, 56.4, 22.6, 21.7. ^{19}F NMR (377 MHz, $CDCl_3$): δ −134.08. MS [ESI$^-$] m/z: 241.2 [M − H]$^-$.

■ ASSOCIATED CONTENT

Supporting Information

The Supporting Information is available free of charge at https://pubs.acs.org/doi/10.1021/acs.jmedchem.1c01913.

Determination of %ee for intermediates (S)- and (R)-**25** (Figure S1); determination of %ee for intermediates (S)- and (R)-**28** (Figure S2); comparison of the relative affinity of hGGPPS inhibitors **12h** and **13c** (Figure S3); comparison of the relative affinity of hGGPPS inhibitors **14a** and **15a** (Figure S4); comparison of the relative affinity of hGGPPS inhibitors **16a** and (S)-**17e** (Figure S5); chiral HPLC of (S)- and (R)-ethyl 2-(3-fluoro-4-methoxyphenyl)-2-hydroxyacetates (Figure S6); and ^{1}H, ^{13}C, and ^{31}P NMR spectra and HPLC chromatograms of key final inhibitors shown in Table 1 (PDF)

Molecular formula strings and biological data (CSV)

■ AUTHOR INFORMATION

Corresponding Author

Youla S. Tsantrizos − *Department of Chemistry, McGill University, Montreal, Quebec H3A 0B8, Canada; Department of Biochemistry, McGill University, Montreal, Quebec H3G 1Y6, Canada;* orcid.org/0000-0002-6231-7498; Phone: +514-398-3638; Email: youla.tsantrizos@mcgill.ca

Authors

Hiu-Fung Lee − *Department of Chemistry, McGill University, Montreal, Quebec H3A 0B8, Canada*

Cyrus M. Lacbay − *Department of Chemistry, McGill University, Montreal, Quebec H3A 0B8, Canada;* Present Address: Evonik Canada, Inc. (Vancouver Laboratories), Burnaby, British Columbia V5J 5J1, Canada

Rebecca Boutin − *Department of Chemistry, McGill University, Montreal, Quebec H3A 0B8, Canada*

Alexios N. Matralis − *Department of Chemistry, McGill University, Montreal, Quebec H3A 0B8, Canada;* Present Address: Alexander Fleming Biomedical Sciences Research Center, Bio-innovation Institute, Athens 16672, Greece.

Jaeok Park − *Department of Chemistry, McGill University, Montreal, Quebec H3A 0B8, Canada; Department of Biochemistry, McGill University, Montreal, Quebec H3G 1Y6, Canada;* Present Address: Biochemistry Department, Memorial University of Newfoundland, St. John's, Newfoundland A1C 5S7, Canada.; orcid.org/0000-0002-8180-3950

Daniel D. Waller − *Department of Medicine, McGill University, Montreal, Quebec H3A 1A1, Canada; Division of Hematology, McGill University Health Center, Montreal, Quebec H4A 3J1, Canada;* Present Address: Terry Fox Laboratory, BC Cancer Research Institute, Vancouver, British Columbia V5Z 1L3, Canada

Tian Lai Guan − *Department of Chemistry, McGill University, Montreal, Quebec H3A 0B8, Canada*

Michael Sebag − *Department of Medicine, McGill University, Montreal, Quebec H3A 1A1, Canada; Division of Hematology, McGill University Health Center, Montreal, Quebec H4A 3J1, Canada*

Complete contact information is available at: https://pubs.acs.org/10.1021/acs.jmedchem.1c01913

Author Contributions

Y.S.T.: conceptualization and coordination of project; M.S.: design of hematology and cellular and *in vivo* studies; H.-F.L., C.M.L., R.B., and A.N.M.: library synthesis of inhibitors; J.P., R.B., and T.L.G.: *in vitro* assays; D.D.W. and T.L.G.: cell-based assays; and H.-F.L.: bone affinity studies.

Notes

The authors declare no competing financial interest.

■ ACKNOWLEDGMENTS

The authors are grateful for ADME/PK studies conducted by Kathryn Skorey, Julien Brault-Turcot, Dr. Zuomei Li, and Sabrina Hammond and their research teams at NuChem Sciences Inc. for conducting the rat PK studies. The authors wish to thank Christina Gagnon for her contributions in screening some of the compounds in biological assays. Financial support for this work was provided by the Canadian Institute of Health Research (CIHR) grants to M.S. and Y.S.T.

■ ABBREVIATIONS USED

ALT, alanine aminotransferase; AP, alkaline phosphatase; AM, amylase; AST, aspartate aminotransferase; Bil, bilirubin; FTase, farnesyl transferase; GGT, γ-glutamyl transferase; GGTase I, II and III, geranylgeranyl transferase I, II, and III; GTPases, GTP-binding proteins; hFPPS, human farnesyl pyrophosphate synthase; hGGPPS, human geranylgeranyl pyrophosphate synthase; HLMs, human liver microsomes; IV, intravenous injection; MTD, maximum tolerated dose; MLMs, mouse liver microsomes; MM, multiple myeloma; PBS, phosphate-buffered saline; RLMs, rat liver microsomes

■ REFERENCES

(1) Takai, Y.; Sasaki, T.; Matozaki, T. Small GTP-binding proteins. *Physiol. Rev.* **2001**, *81*, 153−208.

(2) Nguyen, U. T. T.; Guo, Z.; Delon, C.; Wu, Y.; Deraeve, C.; Fränzel, B.; Bon, R. S.; Blankenfeldt, W.; Goody, R. S.; Waldmann, H.; Wolters, D.; Alexandrov, K. Analysis of the eukaryotic prenylome by isoprenoid affinity tagging. *Nat. Chem. Biol.* **2009**, *5*, 227−235.

(3) (a) Mullen, P. J.; Yu, R.; Longo, J.; Archer, M. C.; Penn, L. Z. The interplay between cell signaling and the mevalonate pathway in cancer. *Nat. Rev. Cancer* **2016**, *16*, 718−731. (b) Clendening, J. W.; Pandyra, A.; Boutros, P. C.; Ghamrasni, S. E.; Khosravi, F.; Trentin, G. A.; Martirosyan, A.; Hakem, A.; Hakem, R.; Jurisica, I.; Penn, L. Z. Dysregulation of the mevalonate pathway promotes transformation. *Proc. Natl. Acad. Sci. U.S.A.* **2010**, *107*, 15051−15056. (c) Sorrentino, G.; Ruggeri, N.; Specchia, V.; Cordenonsi, M.; Mano, M.; Dupont, S.; Manfrin, A.; Ingallina, E.; Sommaggion, R.; Piazza, S.; Rosato, A.; Piccolo, S.; Del Sal, G. Metabolic control of YAP and TAZ by the mevalonate pathway. *Nat. Cell Biol.* **2014**, *16*, 357−366. (d) Laggner, U.; Lopez, J. S.; Perera, G.; Warbey, V. S.; Sita-Lumsden, A.; O'Doherty, M. J.; Hayday, A.; Harries, M.; Nestle, F. O. Regression of melanoma metastases following treatment with the n-bisphosohonate zeledronate and localized radiotherapy. *Clin. Immunol.* **2009**, *131*, 367−373.

(4) Kho, Y.; Kim, S. C.; Jiang, C.; Barma, D.; Kwon, S. W.; Cheng, J.; Jaunbergs, J.; Weinbaum, C.; Tamanoi, F.; Falck, J.; Zhao, Y. A tagging-via-substrate technology for detection and proteomics of farnesylated proteins. *Proc. Natl. Acad. Sci. U.S.A.* **2004**, *101*, 12479−12484.

(5) Review: Lawson, C. D.; Ridley, A. J. Rho GTPase signaling complexes in cell migration and invasion. *J Cell Biol.* **2018**, *217*, 447−457.

(6) Review: Lipton, A. Bisphosphonate therapy in the oncology setting. *Expert Opin. Emerging Drugs* **2003**, *8*, 469−488.

(7) Review: (a) Coleman, R. E. Bisphosphonates in breast cancer. *Ann. Oncol.* **2005**, *16*, 687−695. (b) Fromigue, O.; Lagneaux, L.; Body, J.-J. Bisphosphonates induce breast cancer cell death in vitro. *J. Bone Miner. Res.* **2000**, *15*, 2211−2221. (c) Senaratne, S. G.; Colston, K. W. Direct effects of bisphosphonates on breast cancer cells. *Breast Cancer Res.* **2001**, *4*, 18−23.

(8) (a) Derenne, S.; Amiot, M.; Barillé, S.; Collette, M.; Robillard, N.; Berthaud, P.; Harousseau, J.-L.; Bataille, R. Zoledronate is a potent inhibitor of myeloma cell growth and secretion of IL-6 and MMP-1 by the tumoral environment. *J. Bone Miner. Res.* **1999**, *14*, 2048−2056. (b) Aparicio, A.; Gardner, A.; Tu, Y.; Savage, A.; Berenson, J.; Lichtenstein, A. In vitro cytoreductive effects on multiple myeloma cells induced by bisphosphonates. *Leukemia* **1998**, *12*, 220−229.

(9) Oades, G. M.; Senaratne, S. G.; Clarke, I. A.; Kirby, R. S.; Colston, K. W. Nitrogen containing bisphosphonates induce apoptosis and inhibit the mevalonate pathway, impairing Ras membrane localization in prostate cancer cells. *J. Urol.* **2003**, *170*, 246−252.

(10) Review: (a) Lu, K.-H.; Lu, E. W.-H.; Lin, C.-W.; Yang, J.-S.; Yang, S.-F. New insights into molecular and cellular mechanisms of zoledronate in human osteosarcoma. *Pharmacol. Ther.* **2020**, *214*, No. 107611. (b) Evdokiou, A.; Labrinidis, A.; Bouralexis, S.; Hay, S.; Findlay, D. M. Induction of cell death of human osteogenic sarcoma cells by zoledronic acid resembles anoikis. *Bone* **2003**, *33*, 216−228.

(11) Morgan, G. J.; Davies, F. E.; Gregory, W. M.; Cocks, K.; Bell, S. E.; Szubert, A. J.; Navarro-Coy, N.; Drayson, M. T.; Owen, R. G.; Feyler, S.; Ashcroft, A. J.; Ross, F.; Byrne, J.; Roddie, H.; Rudin, C.; Cook, G.; Jackson, G. H.; Child, J. A. First-line treatment with zoledronic acid as compared with clodronic acid in multiple myeloma (MRC Myeloma IX): a randomized controlled trial. *Lancet* **2010**, *376*, 1989−1999.

(12) Morgan, G. J.; Davies, F. E.; Gregory, W. M.; Szubert, A. J.; Bell, S. E.; Drayson, M. T.; Owen, R. G.; Ashcroft, A. J.; Jackson, G. H.; Child, J. A. Effects of induction and maintenance plus long-term bisphosphonates on bone disease in patients with multiple myeloma: the Medical Research Council Myeloma IX Trial. *Blood* **2012**, *119*, 5374−5383.

(13) Coleman, R. E.; Marshall, H.; Cameron, D.; Dodwell, D.; Burkinshaw, R.; Keane, M.; Gil, M.; Houston, S. J.; Grieve, R. J.; Barrett-Lee, P. J.; Ritchie, D.; Pugh, J.; Gaunt, C.; Rea, U.; Peterson, J.; Davies, C.; Hiley, V.; Gregory, W.; Bell, R. Breast-cancer adjuvant therapy with zoledronic acid. *New Engl. J. Med.* **2011**, *365*, 1396−1405.

(14) Gnant, M.; Mlineritsch, B.; Stoeger, H.; Luschin-Ebengreuth, G.; Heck, D.; Menzel, C.; Jakesz, R.; Seifert, M.; Hubalek, M.; Pristauz, G.;

Bauernhofer, T.; Eidtmann, H.; Eiermann, W.; Steger, G.; Kwasny, W.; Dubsky, P.; Hochreiner, G.; Forsthuber, E. P.; Fesl, C.; Greil, R. Adjuvant endocrine therapy plus zoledronic acid in premenopausal women with early-stage breast cancer: 62-month follow-up from the ABCSG-12 randomised trial. *Lancet Oncol.* **2011**, *12*, 631−641.

(15) Gnant, M.; Mlineritsch, B.; Schippinger, W.; Luschin-Ebengreuth, G.; Pöstlberger, S.; Menzel, C.; Jakesz, R.; Seifert, M.; Hubalek, M.; Bjelic-Radisic, V.; Samonigg, H.; Tausch, C.; Eidtmann, H.; Steger, G.; Kwasny, W.; Dubsky, P.; Fridrik, M.; Fitzal, F.; Stierer, M.; Rücklinger, E.; Greil, R. Endocrine therapy plus zoledronic acid in premenopaisal breast cancer. *New Engl. J. Med.* **2009**, *360*, 679−691.

(16) Coleman, R.; de Boer, R.; et al. Zoledronic acid (zoledronate) for postmenopausal women with early breast cancer receiving adjuvant letrozole (ZO-FAST study): 60-months results. *Ann. Oncol.* **2013**, *24*, 398−405.

(17) (a) Rondeau, J.-M.; Bitsch, F.; Bourgier, E.; Geiser, M.; Hemmig, R.; Kroemer, M.; Lehmann, S.; Ramage, P.; Rieffel, S.; Strauss, A.; Green, J. R.; Jahnke, W. Structural basis for the exceptional *in vivo* efficacy of bisphosphonate drugs. *ChemMedChem* **2006**, *1*, 267−273. (b) Dunford, J. E.; Kwaasi, A. A.; Rogers, M. J.; Barnett, B. L.; Ebetino, F. H.; Russell, R. G. G.; Oppermann, U.; Kavanagh, K. L. Structure-activity relationship among the nitrogen containing bisphosphonates in clinical use and other analogues: Time-dependent inhibition of human farnesyl pyrophosphate synthase. *J. Med. Chem.* **2008**, *51*, 2187−2195.

(18) (a) Chen, T.; Berenson, J.; Vescio, R.; Swift, R.; Gilchick, A.; Goodin, S.; LoRusso, P.; Ma, P.; Ravera, C.; Deckert, F.; Schran, H.; Seaman, J.; Skerjanec, A. Pharmacokinetics and pharmacodynamics of zoledronic acid in cancer patients with bone metastases. *J. Clin. Pharmacol.* **2002**, *42*, 1228−36. (b) Skerjanec, A.; Berenson, J.; Hsu, C.; Major, P.; Miller, W. H., Jr.; Ravera, C.; Schran, H.; Seaman, J.; Waldmeier, F. The pharmacokinetics and pharmacodynamics of zoledronic acid in cancer patients with varying degrees of renal function. *J. Clin. Pharmacol.* **2003**, *43*, 154−162.

(19) Weiss, H. M.; Pfaar, U.; Schweitzer, A.; Wiegand, H.; Skerjanec, A.; Schran, H. Biodistribution and plasma protein binding of zoledronic acid. *Drug Metab. Dispos.* **2008**, *36*, 2043−2049.

(20) (a) Jahnke, W.; Rondeau, J.-M.; Cotesta, S.; Marzinzik, A.; Pellé, X.; Geiser, M.; Strauss, A.; Götte, M.; Bitsch, F.; Hemmig, R.; Henry, C.; Lehmann, S.; Glickman, J. F.; Roddy, T. P.; Stout, S. J.; Green, J. R. Allosteric non-bisphosphonate FPPS inhibitors identified by fragment-based discovery. *Nat. Chem. Biol.* **2010**, *6*, 660−666. (b) Park, J.; Leung, C. Y.; Matralis, A. N.; Lacbay, C. M.; Tsakos, M.; Fernandez De Troconiz, G.; Berghuis, A. M.; Tsantrizos, Y. S. Pharmacophore mapping of thienopyrimidine-based monophosphonate (ThP-MP) inhibitors of the human farnesyl pyrophosphate synthase. *J. Med. Chem.* **2017**, *60*, 2119−2134. (c) Feng, Y.; Park, J.; Li, S.-G.; Boutin, R.; Viereck, P.; Schilling, M. A.; Berghuis, A. M.; Tsantrizos, Y. S. Chirality-driven mode of binding of α-aminophosphonic acid-based allosteric inhibitors of the human farnesyl pyrophosphate synthase (hFPPS). *J. Med. Chem.* **2019**, *62*, 9691−9702.

(21) Rowinsky, E. K. Lately, it occurs to me what a long, strange trip it's been for the farnesyltransferase inhibitors. *J. Clin. Oncol.* **2006**, *24*, 2981−2984.

(22) Martin, N. E.; Brunner, T. B.; Kiel, K. D.; DeLaney, T. F.; Regine, W. F.; Mohiuddin, M.; Rosato, E. F.; Haller, D. G.; Stevenson, J. P.; Smith, D.; Pramanik, B.; Tepper, J.; Tanaka, W. K.; Morrison, B.; Deutsch, P.; Gupta, A. K.; Muschel, R. J.; McKenna, G.; Bernhard, E. J.; Hahn, S. M. A phase I trial of the dual farnesyltransferase and geranylgeranyltransferase inhibitor L-778,123 and radiotherapy for locally advanced pancreatic cancer. *Clin. Cancer Res.* **2004**, *10*, 5447−5454.

(23) (a) Mimura, N.; Hideshima, T.; Anderson, K. C. Novel therapeutic strategies for multiple myeloma. *Exp. Hematol.* **2015**, *43*, 732−741. (b) Melton, L. J., III; Kyle, R. A.; Achenbach, S. J.; Oberg, A. L.; Rajkumar, S. V. Fracture risk with multiple myeloma: a population-based study. *J. Bone Miner. Res.* **2005**, *20*, 487−493.

(24) For a recent review on the biology/physiology and clinical characteristics of multiply myeloma refer to: Bianchi, G.; Munshi, N. Pathogenesis beyond the cancer clone(s) in multiple myeloma. *Blood* **2015**, *125*, 3049−3058.

(25) (a) Thakurta, A.; Pierceall, W. E.; Amatangelo, M. D.; Flynt, E.; Agarwal, A. Developing next generation immunomodulatory drugs and their combination in multiple myeloma. *Oncotarget* **2021**, *12*, 1555−1563. (b) Mukkamalla, S. K. R.; Malipeddi, D. Myeloma bone disease: A comprehensive review. *Int. J. Mol. Sci.* **2021**, *22*, No. 6208. (c) Davis, L. N.; Sherbenou, D. W. Emerging therapeutic strategies to overcome drug resistance in multiple myeloma. *Cancers* **2021**, *13*, No. 1686.

(26) (a) Zhang, Y.; Cao, R.; Yin, F.; Hudock, M. P.; Guo, R.-T.; Krysiak, K.; Mukherjee, S.; Gao, Y.-G.; Robinson, H.; Song, Y.; No, J. H.; Bergan, K.; Leon, A.; Cass, L.; Goddard, A.; Chang, T.-K.; Lin, F.-Y.; Van Beek, E.; Papapoulos, S.; Wang, A. H.-J.; Kubo, T.; Ochi, M.; Mukkamala, D.; Oldfield, E. Lipophilic bisphosphonates as dual farnesyl/geranylgeranyl diphosphate synthase inhibitors: An X-ray and NMR investigation. *J. Am. Chem. Soc.* **2009**, *131*, 5153−5162. (b) Zhang, Y.; Cao, R.; Yin, F.; Lin, F.-Y.; Wang, H.; Krysiak, K.; No, J.-H.; Mukkamala, D.; Houlihan, K.; Li, J.; Morita, C. T.; Oldfield, E. Lipophilic pyridinium bisphosphonates: Potent $\gamma\delta$ T cell stimulators. *Angew. Chem., Int. Ed.* **2010**, *49*, 1136−1138.

(27) Shull, L. W.; Wiemer, A. J.; Hohl, R. J.; Wiemer, D. F. Synthesis and biological activity of isoprenoid bisphosphonates. *Bioorg. Med. Chem.* **2006**, *14*, 4130−4136.

(28) Wills, V. S.; Allen, C.; Holstein, S. A.; Wiemer, D. F. Potent triazole bisphosphonate inhibitor of geranylgeranyl diphosphate synthase. *ACS Med. Chem. Lett.* **2015**, *6*, 1195−1198.

(29) Lacbay, C. M.; Waller, D. D.; Park, J.; Gómez Palou, M.; Vincent, F.; Huang, X.-F.; Ta, V.; Berghuis, A. M.; M Sebag, M.; Tsantrizos, Y. S. Unraveling the prenylation-cancer paradox in multiple myeloma with novel geranylgeranyl pyrophosphate synthase (GGPPS) inhibitors. *J. Med. Chem.* **2018**, *61*, 6904−6917.

(30) (a) Goffinet, M.; Thoulouzan, M.; Pradines, A.; Lajoie-Mazenc, I.; Weinbaum, C.; Faye, J. C.; Séronie-Vivien, S. Zoledronic acid treatment impairs protein geranylgeranylation for biological effects in prostatic cells. *BMC Cancer* **2006**, *6*, No. 60. (b) Guenther, A.; Gordon, S.; Tiemann, M.; Burger, R.; Bakker, F.; Green, J. R.; Baum, W.; Roelofs, A. J.; Rogers, M. J.; Gramatzki, M. The bisphosphonate zoledronic acid has antimyeloma activity in vivo by inhibition of protein prenylation. *Int. J. Cancer* **2010**, *126*, 239−246.

(31) (a) Simon, G. M.; Niphakis, M. J.; Cravatt, B. F. Determining target engagement in living systems. *Nat. Chem. Biol.* **2013**, *9*, 200−205. (b) Durham, T. B.; Blanco, M.-J. Target engagement in lead generation. *Bioorg. Med. Chem. Lett.* **2015**, *25*, 998−1008.

(32) (a) Chesi, M.; Matthews, G. M.; Garbitt, V. M.; Palmer, S. E.; Shortt, J.; Lefebure, M.; Stewart, A. K.; Johnstone, R. W.; Bergsage, P. L. Drug response in a genetically engineered mouse model of multiple myeloma is predictive of clinical efficacy. *Blood* **2012**, *120*, 376−385. (b) Gomez-Palou, M.; Fang, H.; Kremer, R.; Sebag, M. A transgenic model of multiple myeloma bone disease shows profound mesenchymal stem cell impairment. *Blood* **2013**, *122*, No. 130.

(33) Meerwein, H.; Dittmar, G.; Göllner, R.; Hafner, K.; Mensch, F.; Steinfort, O. Verfahren zur herstellung aromatiscer sulfonsäurechloride, eine neue modification der Sandmeyerschen reaction. *Chem. Ber.* **1957**, *90*, 841−852.

(34) Hogan, P. J.; Cox, B. G. Aqueous process chemistry: The preparation of aryl sulfonyl chlorides. *Org. Process. Res. Dev.* **2009**, *13*, 875−879.

(35) (a) McKenna, C. E.; Higa, M. T.; Cheung, N. H.; McKenna, M.-C. The facile dealkylation of phosponic acid dialkyl esters by bromothrimethylsilane. *Tetrahedron Lett.* **1977**, 155−158. (b) Błażewska, K. M. McKenna reaction - which oxygen attacks bromotrimethylsilane? *J. Org. Chem.* **2014**, *79*, 408−412.

(36) (a) Majer, P.; Randad, R. S. A Safe and efficient method for preparation of *N*,*N*′-unsymmetrically disubstituted ureas utilizing triphosgene. *J. Org. Chem.* **1994**, *59*, 1937−1938. (b) Liu, D.; Tian, Z.; Yan, Z.; Wu, L.; Ma, Y.; Wang, Q.; Liu, W.; Zhou, H.; Yang, C. Design, synthesis and evaluation of 1,2-benzisothiazol-3-one derivatives as potent caspase-3 inhibitors. *Bioorg. Med. Chem.* **2013**, *21*, 2960−2967.

https://doi.org/10.1021/acs.jmedchem.1c01913
J. Med. Chem. XXXX, XXX, XXX−XXX

(37) Buck, R. T.; Coe, D. M.; Drysdale, M. J.; Ferris, L.; Haigh, D.; Moody, C. J.; Pearson, N. D.; Sanghera, J. B. Asymmetric rhodium carbene insertion into the Si-H bond: identification of new dirhodium-(II) carboxylate catalysts using parallel synthesis techniques. *Tetrahedron Asymmetry* **2003**, *14*, 791−816.

(38) Neilson, D. G.; Peters, D. V. A new resolution of α-methoxy-α-phenylacetic acid. *J. Chem. Soc.* **1962**, 1519.

(39) Moreno-Dorado, F. J.; Guerra, F. M.; Ortega, M. aJ.; Zubía, E.; Massanet, G. M. Enantioselective synthesis of arylmethoxyacetic acid derivatives. *Tetrahedron Asymmetry* **2003**, *14*, 503−510.

(40) Lock, G. Über die Synthese von 3-Fluor-4-oxy-phenylessigsäure. *Monatsh. Chem.* **1955**, *86*, 511−516.

(41) Yotagai, M.; Ohnuki, T. Asymmetric reduction of functionalized ketones with a sodium borohydride−(L)-tartaric acid system. *J. Chem. Soc. Perkin Trans. 1* **1990**, 1826−1828.

(42) Kavanagh, K. L.; Dunford, J. E.; Bunkoczi, G.; Russell, R. G.; Oppermann, U. The crystal structure of human geranylgeranyl pyrophosphate synthase reveals a novel hexameric arrangement and inhibitory product binding. *J. Biol. Chem.* **2006**, *281*, 22004−22012.

(43) Yang, J.; Copeland, R. A.; Lai, Z. Defining balanced conditions for inhibitor screening assays that target bisubstrate enzymes. *J. Biomol. Screen* **2009**, *14*, 111−120.

(44) Reviews: (a) Acker, M. G.; Auld, D. S. Considerations for the design and reporting of enzyme assays in high-throughput screening applications. *Perspect. Sci.* **2014**, *1*, 56−73. (b) Srinivasan, B. Explicit treatment of non-Michaelis-Menten and atypical kinetics in early drug discovery. *ChemMedChem* **2021**, *16*, 899−918.

(45) (a) Szabo, C. M.; Matsumura, Y.; Fukura, S.; Martin, M. B.; Sanders, J. M.; Sengupta, S.; Cieslak, J. A.; Loftus, T. C.; Lea, C. R.; Lee, H.-J.; Koohang, A.; Coates, R. M.; Sagami, H.; Oldfield, E. Inhibition of geranylgeranyl diphosphate synthase by bisphosphonates and diphosphates: A potential route to new bone antiresorption and antiparasitic agents. *J. Med. Chem.* **2002**, *45*, 2185−2196. (b) Guo, R. T.; Cao, R.; Liang, P. H.; Ko, T. P.; Chang, T. H.; Hudock, M. P.; Jeng, W. Y.; Chen, C. K.; Zhang, Y.; Song, Y.; Kuo, C. J.; Yin, F.; Oldfield, E.; Wang, A. H. Bisphosphonates target multiple sites in both *cis*- and *trans*-prenyltransferases. *Proc. Natl. Acad. Sci. U.S.A.* **2007**, *104*, 10022−10027.

(46) (a) Wiemer, A. J.; Tong, H.; Swanson, K. M.; Hohl, R. J. Digeranyl bisphosphonate inhibits geranylgeranyl pyrophosphate synthase. *Biochem. Biophys. Res. Commun.* **2007**, *353*, 921−925. (b) Barney, R. J.; Wasko, B. M.; Dudakovic, A.; Hohl, R. J.; Wiemer, D. F. 2010. Synthesis and biological evaluation of a series of aromatic bisphosphonates. *Bioorg. Med. Chem.* **2010**, *18*, 7212−7220.

(47) Chen, C. K.-M.; Hudock, M. P.; Zhang, Y.; Guo, R.-T.; Cao, R.; No, J. H.; Liang, P.-H.; Ko, T.-P.; Chang, T.-H.; Chang, S.-C.; Song, Y.; Axelson, J.; Kumar, A.; Wang, A. H.-J.; Oldfiend, E. Inhibition of geranylgeranyl diphosphate synthase by bisphosphonates: A crystallographic and computational investigation. *J. Med. Chem.* **2008**, *51*, 5594−5607.

(48) Cao, R.; Chen, C. K.; Guo, R. T.; Wang, A. H.; Oldfield, E. Structures of a potent phenylalkyl bisphosphonate inhibitor bound to farnesyl and geranylgeranyl diphosphate synthases. *Proteins* **2008**, *73*, 431−439.

(49) (a) Swinney, D. C.; Anthony, J. How were new medicines discovered? *Nat. Rev. Drug Discovery* **2011**, *10*, 507−519. (b) Moffat, J. G.; Vincent, F.; Lee, J. A.; Eder, J.; Prunotto, M. Opportunities and challenges in phenotypic drug discovery: an industry perspective. *Nat. Rev. Drug Discovery* **2017**, *16*, 531−543.

(50) (a) Marma, M. S.; Xia, Z.; Stewart, C.; Coxon, F.; Dunford, J. E.; Baron, R.; Kashemirov, B. A.; Ebetino, F. H.; Triffitt, J. T.; Russell, G. G.; McKenna, C. E. Synthesis and biological evaluation of α-halogenated bisphosphonate and phosphonocarboxylate analogues of risedronate. *J. Med. Chem.* **2007**, *50*, 5967−5975. (b) Ebetino, F. H.; Hogan, A.-M.; Sun, S.; Tsoumpra, M. K.; Duan, X.; Triffitt, J. T.; Kwaasi, A. A.; Dunford, J. E.; Barnett, B. L.; Oppermann, U.; Lundy, M. W.; Boyde, A.; Kashemirov, B. A.; McKenna, C. E.; Russell, R. G. The relationship between the chemistry and biological activity of the bisphosphonates. *Bone* **2011**, *49*, 20−33.

(51) Coxon, F. P.; Helfrich, M. H.; van't Hof, R.; Sebti, S.; Ralston, S. H.; Hamilton, A.; Rogers, M. J. Protein geranylgeranylation is required for osteoclast formation, function and survival: Inhibition by bisphosphonates and GGTI-298. *J. Bone and Miner. Res.* **2000**, *15*, 1467−1476.

(52) Jahnke, W.; Henry, C. An in vitro assay to measure targeted drug delivery to bone mineral. *ChemMedChem* **2010**, *5*, 770−776.

(53) Jahnke, W.; Bold, G.; Marzinzik, A. L.; Ofner, S.; Pellé, X.; Cotesta, S.; Bourgier, E.; Lehmann, S.; Henry, C.; Hemmig, R.; Stauffer, F.; J Hartwieg, J. C. D.; Green, J. R.; Rondeau, J.-M. A general strategy for targeting drugs to bone. *Angew. Chem., Int. Ed.* **2015**, *54*, 14575−14579.

(54) Review: (a) Onakpoya, I. J.; Heneghan, C. J.; Aronson, J. K. Worldwide withdrawal of medicinal products because of adverse drug reactions: a systematic review and analysis. *Crit. Rev. Toxicol.* **2016**, *46*, 477−489. (b) Monroe, J. J.; Tanis, K. Q.; Podtelezhnikov, A. A.; Nguyen, T.; Machotka, S. V.; Lynch, D.; Evers, R.; Palamanda, J.; Miller, R. R.; Pippert, T.; Cabalu, T. D.; Johnson, T. E.; Aslamkhan, A. G.; Kang, W.; Tamburino, A. M.; Mitra, K.; Agrawal, N. G. B.; Sistare, F. D. Application of rat liver drug bioactivation transcriptional response assay early in drug development that informs chemically reactive metabolite formation and potential for drug-induced liver injury. *Toxicol. Sci.* **2020**, *177*, 281−299.

(55) (a) Haney, S. L.; Chhonker, Y. S.; Varney, M. L.; Talmon, G.; Murry, D. J.; Holstein, S. A. Preclinical investigation of a potent geranylgeranyl diphosphate synthase inhibitor. *Invest. New Drugs* **2018**, *36*, 810−818. (b) Haney, S. L.; Chhonker, Y. S.; Varney, M. L.; Talmon, G.; Smith, L. M.; Murry, D. J.; Holstein, S. A. In vivo evaluation of isoprenoid tyriazole bisphosphonate inhibitors of geranylgeranyl diphosphate synthase: Impact of olefin stereochemistry on toxicity and biodistribution. *J. Pharmacol. Exp. Ther.* **2019**, *371*, 327−338.

(56) Jiang, L.; Cui, X.; Ma, H.; Tang, X. Comparison of denosumab and zoledronic acid for the treatment of solid tumors and multiple myeloma with bone metastasis: a systematic review and meta-analysis based on randomized controlled trials. *J. Orthop. Surg. Res.* **2021**, *16*, No. 400.

(57) Lai, L.; Li, A. N.; Zhou, J.; Guo, Y.; Lin, L.; Chen, W.; Wang, R. Mg(OMe)2 promoted allylic isomerization of γ-hydroxy-α,β-alkenoic esters to synthesize γ-ketone esters. *Org. Biomol. Chem.* **2017**, *15*, 2185−2190.

https://doi.org/10.1021/acs.jmedchem.1c01913
J. Med. Chem. XXXX, XXX, XXX−XXX